EFFECT OF WAVE GROUPİNG, SPECTRAL SHAPE AND EXTREME WAVES IN A WAVE TRAIN ON THE STABILITY OF RUBBLE MOUND BREAKWATERS

A THESIS SUBMITTED TO
THE GRADUATE SCHOOL OF NATURAL AND APPLIED SCIENCES
OF
MİDDLE EAST TECHNICAL UNIVERSITY

BY

BERGÜZAR ÖZTUNALI ÖZBAHÇECİ

IN PARTIAL FULFILLMENT OF THE REQUIREMENTS FOR THE
DEGREE OF DOCTOR OF PHILOSOPHY
IN
THE DEPARTMENT OF CIVIL ENGINEERING

JULY 2004

Approval of the Graduate School of the Natural and Applied Sciences

_____

Prof. Dr. Canan Özgen
Director

I certify that this thesis satisfies all the requirements as a thesis for the degree of Doctor of Philosophy

_____

Prof. Dr. Erdal Çokca
Head of Department

This is to certify that we have read this thesis and that in our opinion it is fully adequate, in scope and quality, as a thesis for the degree of Doctor of Philosophy.

_____

Prof. Dr. Ayşen Ergin
Supervisor

Examining Committee Members

Prof. Dr. Yalçın Yüksel _____

Prof. Dr. Ayşen Ergin _____

Prof. Dr. Melih Yanmaz _____

Assoc. Prof. Dr. A. Cevdet Yalçıner _____

Assoc. Prof. Dr. E. Can Balas _____

I hereby declare that all information in this document has been obtained and presented in accordance with academic rules and ethical conduct. I also declare that, as required by these rules and conduct, I have fully cited and material and referenced all material and results that are not original to this work.

Name, Last name: Bergüzar ÖZTUNALI ÖZBAHÇECİ

Signature :

ABSTRACT

EFFECTS OF WAVE GROUPING, SPECTRAL SHAPE AND
EXTREME WAVES IN A WAVE TRAIN
ON THE STABILITY OF RUBBLE MOUND BREAKWATERS

Özbahçeci Öztunalı, Bergüzar
Ph.D., Department of Civil Engineering
Supervisor: Prof. Dr. Ayşen Ergin

July 2004, 135 pages

There are some empirical formulas used in the design of rubble mound breakwaters to find the weight of armour layer stone. The effect of wave grouping and spectral shape could not put into these design formulas since their effects are still under question. The influences of wave groups and spectral shape on the stability of rubble mound breakwaters have been investigated by several researchers up to now. However, results were not conclusive in these researches, where different wave grouping and spectral shape parameters were used.

This study aims to investigate the influences of wave groups and spectral shape on the stability of rubble mound breakwaters by means of hydraulic model experiments. According to the result of the experiments, the damage to breakwater armour layer is almost same for different spectrum shapes and pronounced wave grouping, under the condition of similar wave statistics. Experiments also indicated that the wave trains with same significant wave height, $H_{1/3}$, but with different distribution of the heights of

extreme waves which were defined as wave heights higher than $H_{1/3}$ in this study, cause different damage levels. Based on these results, extended experiments were conducted to observe the effect of heights of extreme waves in a wave train on the stability of rubble mound breakwaters. Results of the experiments showed that the higher the extreme waves are, the more destructive the wave train is. By carrying experimental results into design conditions, it was shown that a wave train with high extreme waves may affect the design weight of armour stone.

Finally, in order to achieve more practical tools for engineering applications, occurrence probabilities of extreme waves under different spectral shapes were obtained by a numerical simulation. As a result, for different occurrence probabilities of extreme waves under the most widely used spectrums of PM and JONSWAP, necessary weight of armour stone was given in a range comparing with the formula of Meer. Moreover, it was noted that the spectral shape indirectly affects the stability not due to the wave grouping but due to the extreme waves in a wave train since the occurrence probability of the high extreme waves becomes higher as the spectral shape becomes narrower under same significant wave height condition.

Keywords: Wave grouping, Spectral shape, Wave statistics, Stability, Rubble Mound Breakwater

ÖZ

DALGA KÜMELEŞMESİ, DALGA SPEKTRUMUNUN BİÇİMİ VE
BİR DALGA DİZİSİNDEKİ AŞIRI DALGALARIN
TAŞDOLGU DALGAKIRANLARIN DENGESİNE ETKİSİ

Özbahçeci Öztunalı, Bergüzar
İnşaat Mühendisliği Bölümü
Tez Yöneticisi: Prof. Dr. Ayşen Ergin

Temmuz 2004, 135 sayfa

Taşdolgu dalgakıranların tasarımında koruma tabakası taş ağırlığının bulunması için deneysel denklemler kullanılmaktadır. Bu denklemlerde dalga yüksekliği, periyodu, yapı eğimi, taşın ve suyun birim ağırlığı, fırtına süresi, hasar seviyesi ve yapının geçirgenliği dikkate alınırken, dalga kümeleşmesi, ve spektrum biçiminin etkisi belirsizliğini korumasından dolayı denge denklemlerinde yer almamıştır. Dalga kümeleşmesi ve dalga spektrumunun biçiminin taşdolgu dalgakıranların stabilitesine etkisi pek çok araştırmaya konu olmuştur. Ancak araştırmalarda dalga kümeleşmesi ve spektrum biçimini ifade eden farklı değişkenler kullanılmış ve birbiriyle çelişen sonuçlar ortaya çıkmıştır.

Sözkonusu tez, hidrolik örnekleme çalışması yardımıyla bu konulara açıklık getirmeyi amaçlamıştır. Deney sonuçlarına göre spektrum biçimi değişmesine ve dalga kümeleşmesi artmasına rağmen dalga yüksekliği dağılımı aynı kaldığı sürece koruma tabakasındaki hasarda önemli bir değişiklik olmamaktadır. Deneyler aynı zamanda, belirgin dalga yüksekliği ($H_{1/3}$) sabit olan dalga dizilerinden, aşırı dalgaların yani $H_{1/3}$ ten büyük

dalgaların farklılığının, hasarda da farklılığa yol açtığını göstermiştir. Bu deney sonuçlarına dayanılarak aşırı dalgaların taşdolgu dalgakıranların dengesine etkisi genişletilmiş deneylerle incelenmiştir. Deneyler dalga serilerinden aşırı dalgaları daha yüksek olanının dalgakırana daha fazla hasar verdiğini ortaya çıkarmıştır. Daha sonra, deney sonuçları tasarım koşullarına taşınmış ve aşırı dalgaların tasarımda bulunan taş ağırlığını etkileyebileceği gösterilmiştir.

Son olarak mühendislik uygulamalarında kolaylık sağlaması amacıyla, bir dalga dizisindeki aşırı dalgaların olasılık dağılımları değişik spektrum biçimleri için sayısal benzeşim yöntemiyle bulunmuştur. Böylece özellikle kullanımı yaygın olan PM ve JONSWAP spektrumları için aşırı dalgaların farklı oluşma olasılıklarında, koruma tabakasındaki taş ağırlığının Meer denkleminde bulunana göre nasıl bir aralıkta değişebileceği ortaya konmuştur. Çalışma sonuçlarına göre, spektrum biçiminin dalga kümeleşmesi nedeniyle değil ama aşırı dalgaların oluşma olasılığını değiştirebildiği için dengeyi dolaylı olarak etkilediği söylenebilir.

Anahtar Kelimeler: Dalga Kümeleşmesi, Spektrum Biçimi, Dalga İstatistiği, Aşırı Dalgalar, Taşdolgu Dalgakıran

To my dear grandparents who transmitted me the gene of doing research with love and patience,

To my uncle Prof. Dr. Dr. Hc. Önder Öztunalı for his encouragement, light and guidance,

To my unborn child who has been waiting for the completion of mother's Ph.D. study to born, with endurance.

ACKNOWLEDGEMENTS

The author would like to express her gratitude to her supervisor, Prof. Dr. Ayşen Ergin for her guidance, concern, positive energy and patience.

The author would like gratefully thank to Prof. Dr. Tomotsuka Takayama, author's advisor in Kyoto University, for his acceptance of author as a research student to his laboratory in Disaster Prevention Research Institute of Kyoto University and for his patient guidance and his support and care for the life of the author in Japan. The author is also thankful to Assoc.Prof. Dr. Hajime Mase from Kyoto University for his valuable suggestions on the study. The author is also grateful to dear Shiego Fujiki, technician of the laboratuary, for his help and support during the experiments. Thanks are extended to secretary of the laboratory, Ms Yumiko Okamoto, and the all members but especially Yamato San, Murayama San, Amomori San and Higashira San for their help during the experiments.

The author would like to thank to Prof. Dr. Melih Yanmaz and Assoc. Prof. Dr. Can Balas for serving on her doctoral committee and for their suggestions.

The author is thankful to Engin Bilyay, Gülsen Kiziroğlu and Selahattin Bacanlı for their support, help, friendship and patience in the office.

The author would also like to thank to her parents for their encouragement and support whenever she needs.

Special thanks go to author's husband Murat Özbahçeci for his love and endless support on the author's career even being 10000 km far away is necessary. The author is also grateful to his family for their care.

TABLE OF CONTENTS

LIST OF TABLES

TABLE

LIST OF FIGURES

FIGURE

LIST OF SYMBOLS

W	=	Weight of individual armour stone
γ_σ	=	Unit weight of stone
γ_ω	=	Unit weight of water
Δ	=	Relative mass density= $(\gamma_s-\gamma_w)/\ \gamma_w$
ρ_s	=	Density of stone
D_n	=	Nominal diameter $=(M_{50}/\rho_s)^{1/3}$
D_{n15}	=	Nominal diameter of stone with 15% value of distribution curve
D_{n50}	=	Nominal diameter of stone with 50% value of distribution curve
D_{n85}	=	Nominal diameter of stone with 85% value of distribution curve
M_{50}	=	Mass of stone with 50% value of distribution curve
α	=	Angle between breakwater and horizontal
K_D	=	Damage coefficient or empirical stability coefficient
H_s	=	Zero-up crossing Significant wave height ($H_{1/3}$)
$H_{1/10}$	=	Average of the heighest 1/10 waves
$H_{1/20}$	=	Average of the heighest 1/20 waves
$H_{1/100}$	=	Average of the heighest 1/100 waves
H_{max}	=	Maximum wave height
T_s	=	Zero-up crossing Significant wave period ($T_{1/3}$)
T_m	=	Zero-up crossing mean wave period
T_p	=	Spectral peak period
ξ	=	Irribaren number or Surf similarity parameter,
ξ_m	=	Irribaren number calculated by T_m
s	=	Wave steepness,
N_s	=	Stability number
S	=	Damage level,
A_e	=	Erosion area in a cross-section
N	=	Number of waves (Storm duration)
P	=	Permeability coefficient of the structure

α	=	Envelope exceedance coefficient
$\alpha_{extreme}$	=	Extreme wave parameter
GF	=	Groupiness factor
mrl	=	Mean run length
γ	=	Spectrum peak enhancement factor
S(f)	=	Frequency spectrum
f	=	Frequency
f_p	=	The peak frequency of the spectrum
m	=	A coefficient that determines the high frequency slopes of the spectrum
n	=	A coefficient that determines the low frequency slope of the spectrum

CHAPTER 1

INTRODUCTION

Rubble mound breakwaters are the oldest and still the most common type of breakwater. The vast amount of published researches reflects clearly importance of these structures. Especially to obtain a reliable design equation for the stability of armour layer has been an attractive topic for the researchers.

The well known Hudson formula has been widely used due to its simplicity and the wide range of armour units and configurations for which values of stability coefficient K_D have been derived. The Hudson formula also has many limitations (Meer, 1993). Briefly saying, wave period, storm duration, and permeability were not taken account in the formula. Moreover since the formula was based on the results of regular wave tests, some parameters related to wave irregularity like wave height distribution, spectral shape and wave grouping do not take place in Hudson's formula.

The wave spectrum describes how the wave energy is spreading over a range of frequency and that of direction. The distribution of wave energy over the frequency is represented by the frequency spectrum S(*f*). It is very important to reveal the structure of wave spectra so as to clarify the nature of sea waves.

Although sea waves may look random, inspection of wave records indicates that high waves fall into groups rather than appear individually. The existence of wave groups has been known to seafarers for a long time. Out of their experiences have come the saying that 'every seventh wave is large' and old Icelandic saying that 'large waves seldom come alone'. Surf riders

are also aware of this phenomenon. They say that ‘big waves come in three by three’. Engineers and scientists, however, have neglected this phenomenon until the phenomenon has been recognized, by a number of events which proved the necessity of taking them seriously in technical sense (Bruun, 1985)

After irregularity of the waves which is the real case in the nature gained importance in coastal engineering, it was attempted to apply the Hudson formula directly to irregular wave fields with appropriate design wave height representing sea state. Therefore, in most of the previous studies, only the problem as to how to determine the statistic design wave height with a stability conception of regular wave condition was discussed. Firstly, significant wave height ($H_{1/3}$) was put into Hudson formula instead of regular wave height. Then, Shore Protection Manual (SPM 1984) proposed to use $H_{1/10}$ in the Hudson formula as representative of extremely irregular wave action. However, depending on the design wave selected, the design weight of armour of rubble mound breakwaters varies in wide range and many different results have been reported.

Then, in 1988, Van der Meer derived new stability formulas for rubble mound breakwaters under random wave attack as a result of comprehensive model investigation. These formulas include parameters such as the wave period, storm duration and permeability of the structure. But still the wave grouping and spectral shape were not taken into account since Meer concluded from his experiments that there was no significant correlation of spectral shape with armour damage. Significant wave height was used in derivation of stability formulae and it was proposed to use the ratio $H_{2\%}/H_s$ or a similar one with $H_{1\%}$ or $H_{5\%}$ for the effect of non-Rayleigh distribution of individual wave heights.

The influences of wave groups and spectral shape on the stability of rubble mound breakwaters have been investigated by several researchers up to now. But, results were not conclusive in these researches, where different wave grouping and spectral shape parameters were used. Moreover it has

still been discussed which is the best characteristic wave height to be used in the design under irregular wave conditions.

This thesis aims to find the answers to those questions by means of hydraulic model experiments. First of all, experiments were conducted to investigate the wave groups and spectral shape on the stability of rubble mound breakwaters. A model of rubble mound breakwater with 1:1.5 slope was installed inside the wave channel of hydraulic laboratory of the Disaster Prevention Research Institute of Kyoto University. Time series, approximately equal to 1000 waves, with similar wave height statistics but different degrees of wave grouping and spectral shape were generated. In Chapter 3, experimental set-up, model cross-section, test program, wave generation, damage measurement and calculation, wave analysis and test results are presented with discussions.

Based on the results of the experiments which indicated that the wave trains with same significant wave height, $H_{1/3}$, but with different extreme waves which was defined as wave heights higher than $H_{1/3}$ in this study, cause different damage levels, extended experiments were conducted to observe the effect of heights of extreme waves in a wave train on the stability of rubble mound breakwaters. Rubble mound breakwater models which were installed inside the wave channel of hydraulic laboratory of the Disaster Prevention Research Institute of Kyoto University with two different slopes of 1:1.5 and 1:3 were tested since those are the limits of mostly applied slope angle range. Time series, approximately equal to 1000 waves, with similar significant wave height but different distribution of the heights of extreme waves were generated. Damage curves and stability curves were plotted according to the experimental results. Then, by using stability curves, experimental results were carried into design conditions and it was shown that a wave train with high extreme waves may affect the design weight of armour stone. Experiment cases, results of the experiments, damage and stability curves and design considerations are given in Chapter4.

Finally, in order to achieve more practical tools for engineering applications, occurrence probabilities of extreme waves under different spectral shapes were obtained by a numerical simulation. Details of numerical simulation and engineering application are presented in Chapter 5. Chapter 6 provides the conclusions and recommendations of future studies.

Summary of the previous studies on wave grouping, spectral shape, extreme waves in a wave train, stability of rubble mound breakwaters and the effects of wave grouping, spectral shape and the extreme waves on the stability of rubble mound breakwaters are given in Chapter 2.

CHAPTER 2

LITERATURE SURVEY

Coastal engineering is a well-established branch of civil engineering with a history of more than half a century. Although since the early 19th century, the mathematical theory of water waves began to be developed by mathematicians and physicists, many pieces of knowledge in various fields of science and engineering were amalgamated in the furnace of Second World War to give birth to this new interdisciplinary branch of coastal engineering. The motivation was the military needs to forecast the sea condition for the amphibious operation at the coast occupied by the enemy (Goda, 1998).

Sverdrup and Munk of the Scripps Institute of Oceanography at the university of California devised the unique concept of significant wave, while striving for creation of a rational method of wave forecasting. It was a simple representation of irregular sea waves with a single height and period. The height was defined as the average of the heights one-third waves of the whole individual waves and the period was the average of the periods of the same waves (Goda, 1998).

2.1 Spectral Shape

When Sverdrup and Munk introduced the concept of significant wave as a mean to represent the sea state in 1946, they were fully aware of the randomness of ocean waves and it is brought forth by the presence of a large number of wave components of different frequencies and amplitudes, which are contained in the wave spectrum. Oceanographers endeavoured

to reveal the structure of wave spectra so as to clarify the nature of ocean waves (Goda, 1998)..

Neumann was the first in proposing a functional form of wave spectrum in 1953. He visually measured the heights and periods of individual waves from a ship in the ocean, and derived a power spectrum from the histogram of wave energy of individual waves in the respective classes of wave periods. Although this method of analysing wave spectra is not accepted nowadays, Neumann's spectrum was welcomed by oceanographers as the basis to build a more rational wave forecasting method. The first spectral method of wave forecasting was presented by Pierson, Neumann, and James in 1955 in the form of a technical manual form the US Navy Hydrographic Office, which is often called the PNJ method (Goda, 1998).

The wave spectrum describes how the wave energy is spreading over a range of frequency and that of direction. The distribution of wave energy over the frequency is represented by the frequency spectrum $S(f)$, while the energy spreading over the direction is described with the directional spreading function $G(\theta,f)$. Thus, the ocean wave spectrum is expressed as

$$S(f,\theta) = S(f)\, G(\theta,f) \qquad (2.1)$$

In which (f) denotes the frequency and θ is the angle from the principal direction of wave propagation. The wave spectrum is given the dimension of energy density such as m^2s, and this dimension is assigned to the frequency spectrum $S(f)$. The directional spreading function is made dimensionless and normalised such that its integral over a full direction is unity (Goda, 1998).

The PNJ method employed Neumann's spectrum for the frequency spectrum and a cosine squared law of the following for the directional spreading function.

$$G(\theta,f) \cong \begin{cases} \frac{2}{\pi}\cos^2\theta : |\theta| \le \frac{\pi}{2}, \\ 0 \ : \qquad |\theta| > \frac{\pi}{2}. \end{cases} \tag{2.2}$$

The above function seems to have been introduced by the intuition of oceanographers without any measurement data. The function also assumption is not correct in the light of the detailed ocean wave measurements by Mitsuyasu et al. (1975) and others, but the overall characteristics of directional energy spreading are well described by Eq.(2.2) at least for the wind waves (Goda, 1998).

With many wave measurements in the ocean since the late 1940s, the structure of wave spectrum became gradually known. The frequency spectrum of fully-developed wind waves was given by Pierson and Moskowitz in 1964. The original functional form included the wind speed as a parameter, but in 1970 Mitsuyasu rewrote it with the significant wave height H1/3 and the significant wave period T1/3 as follows:

$$S(f) = 0.257 H_{1/3}^2 T_{1/3}^{-4} f^{-5} \exp\left[-1.05(T_{1/3} f)^{-4}\right]. \tag{2.3}$$

The functional form of Eq.(2.3) is called the Bretschneider-Mitsuyasu spectrum because of the initial contribution by Bretschneider in 1959.

Storm waves generated by strong winds in a relatively small sea area are known to have a feature that the wave energy is concentrated in a narrow frequency range; i.e., the frequency spectrum exhibits a sharp peak. This feature was examined in detail by joint wave observation project in the North Sea. The result of spectral measurements was compiled in a form of modification to the Pierson-Moskowitz spectrum by enhancing the spectral peak, as reported by Hasselmann et al. (1973). The resultant spectral function is called the JONSWAP spectrum after the name of project. The original expression included the wind speed as the parameter, but it has

been rewritten by Goda (1985) with the significant wave height and spectral peak period as follows:

$$S(f) = \beta H_{1/3}^2 T_p^{-4} \exp\left[-1.25(T_p f)^{-4}\right] \gamma^{\exp\left[-(T_p f - 1)^2 / 2\sigma^2\right]} \quad (2.4)$$

Where γ is the peak enhancement factor, f_p the peak frequency, $Tp=1/f_p$, and

$$\beta_j \cong \frac{0.0624[1.094 - 0.01915 \ln \gamma]}{0.230 + 0.0336\gamma - 0.185(1.9 + \gamma)^{-1}} \quad (2.5)$$

$$Tp \cong T_{1/3} / \left[1 - 0.032(\gamma + 0.2)^{-0.559}\right] \quad (2.6)$$

$$\sigma \cong \begin{cases} 0.07 : f \le f_p, \\ 0.09 : f > f_p. \end{cases} \quad (2.7)$$

Hasselmann et al. (1973) reported the peak enhancement factor γ varying between 1 and 7 with the mean of 3.3. Equation (2.4) can also represent the swell spectrum by setting γ=7 to 15 as indicated by Goda (1983) in his analysis of the swell travelling over a distance of 7000 to 9000 km.

Various parameters were developed to describe the width of the spectrum. Well known parameters are ε by Cartwright and Longuet Higgins in 1956, $\kappa(\tau)$ by Battjes in 1974 and ν, which is introduced by Longuet Higgins in 1975. They are defined as follows:

$$\varepsilon = \left[1 - m_2^2 / (m_0 m_4)\right]^{1/2} \quad (2.8)$$

$$\nu^2 = (m_0 m_2 - m_1^2) / m_1^2 \quad (2.9)$$

$$\kappa(\tau) = [(\int_0^\infty S(f)\cos(2\pi f\tau)df)^2 + (\int_0^\infty S(f)\sin(2\pi f\tau)df)^2]^{1/2} / m_0 \quad (2.10)$$

Where;

$$m_n = \int_0^\infty f^n S(f)df \quad (2.11)$$

$\tau = T_m$ and $T_m = \sqrt{m_0 / m_2}$

The peakedness of spectral shape is given by parameter Qp of Goda (1985) Qp is defined as:

$$Q_p = \frac{2\int_0^\infty fS^2(f)df}{m_0^2} \quad (2.12)$$

2.2 Wave Grouping

Although sea waves may look random, inspection of wave records indicates that high waves fall into groups rather than appear individually. Visual observations show that ocean surface waves commonly appear in groups. The existence of wave groups has been known to seafarers for a long time. Out of their experiences have come the saying that 'every seventh wave is large' and old Icelandic saying that 'large waves seldom come alone'. Surf riders are also aware of this phenomenon. They say that 'big waves come in three by three'. Engineers and scientists, however, have neglected this phenomenon until recently, when the phenomenon has been recognized, by a number of events which proved the necessity of taking them seriously in technical sense (Bruun, 1985).

Five decades ago, Tucker identified the presence of waves in the surf zone with periods between 1 and 5 min. and suggested that these long waves were generated by wave groups. Although Tucker noted the importance of

wave groups in the analysis of harbour resonance, wave groupiness did not receive much real attention until the seminal study by Goda(1970).

The analysis of wave groups is complicated. As one is faced with a problem which involves a description of succession of wave heights (periods), it is necessary to work in the time domain (or horizontal space at a given time instant). One type of approach which has been attempted involves a statistical theory of runs, where a run is defined as a sequence of wave heights exceeding some prescribed threshold. Examples of this type of analysis have been presented by Goda (1970), Wilson and Baird in 1972 and by Rye in 1974. Another approach is to work with envelope statistics, where the envelope is defined (for a narrow banded process) as the curve which combines the maxima of the time trace. Approaches along these lines have been attempted by Nolte and Hsu in 1972, Ewing in 1973 and Arhan and Ezraty (1978). Wave groups have also been analysed by means of squaring and smoothing the time trace. Such approaches have been attempted by Funke and Mansard (1979) and Nelson in 1980. Funke and Mansard (1979) introduced the Smoothed Instantenous Wave Energy History (SIWEH) method to estimate the low frequency component of $\eta^2(t)$ in their analyses of the slow oscillations of floating structures. SIWEH is the computation of the distribution of wave energy along the time axis where wave energy would be defined as the square of the water surface elevation averaged over a period which is a function of the peak frequency (Medina et.al 1990).

$$E(t) = \frac{1}{T_p} \int_{-\infty}^{\infty} \eta^2(t+\tau) Q(\tau) d\tau \qquad (2.13)$$

and

$$Q(\tau) = \begin{cases} 1 - \dfrac{|\tau|}{T_p}; |\tau| < T_p \\ 0; |\tau| \geq T_p \end{cases} \qquad (2.14)$$

where Tp is the spectral peak period, $\eta(t)$ the water surface variation, $Q(\tau)$ the triangular data window, and τ the time lag.

Groupiness factor (GF) is defined as the variation coefficient of SIWEH.

$$GF = \sqrt{\frac{1}{Tn}\int_0^{Tn}(E(t)-\bar{E})^2 dt}\,/\,\bar{E}$$
$$\bar{E} = \frac{1}{Tn}\int_0^{Tn} E(t)dt \qquad (2.15)$$

E(t) is Smoothed Instantenous Wave Energy History

Tn= Duration of the wave records

$\bar{E}$ = The time avaraged value of E(t)

Medina et al. (1994) derived the envelope exceedance coefficient, α, which is given as:

$$\alpha = \frac{\alpha'}{E(\alpha')} \qquad (2.16)$$

$$\alpha' = \frac{1}{N}\sum_{n=1}^{N}(\Delta H_n)^2 U(\Delta H_n) \qquad (2.17)$$

$$\Delta H_n = \frac{H(x_0, n\Delta t)}{H_*} - 1 \qquad (2.18)$$

where; $E(\alpha')$= expected value of α'; U( )= Heaviside step function; N= total number of data points in a discrete time sequence; Δt= discrete time interval; $H(x0,n\Delta t)$= wave height function at x=x0; and H*= characteristic wave height. Eq. (2.16) is used to make parameter α' in Eq. (2.17) normalized.

Liu (2000) used wavelet spectrum obtained by wavelets and wavelet transforms for wave grouping analysis. The wavelet spectrum is energy density contours in the two dimensional time-frequency plane. The distinctive energy density parcels in the time-frequency domain of wavelet spectrum can indicate the wave groups. The boundary size of a wave group

can be readily specified in the wavelet spectrum by setting an appropriate threshold energy level.

The Hilbert-Huang Transform (HHT) method for nonlinear and non-stationary time series was applied by Veltcheva (2002) to wave field data from the nearshore area. The frequency-time distribution of the energy, designated as a Hilbert spectrum is utilized for the examination of the sea waves and their group structures.

It has been recognized that wave grouping plays an important role in various fields of coastal and ocean engineering. As it is stated by Goda (1985), the grouping of high waves may influence: 1) long-period oscillation of moored vessels and other floating structures which are subject to irregular waves, 2) surf beat i.e. irregular fluctuation of the mean water level near the shoreline with a period of several minutes, 3) effective number of consecutive waves necessary to produce resonance in structures and capsize ships, 4) stability of armour stones and blocks of sloping breakwaters, and 5) fluctuation of wave overtopping quantity of seawalls.

The effect of spectral shape upon wave grouping (the length of runs) has been demonstrated by Goda (1970) with analysis of linearly simulated irregular waves having various energy spectra and with analysis of field data (Goda, 1983). According to his conclusion, the wave grouping (the length of runs) increases with sharpening in spectral peaks even the scatter of field data is large. Then, this idea became a general assumption among the engineers. However, it is also possible to get the wave time series with same energy spectrum but having totally different wave groupiness. In their study (Ozbahceci et.al, 2002), considering two main properties of wave grouping: 'sequence and exceedance', average values and probability density functions of wave grouping were obtained for different spectral shapes. Thus, the relation between wave grouping and spectral shape is shown in a probabilistic manner.

In many laboratories the waves have been generated using a given spectrum and with random phases. Little work has been done to confirm that the wave groupings so produced are those in real seas (Burcharth, 1979). However, it is quite possible to get wave trains with equal wave spectra but apparently different groupiness. In fact, this may be one reason of contradictory results obtained by different laboratories for the effect of wave grouping on the stability of rubble mound breakwaters.

2.3 Extreme Waves in a Wave Train

The random nature of ocean waves can be observed from field measurements. It can be found that some 13 waves have the height greater than the significant wave $H_{1/3}$ in a continuous record of 100 waves. Those waves are called as extreme waves in this thesis.

Individual wave heights of actual ocean waves which have spectra spreading broad frequency bands, are known to follow the Rayleigh distribution approximately. The distribution of wave heights immediately raises the problem of how to select the design wave height for the designated sea state. The selection depends on the type of structures under design. For rubble mound breakwaters, the wave height was a single value parameter without any clear concept of wave randomness at the beginning. The Hudson formula in 1952 for the minimum weight of armour stones was derived from a series of laboratory tests with regular waves. Engineers tacitly input the significant wave height in the place of wave height H of the Hudson formula (Goda, 1998). But as many laboratories conducted model experiments using irregular wave trains, the problem raised to what definition of wave heights such as $H_{1/3}$, $H_{1/10}$, H_{max} should be used for Hudson formula. However, depending on the design wave selected, the design weight of rubble varies in wide range and many different results have been reported.

Because of wave randomness, any quantity derived from measurements is susceptible to statistical variability. For example, the significant wave height calculated from a record of 100 waves is expected to have a standard deviation of 6 % (Goda,1998). The variability of irregular wave tests would bring some trouble in the judgement of stability of rubble mound breakwaters. Under the same input wave spectrum, some train of irregular waves may exhibit a large fluctuation of instantaneous wave energy, while another train may not show such a fluctuation. By carrying out tests with a sufficient number of wave trains corresponding to a designated duration of storm waves, various degrees of energy fluctuation will be automatically reproduced and the stability (or amount of damage) of a breakwater against storm waves will be revealed in a probabilistic term. Examination of armour stone damage from the probabilistic point of view is needed for establishment of the reliability- based design method (Goda, 1998).

2.4 Stability of Rubble Mound Breakwaters

In 1951 Hudson (Hedar, 1986) modified the Iribarren formula and in 1958 Hudson presented an empirical formula based upon small scale tests. The Hudson equation is given as :

$$W = \frac{\gamma_s H_{D=0}^3}{K_D \cot\alpha \left(\frac{\gamma_s}{\gamma_w} - 1 \right)^3} \qquad (2.19)$$

where:

W	=	Weight of individual armour unit	(N)
γ_s	=	Unit weight of stone	(N/m^3)
$H_{D=0}$	=	Design wave height for zero damage (1% to 5% damage)	(m)
K_D	=	Damage coefficient or empirical stability coefficient	
γ_w	=	Unit weight of water	(N/m^3)
α	=	Angle between breakwater and horizontal	(degrees)

Hudson Formula can be written as following:

$$\frac{H_{D=0}}{\Delta D_n} = (K_D \cot\alpha)^{1/3} \qquad (2.20)$$

where:

Δ = Relative mass density= $(\gamma_s-\gamma_w)/\gamma_w$

D_n = Nominal diameter of stone= $(W/\gamma_s)^{(1/3)}$

The main advantages of the Hudson formula are its simplicity, and the wide range of armour units and configurations for which values of K_D have been derived. The Hudson formula also has many limitations (Meer, 1993). Briefly they include:

Potential scale effects due to the small scales at which most of the tests were conducted,

The use of regular waves only,

No account taken in the formula of wave period or storm duration,

No description of the damage level,

The use of non-overtopped and permeable core structures only.

Due to shortcomings of Hudson formula, researches have been continued in order to obtain a reliable design formulae for the stability of the rubble mound breakwaters.

In 1988, Van der Meer derived two formulas which describe the stability of rubble mound revetments and breakwaters consisting of rock as a first step. The formulae were based upon a series of more than two hundred and fifty model tests which were conducted using irregular wave train (Meer, 1988). The stability formulae derived are:

For plunging waves,

$$\frac{H_s}{\Delta D_{n50}} = 6.2\, P^{0.18}\left(\frac{S}{\sqrt{N}}\right)^{0.2} \xi_z^{-0.5} \qquad (2.21)$$

and for surging waves,

$$\frac{H_s}{\Delta D_{n50}} = 1.0\, P^{-0.13}\left(\frac{S}{\sqrt{N}}\right)^{0.2}\sqrt{\cot\alpha}\;\xi_z^P \qquad (2.22)$$

where:

H_s (m) = Significant wave height at toe of structure

ξ_m = Surf similarity parameter, $\xi_m = \frac{\tan\alpha}{\sqrt{s_m}}$

S_m = Wave steppness, $s_m = \frac{2\Pi H_s}{gT_m^2}$

T_m (s) = Zero up-crossing mean wave period

α = Slope angle

ρ_a (kg/m^3) = Mass density of stone or unit

ρ (kg/m^3) = Mass density of water

D_{n50} (m) = Normal diameter of stone $D_{n50} = \left(\frac{W_{50}}{\rho_a}\right)^{1/3}$

P = Permeability coefficient of the structure

S = Damage level, $S = \frac{A}{D_{n50}^2}$

A(m^2) = Erosion area in a cross-section

g(m/s^2) = Gravitational acceleration

N = Number of waves (Storm duration)

During the last decade, a controversy has surfaced regarding especially the correlation of wave groupiness with damage to breakwater armour layers. While wave steepness and storm duration have been correlated with damage to breakwater armour layers, contradictory results have been presented regarding the influence of wave groupiness.

Johnson et al., (1978) reported that grouped waves caused worse damage to dolos blocks than non-grouped waves even when their significant wave heights and spectra were the same.

Burcharth (1979) conducted several experiments to determine run-up and run-down and block stability for a 1 in 1.5 slope protected by dolos blocks. The model was subjected to the three different wave patterns. Pattern 1 is a regular sine wave which can be regarded as a reference. Pattern 2 consists of a big wave followed by a small wave and it was chosen because one might accept large wave run-up values due to minimum backwash from the proceeding small wave. Pattern 3, a strongly grouped wave train made of two sine waves. Degree of damage is defined as blocks start rocking, few blocks start moving armour layer remains stable and slow breakdown of armour layer.

As the normal design conditions for a dolos armour layer is chosen between degrees of damage 2 and 3, in those cases, wave pattern 2 is the most critical according to the result of the experiments. Therefore it was concluded that a jump in wave heights where a small wave is followed by a big wave has a significant effect.

Bruun (1985) strongly emphasized the influence of wave groupiness on armour damage. However, The Shore Protection Manual (SPM 1984) describes a conventional, emprical-based design for breakwater armour layers using $H_{1/10}$ as representative of extremely irregular wave action. Storm duration, mean wave period, wave steepness and wave groupiness are not considered in the SPM design methodology; instead physical modeling is recommended for a cost effective design of rubble mound breakwaters.

Sawaragi et al (1985) investigated the effects of the grouping characteristics of irregular waves to the stability of rubble mound structures by model testing using 7 kinds of simulated irregular waves, which have different spectrum shapes.

In their study, it is said that the run length is only number of waves satisfying a certain wave condition, and it is not adequate to use as a parameter of external force of group formed waves and a new parameter which can represent the grouping wave force called as run-sum is proposed. Run-sum means the energy sum of a run satisfying a critical wave condition. Based on the experiment result it was found that the run-sum of the conditional run of ζ^*_0 under the condition of critical wave height H_c was the most suitable parameter to express the destruction process of rubble mound structures, where ζ^*_0 is a breaker index on the steep slopes as expressed which the value lies between 1.5 and 2.5. ($\xi = \tan\theta / \sqrt{H/L}$, $\xi_o = 2.65\tan\theta$). Also it was found that run sum is the most closely correlated parameter to spectrum peakedness parameter Q_p among the various grouping definitions. Using the correlations between Q_p, run-sum of grouping waves, and percentage of destruction, a new design method in which the irregular wave force, the allowable percentage of damage, and effect of wave period on the stability are directly taken into account was developed.

Van der Meer (1988) used the parameter κ to describe the width of the spectrum since κ can be computed in both the time and frequency domain even it was shown that κ calculated in time domain is consistently larger than it is calculated from time domain. He used three spectra of a very narrow spectrum, a Pierson Moskowitz spectrum and a rather wide spectrum with almost the same significant wave height and average period. The value of κ increased as spectrum became narrower. The test series with a slope angle of $\cot\alpha$=3 was performed with all of three spectrums and it was concluded that there was no significant correlation of spectral shape with armour damage.

T. Okuno, H. Uji-ie, M. Sawamoto (1989), studied the effect of wave grouping on the tetrapod block stability under non-breaking and breaking wave conditions in the non-resonant region of 3.5< ξ <7. The relationship between the wave irregularity and block stability was also investigated. A summary of the results is as follows:

1-Wave grouping causes instability in armor units, facilitating their removal from the armor layer.
2-The damage probability to blocks from a single wave group depends on the degree of its groupiness. Existence of a high wave such as a maximum wave or 1/10 maximum wave in a wave train does not necessarily result in high damage probability; the grouping of successive high waves more effectively increases the damage probability.
3-The wave grouping contributes more significantly to block instability under non-breaking wave conditions, because the structure of a wave group collapses as waves break and the power of successive attacks on an armor layer is reduced except for waves just breaking on the breakwater slope.
4-The mean run-length of incident irregular waves is related to the block stability and wave grouping brings about more serious disturbance of blocks.

Their study indicated that both non-breaking and breaking wave sequences could affect the block stability, but non –breaking wave sequence would have greater influence.

Kevin R. Hall, (1994) assessed the effect of wave groups on the stability of berm breakwaters in a two-dimensional wave flume. Profiles of the structure during the various stages of reshaping were measured using a profiler developed for this study. Four gradations of armour stones were used, giving a range of uniformity coefficients (D_{85}/D_{15}) of 1.35-5.4. Groupiness was determined using the method of Mansard and Funke (groupiness factor, GF). The volume of stones and the initial berm width required for development of a stable profile and the extent to which the toe of the structure progressed seaward were chosen as representative parameters of the reshaped breakwater. These parameters were found to be insensitive to changes in wave groupiness factor ranging from 0.5 to 1.1. Therefore it was concluded that wave groupiness does not have significant effect on the reshaping of dynamivally stable breakwaters.

Josep R. Medina (1994) analyzed the effects of wave groups on damage to the armor layer for nonovertopped, rubble mound breakwaters by a large-

scale experiment. Two independent wave grouping parameters were evaluated in the experiment: (1) The mean run length correlated with the spectral peakedness parameter γ; and (2) an envelope exceedance coefficient α, correlated with a wave height function H(x,t) given in Eq.(2.16)-(2-18).

The observed damage levels of the armour layer were found to be correlated with α; on the contrary, no significant correlation was found between armor damage and spectral peakedness parameter γ, or mean run length. Because only 224 damage observations were obtained, the experiment did not allow for a complete and reliable modelling of the armour response under wave group attack. According to his conclusion, the positive correlation between the envelope exceedance coefficient α and armour damage may be of the same order of magnitude as the storm duration, and should be considered in both preliminary designs and in analyses of experimental data for armour damage from random waves.

CHAPTER 3

EFFECT OF WAVE GROUPING AND SPECTRAL SHAPE

3.1 Definition and Properties of Spectral Shape And Wave Grouping

3.1.1 Spectral shape

The wave spectrum describes how the wave energy is spreading over a range of frequency and that of direction. The distribution of wave energy over the frequency is represented by the frequency spectrum S(f). Frequency spectrum model for sea waves can be formulated as follows:

$$S(f) = \beta H_{1/3}^2 T_p (T_p f)^m \exp[-(m/n)(T_p f)^n] \gamma^{\exp[-(T_p f - 1)^2 / 2\sigma^2]} \quad (3.1)$$

where γ is the peak enhancement factor, f_p is the peak frequency, $T_p=1/f_p$, m and n are the coefficients which determine the high, and low frequency slopes of the spectrum, respectively, and

$$\beta \cong \frac{0.0624}{0.230 + 0.0336\gamma - 0.185(1.9 + \gamma)^{-1}} \quad (3.2)$$

$$\sigma \cong \begin{cases} 0.07 : f \le f_p, \\ 0.09 : f > f_p. \end{cases} \quad (3.3)$$

It is possible to get wave energy spectrum in different shapes by changing the parameters in the Eq. (3.1). Spectral shapes used in this study are listed in Table (3.1) and shown in Fig. (3.1).

Table 3.1 Spectral Shapes Used in Simulations

Spectrum Shape	γ	m	n	ν	$\kappa(T_m)$	Q_p
I- PM (Pierson Moskowitz)	1	-5	-4	0.403	0.422	2.00
II- J33 (JONSWAP)	3.3	-5	-4	0.371	0.565	3.14
III- J10 (JONSWAP)	10	-5	-4	0.310	0.724	5.62
IV- W (Swell)	10	-8	-8	0.127	0.854	8.25

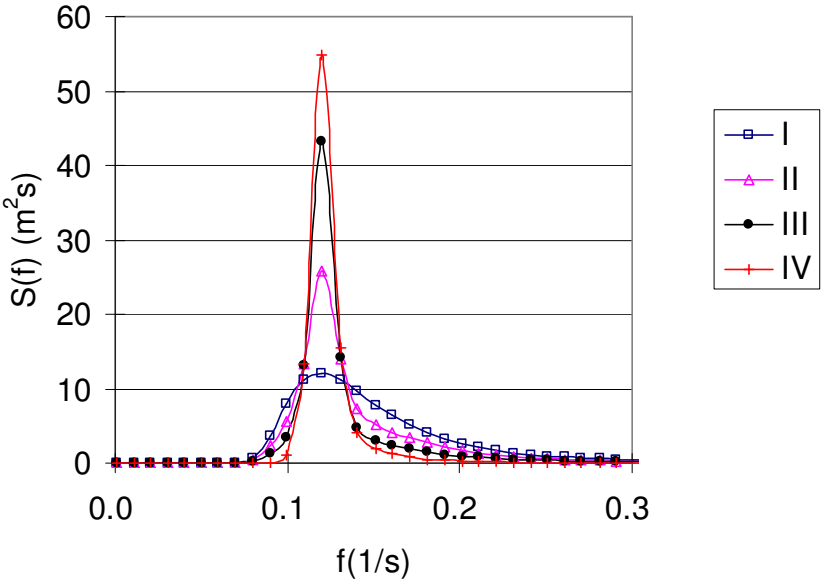

Fig. 3.1 Spectral shapes given in Table 3.1 (H1/3=4m. T1/3=8sec)

These four shapes of energy spectrum were chosen since they are very popular among the engineers and also in order to investigate the effect of spectral shape from broad to very narrow and sharp one. In this study, narrowness of the spectral shape is given in Table (3.1) by two parameters: one is,ν, by Longuet Higgins and the other parameter is $\kappa(\tau)$ introduced by Battjes. Their definitions are given in Eq.(2.9) and Eq.(2.11), respectively. Sharpness of spectral shape is given by parameter Qp of Goda defined in Eq. (2.12).

Calculated values of these three parameters listed in Table (3.1) show that spectral shape becomes narrower and sharper from spectrum I to IV. During the calculation of the above parameters, integration limit was taken as eight times of f_p in order to avoid from the effect of upper integration limit.
Spectral shape IV can represent swell having travelled over a long distance. Because according to swell analysis by Goda (1983), the peak enhancement factor, γ should be taken at the value of 8-9 on the average. Moreover, the slope of wave spectrum at the higher frequency side (m in this case) varies from -4.4 to -10.9.

3.1.2 Wave Grouping

Basic definition of a wave group can be given as the sequence of high waves in a wave train. Up to now, many parameters and different methodologies have been used to characterize wave groups. In fact, even it can be understood from the above simple definition, wave grouping has two main properties. One of them is '*sequence*' which shows the loneliness of the high waves, i.e. a high wave comes alone or it is accompanied by the other high waves. In this study, the mean run length defined by Goda (1985) is used to check sequence property of wave grouping. According to his definition, the *run length* is the number of waves exceeding a specified value of the wave height H_c ($H_{1/3}$ in this study) without falling below that height. A succession of such high waves is called as a *run* of high wave heights. *Mean run length (mrl)* is the sum of run lengths divided by number of runs in a wave series. An example of calculation of mrl is given here. Fig. 3.2 is the plot of 250 sec duration of an example surface profile. It is possible to calculate individual wave heights by zero-up crossing method using surface profile data. The individual wave heights calculated from whole surface profile are given in Fig. 3.3. Significant wave height ($H_{1/3}$) which is specified to calculate mrl is 4m and it is plotted on the same figure, also. As it can be seen from Fig. 3.3, there are 20 waves with heights higher than $H_{1/3}$ and 8 runs whose lengths are between 1 and 8. Thus, mrl is calculated as 20/8=2.5.

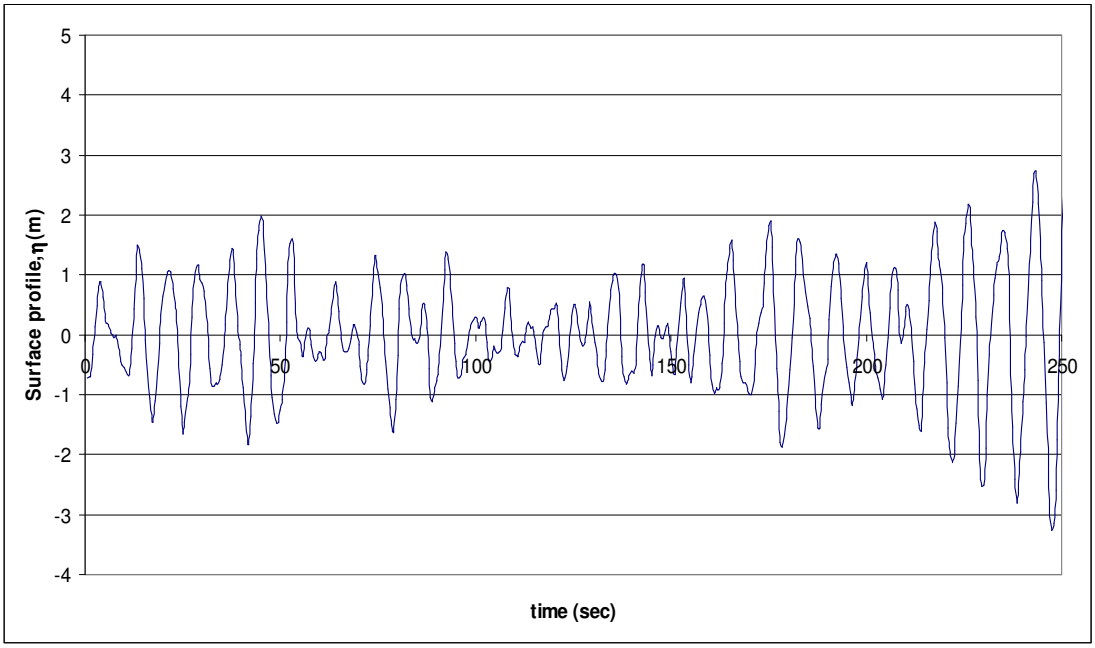

Fig. 3.2 An example of Surface Profile

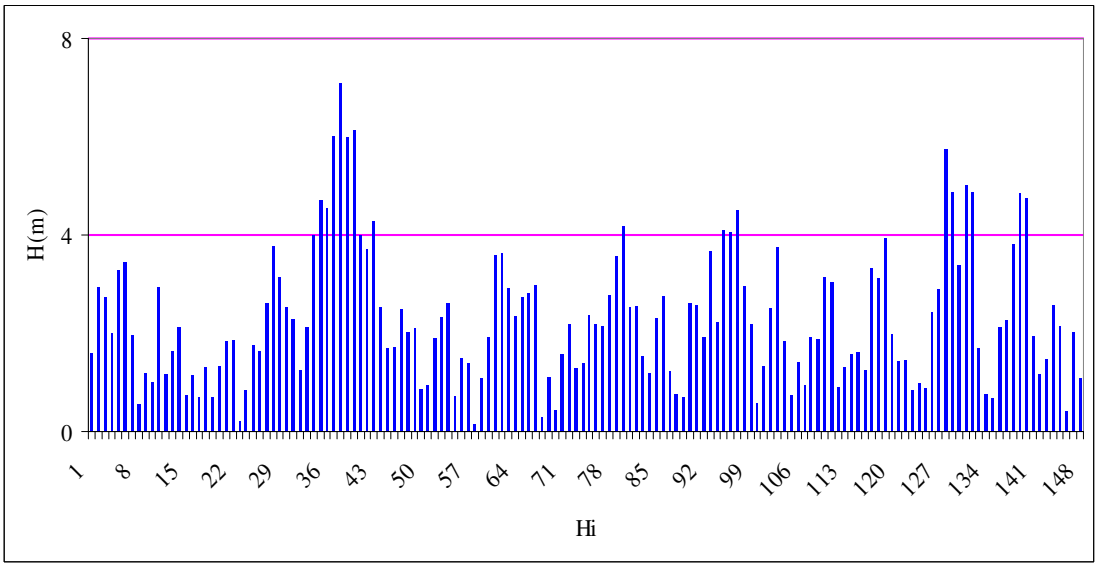

Fig. 3.3 Individual wave heights calculated by zero-up crossing method

The other property is '*exceedance*' which shows the how high the waves are in a group. Especially, from the structural stability point of view, this property is very important because it gives an idea about the grouping wave force, which is necessary to discuss the stability of the structures. The run length

is only the number of waves satisfying a critical wave condition and it is not adequate for that purpose (Sawaragi et al., 1985). Since the flux of wave energy is approximately proportional to square of wave height, it will be meaningful to use a parameter related with that one. In order to check exceedance property, wave grouping parameters like Groupiness Factor, GF, by Funke and Mansard (1979) and envelope exceedance coefficient,α, by Medina et al.(1994) can be used.

Focusing on the results of the past researches, it can be noticed that while no significant correlation was found between either the spectral shape or the mean run length parameters and armour damage, wave grouping parameters like Groupiness Factor, GF, by Funke and Mansard (1979) and envelope exceedance coefficient,α, by Medina et al.(1994) were found to be correlated with armour damage.

Both GF and α are the parameters which indicate how high the waves are in a group rather than length of the group. Vidal et al. (1995) found in their numerical study that there is a strong correlation between GF and extreme wave parameters like $H_{1/10}$, $H_{1/20}$, $H_{1/100}$ under the same $H_{1/3}$ condition. Similar numerical investigation is done for the exceedance parameter,α. Characteristic wave height is taken as $H_{1/10}$ in the simulations. According to the results as they are shown in Figure 1 and 2, the value of α is highly correlated to $H_{1/20}$ and $H_{1/100}$ similar to the parameter GF.

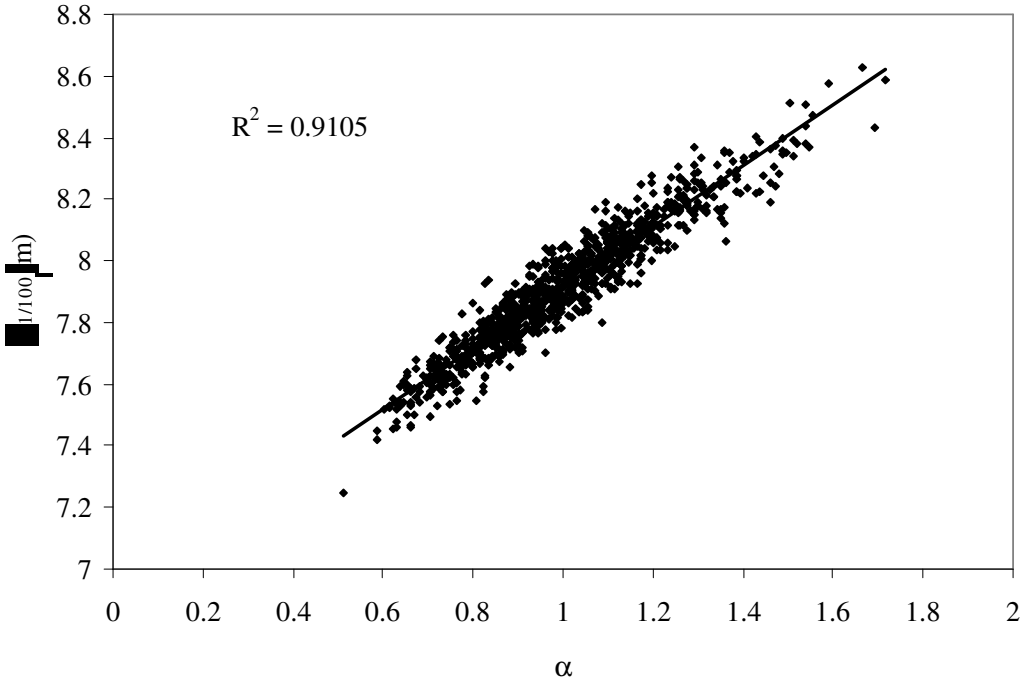

Fig. 3.4 Correlation between Exceedance Parameter of Medina, α and $H_{1/100}$

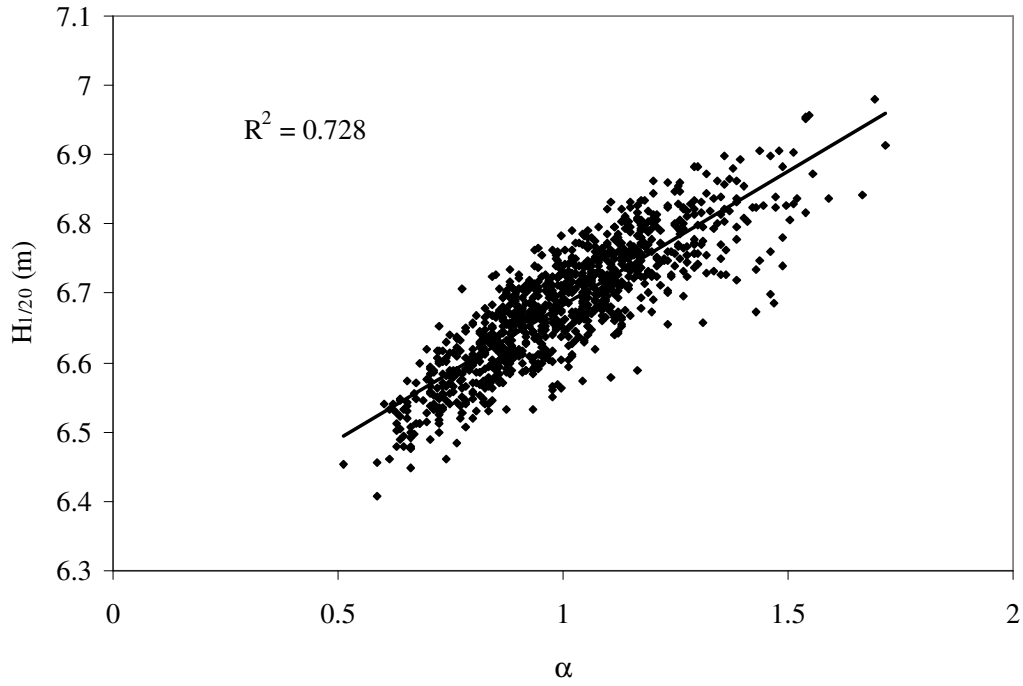

Fig. 3.5 Correlation between Exceedance Parameter of Medina, α and $H_{1/20}$

Therefore it has remained as a question up to now that a decrease in the armour stability is due to sequence of high waves which may be related to narrow banded spectrum or due to only high waves even they come alone. This study tries to find an answer to that question by means of hydraulic model experiment.

Regarding Figs. 3.4 and 3.5, it will be better to consider α' (non-normalized form of α) as a parameter for evaluating the effects of the individual highest waves in a random wave train (such as waves equal or higher than $H_{1/3}$, named as extreme waves in this study) rather than a grouping parameter.

In order to study the effect of high waves forming a group, another parameter called modified exceedance parameter (Exc2) is redefined which isolates the effect of an individual high wave coming as a single wave not within a group. The modified exceedance parameter (Exc2) used in the analysis is given as:

$$Exc2 = \frac{1}{N}\sum_{n=1}^{N}(\Delta H_n)^2 U_2(\Delta H_n) \tag{3.4}$$

$$\Delta H_n = \frac{H_n}{H_*} - 1 \tag{3.5}$$

$$U_2(\Delta H_n) = \begin{cases} 1; & H_i \text{and} H_{i+1} > H_* \\ 0; & \text{otherwise} \end{cases} \tag{3.6}$$

where; U( )= Heaviside step function; N= total number of waves; H_n= nth wave height ; and H_*= a characteristic wave height ($H_{1/3}$ in this case)

Similar to modified exceedance parameter, modified mean run length (mrl2) is redefined. For modified mean run length a run is counted if at least two succeeded waves exceed wave height $H_{1/3}$. Those modifications are done to separate the effect of isolated high waves from the groups of high waves. Therefore now it would be possible to make it clear that if there is an effect to the damage, it is due to high waves even they come alone or they are effective if they come as group.

In order to check extreme waves in an irregular wave train defined as the waves whose heights are higher than $H_{1/3}$ in this case, the parameter, $\alpha_{extreme}$ is proposed. It is given as:

$$\alpha_{extreme} = \frac{1}{N}\sum_{n=1}^{N}(\Delta H_n)^2 U(\Delta H_n) \tag{3.7}$$

$$\Delta H_n = \frac{H_n}{H_*} - 1 \tag{3.8}$$

Extreme wave parameter $\alpha_{extreme}$ is very similar to the envelope exceedance parameter of Medina et al.(1994). But in this case instead of wave height function, individual wave heights determined by zero-upcrossing definition are used.

3.2 Hydraulic Model Experiments

3.2.1 Experimental Set-up

A model of rock armored rubble mound breakwater with 1:1.5 slope was installed inside the wave channel of hydraulic laboratory of the Disaster Prevention Research Institute of Kyoto University. The experimental set-up is shown in the Fig. 3.6 as schematically. Time series, approximately equal to 1000 waves, with similar wave height statistics but different degrees of wave grouping and spectral shape were first generated numerically then they were inputted to the wave generator. Four different shapes of energy spectra as given in Table 3.1 were used.

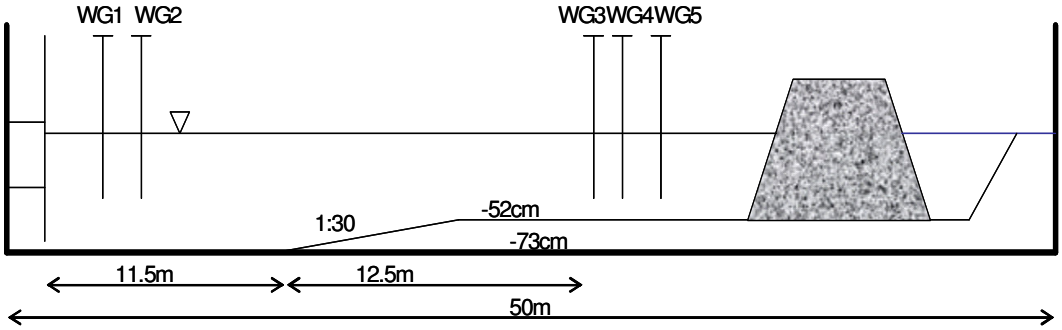

Fig. 3.6 Experimental set-up in the wave channel

Model cross-section is given in Fig. 3.7. The model is consisted of a permeable core layer, a filter and armour layer with two stones thicknesses.

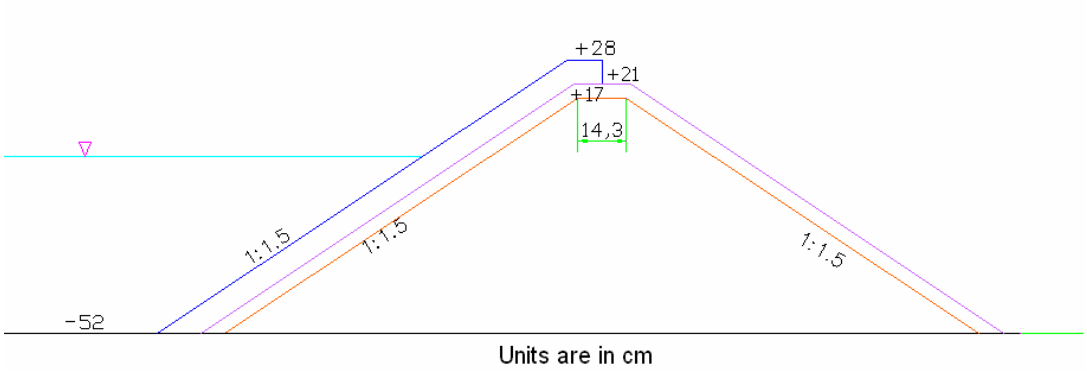

Fig. 3.7 Cross-section of the model with the slope of 1:1.5

Mass distributions of armour, filter and core layer stones are given in Fig. 3.8-3.10, respectively.

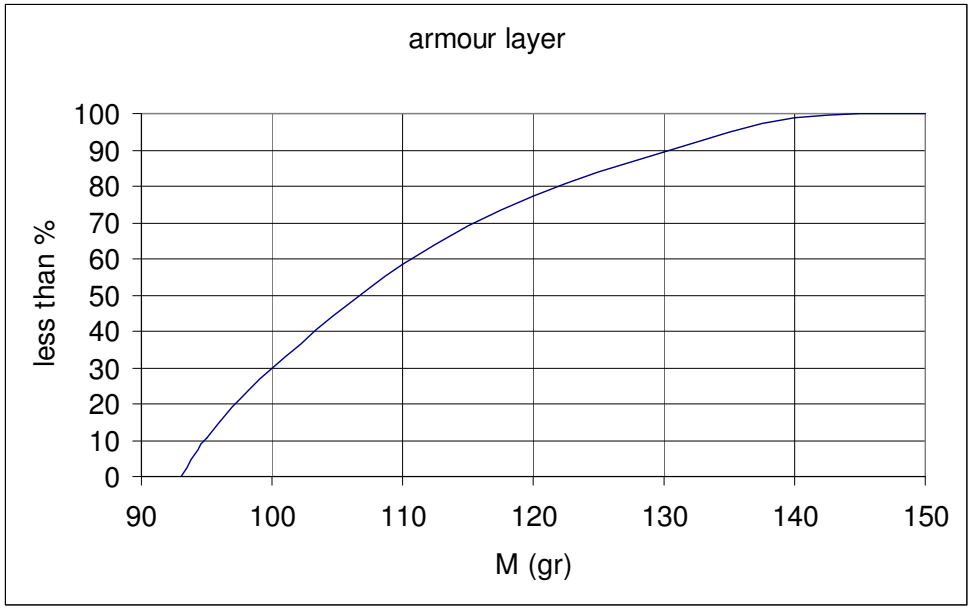

Fig. 3.8 Mass distribution of armour layer stones

According to the Fig. 3.8, M_{50}= 107 gr, M_{15}=96 gr and M_{85}=125.5 gr for armour stones. Mass density of the stone, ρ, is 2.64t/m^3. Then D_{n50}, D_{n85} and D_{n15} are calculated as 0.034, 0.036, 0.033, respectively using Eq.(2.20). D_{n85} / D_{n15}= 1.1 which indicates the uniformity of armour stones.

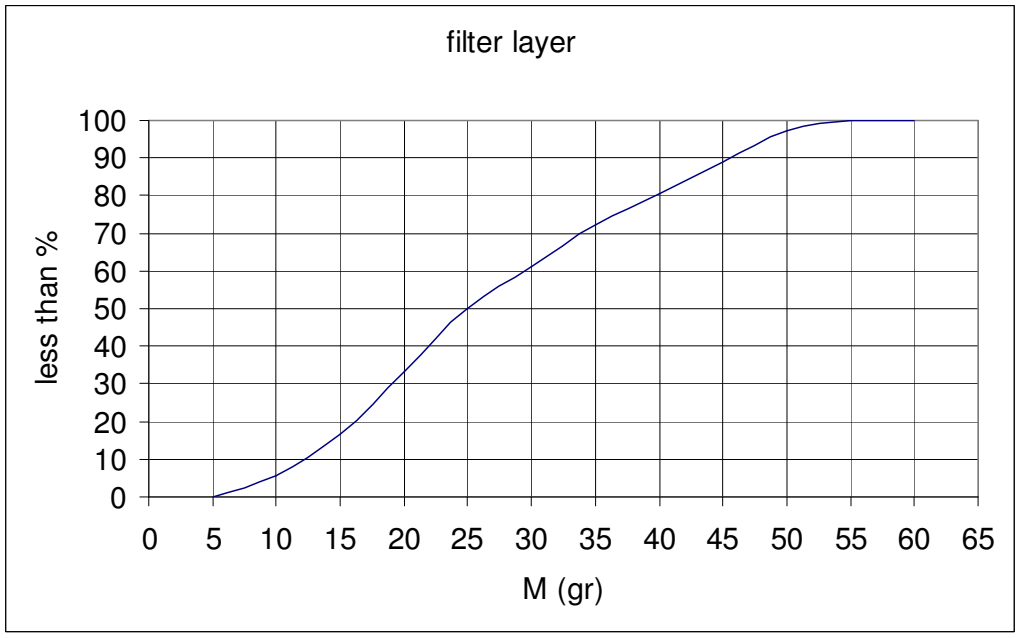

Fig. 3.9 Mass distribution of filter layer stones

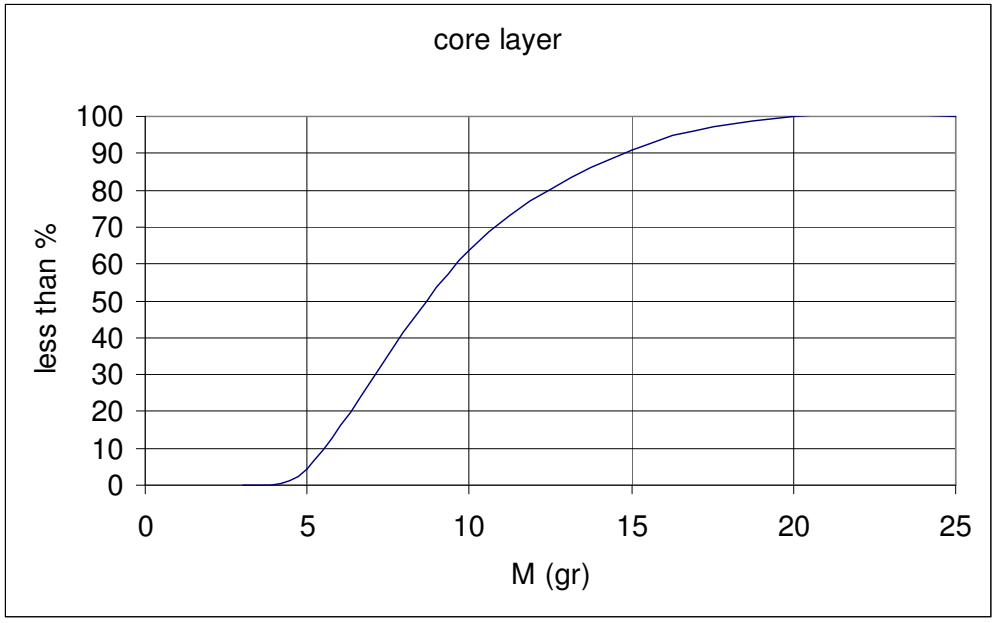

Fig. 3.10 Mass distribution of core layer stones

As it can be seen in Fig. 3.9 and Fig. 3.10, M_{50}= 25 gr for filter stones and it is 8.5 gr for core layer stone. Therefore, D_{n50} is calculated as 0.021m and 0.0148m for filter and core layer stones, respectively using Eq.(2.20). $D_{n50(armour)}/ D_{n50(filter)}$=1.62 and $D_{n50(armour)}/ D_{n50(core)}$=2.33.

3.2.2 Wave Generation

For numerical generation of wave time series, Deterministic Spectral Amplitude (DSA) model with FFT algorithm was used. It is possible to get different time series with a same target spectrum in DSA model by setting up the target spectrum and using random numbers for phase angles. The simulation procedures for the DSA model are summarized by the following: (Tuah et al., 1982)

1- Generation of a sequence of random phase angles, θ_n, which are uniformly distributed in the interval [0, 2π]

2- Computation of A_n by

$$A_n = N[0.5S(f)\Delta f]^{1/2} \exp + i\theta n \tag{3.9}$$

in which S(f) is the target wave energy spectral density at frequency f, f=(n-1)Δf; n=1,2,…,N; N= total data number which should be equal to 2^m, t=jΔt; j=1,2,…,N, and $\Delta f \Delta t = N^{-1}$

3- Synthisization of the sequence A_n by inverse FFT to obtain discrete time sequence, $\eta(j)$ according to Eq. 5

$$\eta(j) = N^{-1} \sum_{j=1}^{N} A_n \exp i\left[\frac{2\pi(n-1)(j-1)}{N}\right] \tag{3.10}$$

DSA model is a linear algorithm. Comparisons of statistics of wave groups observed in the field with those predicted by numerical simulations demonstrate that wave group statistics are not inconsistent with a linear, Gaussian sea surface except surf zone (Goda, 1983; Elgar et al. 1984, Liu et al. 1993).

It is possible to generate thousands of time series with different wave grouping and wave statistics by DSA model. After choosing appropriate time series, those are inputted to the wave generator.

3.2.3 Experiment Cases

In the experiments, four different time series with same significant wave height, period ($H_{1/3}$=10.8cm, $T_{1/3}$=1.9sec) and $\alpha_{extreme}$ (0.007) but with different spectral shapes of PM, J33, J10 and W were generated and named Case 1. Spectrum shapes were defined as earlier. The test belong to each spectral shape was repeated three times e.g. PM1, PM2, PM3.

In the experiments named Case 2, again four different time series with same significant wave height, period ($H_{1/3}$=10.8cm, $T_{1/3}$=1.9sec) and $\alpha_{extreme}$ but with different spectrum shapes were generated. In Case 2, significant wave height and period were same as those in Case 1, but $\alpha_{extreme}$ =0.0105, higher than the Case1.

In Case3 and Case 4 were similar to Case1 and Case, respectively, but significant wave height and period changed ($H_{1/3}$=13.0cm, $T_{1/3}$=2.1sec) while wave steepness kept as almost same as in the Cases 1 and 2. Experiment cases are tabulated in Table 3.2.

Table 3.2 Experiment Cases

Case no	$H_{1/3}$	$T_{1/3}$	Spectrum	$\alpha_{extreme}$	Test no
1	10.8	1.9	PM	0.007	3
1	10.8	1.9	J33	0.007	3
1	10.8	1.9	J10	0.007	3
1	10.8	1.9	W	0.007	3
2	10.8	1.9	PM	0.0105	3
2	10.8	1.9	J33	0.0105	3
2	10.8	1.9	J10	0.0105	3
2	10.8	1.9	W	0.0105	3
3	13.0	2.1	PM	0.007	1
3	13.0	2.1	J33	0.007	1
3	13.0	2.1	J10	0.007	1
3	13.0	2.1	W	0.007	1
4	13.0	2.1	PM	0.0105	1
4	13.0	2.1	J33	0.0105	1
4	13.0	2.1	J10	0.0105	1
4	13.0	2.1	W	0.0105	1

3.2.4 Wave Recording and Analysis

After the generation of waves started, waves were recorded with 8192 data with dt=0.16 sec. Since the absorption mode of wave generator was used, multi reflection due wave generator was decreased but there was reflection due to model in the channel. Therefore, it was compulsory to separate incident waves from reflected waves. Incident wave energy spectrum was obtained by using the separation method introduced by Goda and Suzuki (1976). Three wave gauges in front of the model were used for the separation. After incident wave spectrum was obtained, incident wave train was formed by inverse FFT method. Then individual wave heights were determined by zero-up crossing method by using incident wave train. Finally, wave grouping parameters of mrl, mrl2, Exc2 and extreme wave parameter $\alpha_{extreme}$ were computed.

As it is shown in Fig. 3.11, spectral shape becomes narrower and sharper from PM to W. Wave grouping parameters of mrl, mrl2 and Exc2 increase from PM to W as indicated in Figs. 3.12, 3.13 and 3.14, respectively. In Fig. 3.15, measured wave heights $H_{1/3}$, $H_{1/10}$, $H_{1/20}$, spectral significant wave height H_{m0} and wave period $T_{1/3}$ are plotted for each test. In all of these Figs. 3.12, 3.13, 3.14 and 3.15, it is seen that wave grouping is pronounced from PM to W while significant wave height, period and $\alpha_{extreme}$ are almost similar.

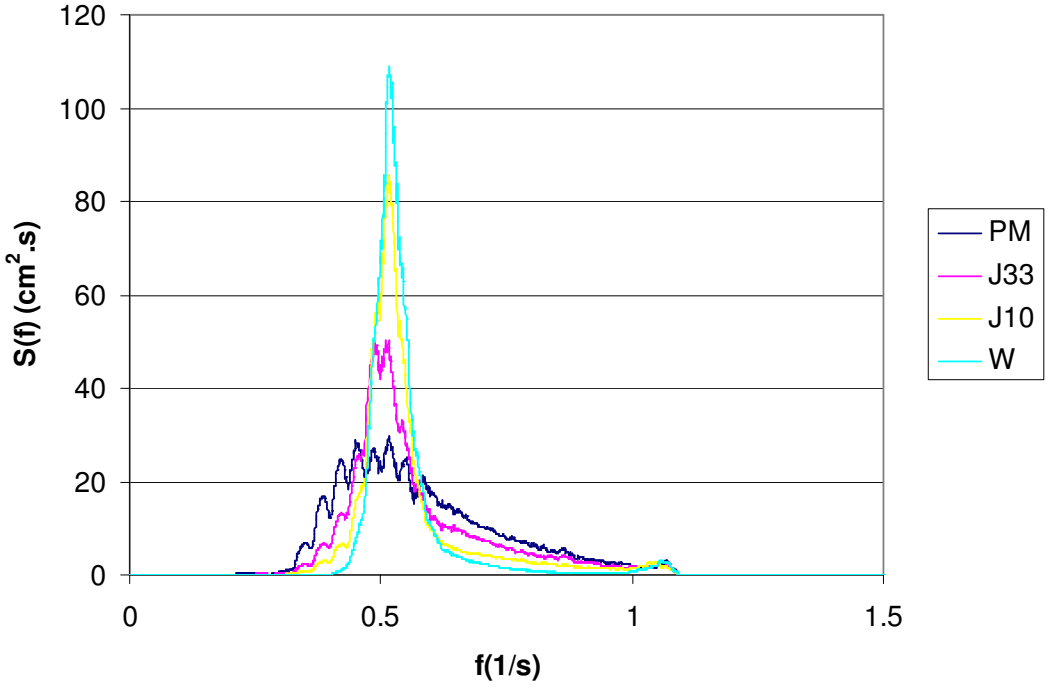

Fig. 3.11 Incident wave spectras obtained during the experiment Case 1

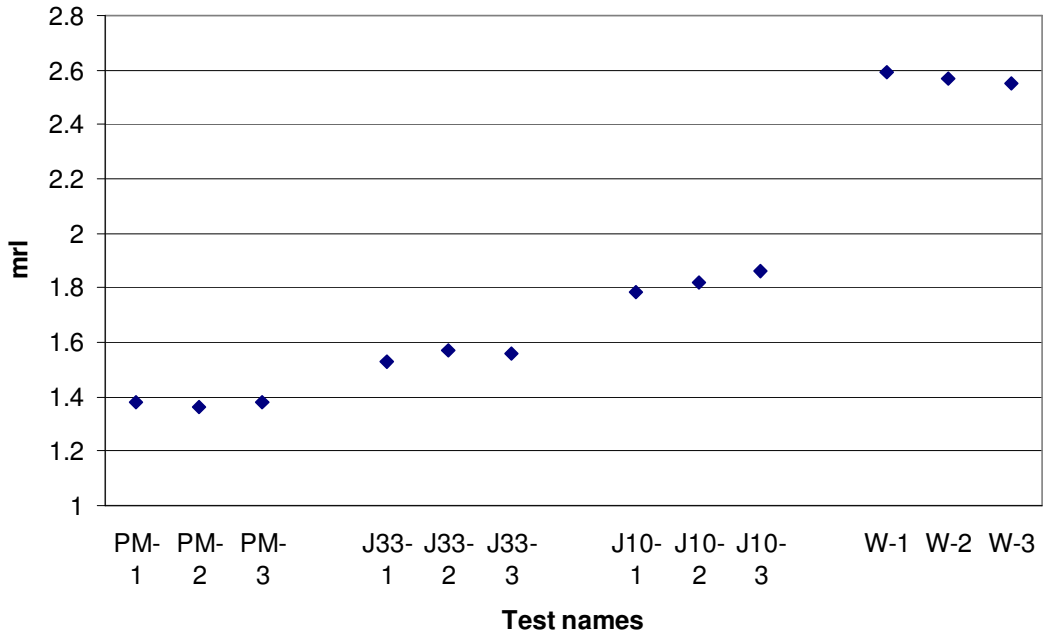

Fig. 3.12 Measured mean run length (mrl) of generated time series belongs to different type of wave spectra

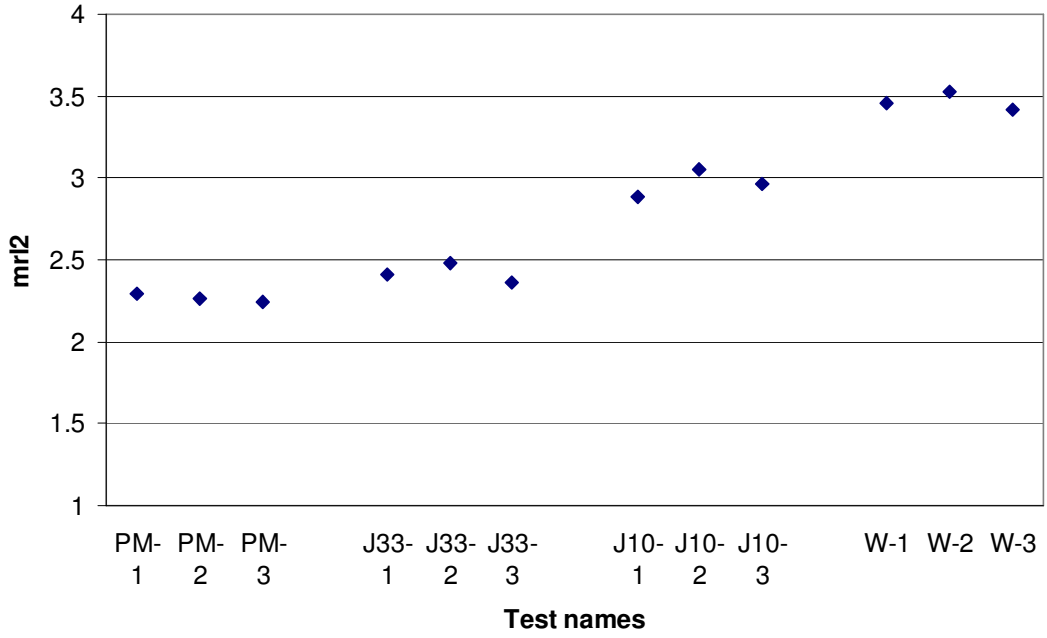

Fig. 3.13 Measured modified mean run length (mrl2) of generated time series belong to different type of wave spectra

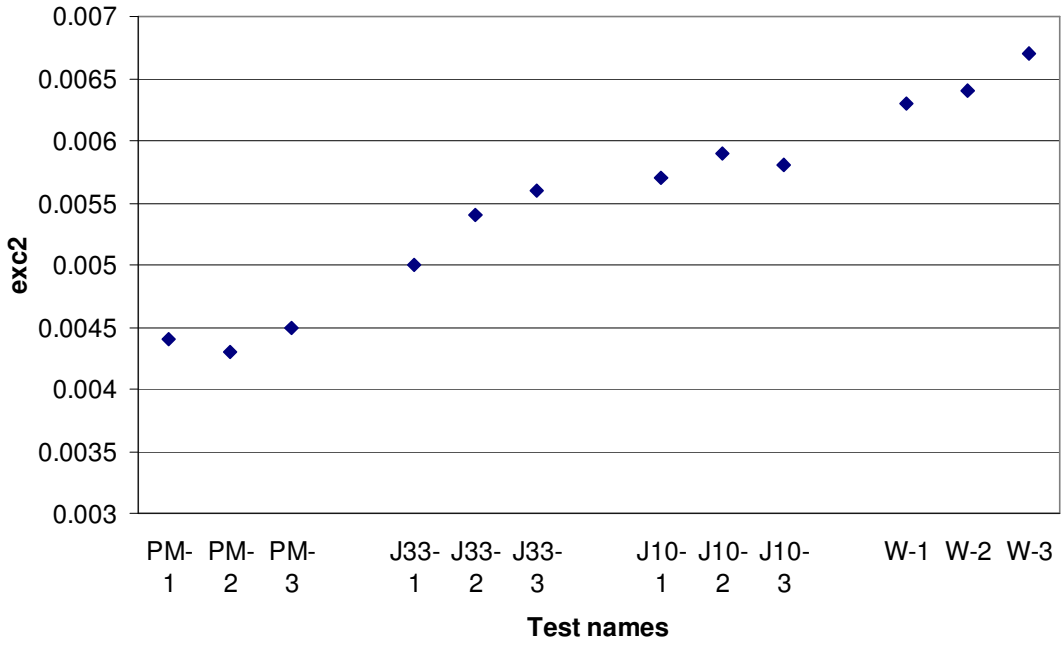

Fig. 3.14 Measured exc2 parameter of generated time series belong to different type of wave spectra

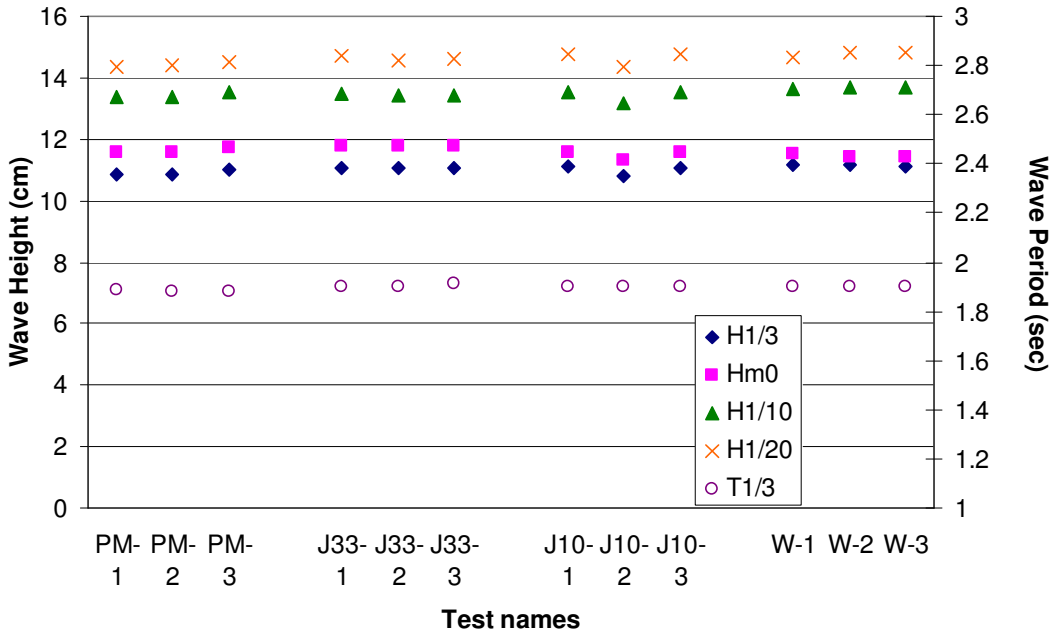

Fig. 3.15 Measured wave heights and wave period in each test

3.2.5 Damage Definition

After each test damage to the breakwater was calculated. Van der Meer's (1988) definition of damage was used in the calculations as:

$$S = A_e / D_{n50}^2 \qquad (3.11)$$

where; A_e= Eroded area, $D_{n50=}$ nominal diameter of armour stone

In order to get eroded area, the profile of armour layer was measured by laser equipment through nine lines along the section. Laser equipment is a sophisticated profiler but it requires the wave flume to be either fully drained or fully flooded so that measurements are made in either the dry or in the wet so measurement through the air-water interface is difficult. During the experiments, the flume was drained after completion of each test which was very time consuming. After the profile was measured the model armour layer was re-constructed for each test.

Laser profiler was put on an automatically controlled carriage which moves in the track on the top of flume wall. While laser profiler was measured the profile along the section, horizontal position of carriage was also being recorded. Data interval was 0.5 cm. Therefore, one armour stone with diameter 3.4 cm was recorded by almost 7 data. One measurement line starts from the almost crest level of the model and continued up to toe of the model. After finishing measurement of one line, laser profile was moved to the next position (dx= 9 cm) automatically and the next line was measured. Total measurement distance was 72 cm which was centred on 100cm channel width. The remaining part was not measured because of possible side wall effect. During the measurements, it was determined that the error in the reading of laser profiler was in the order of 10^{-1} cm. Measurements were done before wave generation and after the storm. Then eroded area was calculated for each line and then the resulted damage level was computed from the average eroded area of nine lines using Eq. 3.11. During eroded area calculation, differences in the profiles of before and after the storm due small sliding or settlement were ignored. An example of profile plots of before and after the storm was given in Fig. 3.16. As it can be seen from Fig. 3.16, maximum erosion occurs near SWL.

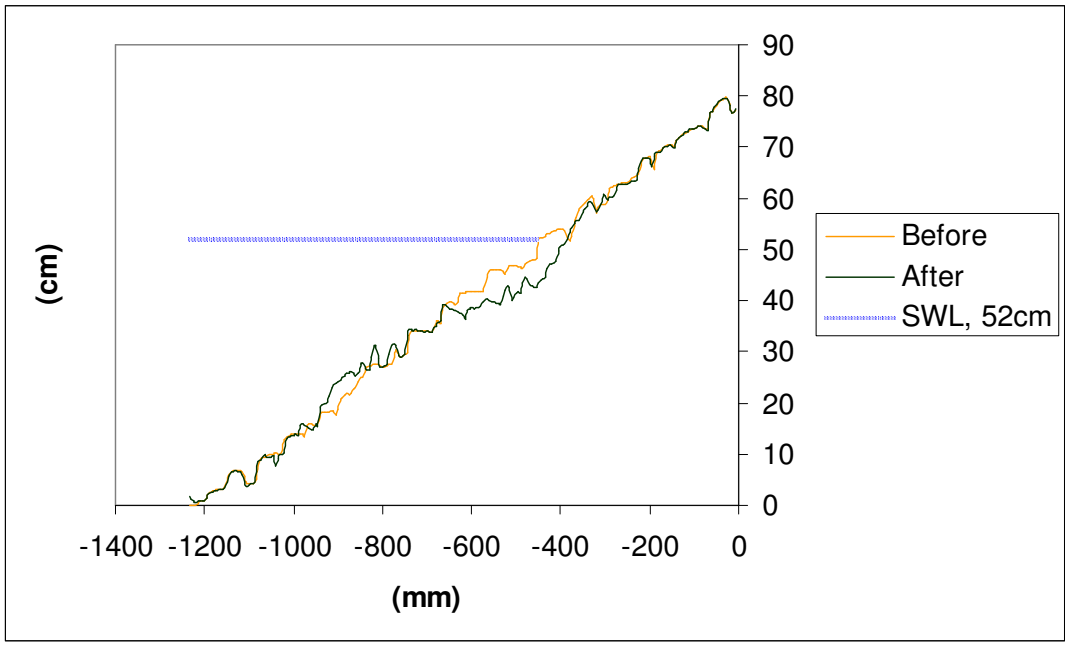

Fig. 3.16 An example of profile plots of before and after the storm

3.2.6 Results and Discussions

Damage results of Case 1 are shown in Fig. 3.17. As it can be seen from the figure, there is no such a tendency that the damage increases as spectral shape becomes narrower or wave grouping is pronounced.

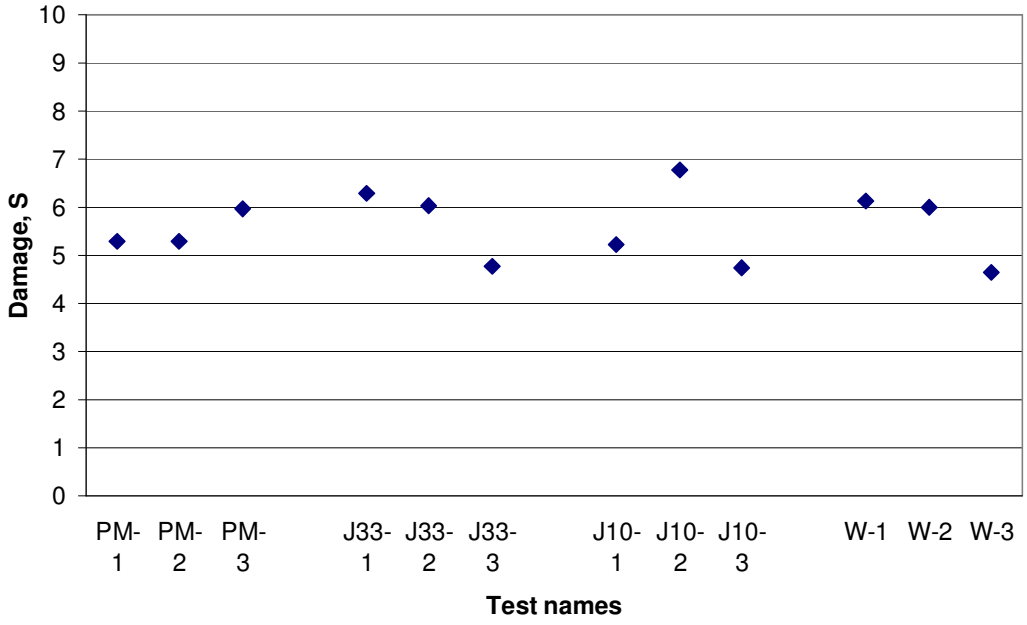

Fig. 3.17 Damage result of waves with different wave spectra (Case 1)

In Case 2 significant wave height and period were same as those in Case 1, but $\alpha_{extreme}$ =0.0105, higher than the Case1. Therefore extreme wave heights in the trains of are higher than the first case. Wave grouping parameters of mrl, mrl2 and Exc2 of Case 2 increase from PM to W same as it is in the Case 1. In Fig. 3.18 damage results are plotted together with the results of the first case.

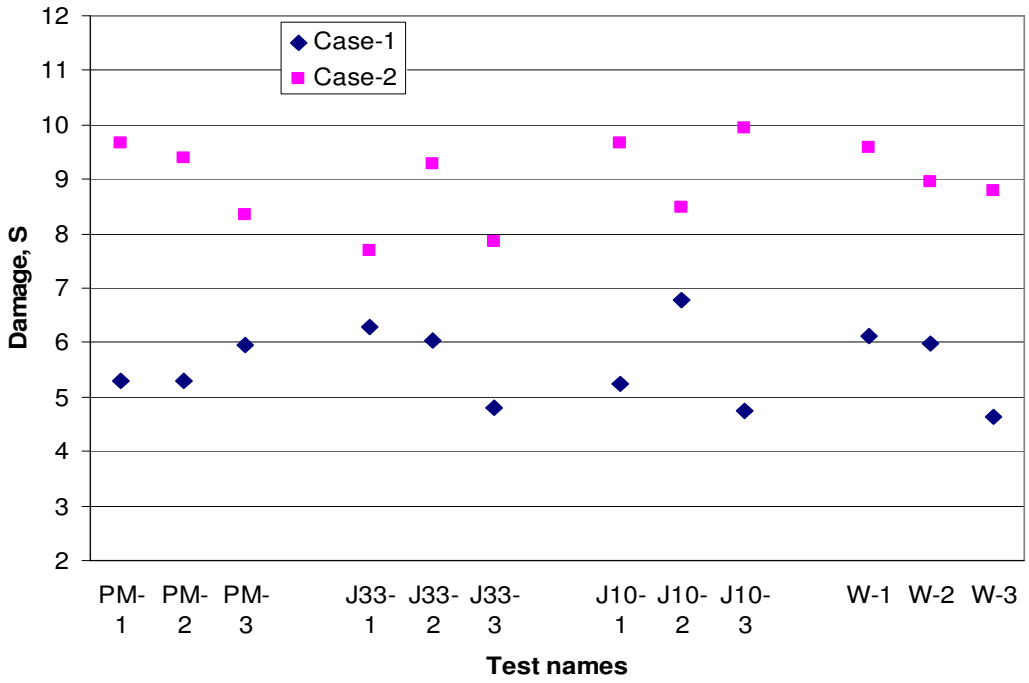

Fig. 3.18 Comparison of damage results of Case 1 and Case 2

According to the Fig. 3.18, even the spectral shape and wave grouping changes, damage results are almost same unless values of extreme waves change. The same result is true for new set up of experiments named Case3 and Case 4 which significant wave height and period changes but wave steepness is almost same as in the Cases 1 and 2. Damage results of Case 3 and Case 4 are given in Fig. 3.19.

According to the results of tests with same significant wave height, period ($H_{1/3}$=10.8cm, $T_{1/3}$=1.9sec) and $\alpha_{extreme}$ (0.007) but with different spectral shapes of PM, J33, J10 and W in which wave grouping were pronounced, it may be stated that even the spectral shape and wave grouping changes, damage results are almost same unless values of extreme waves change

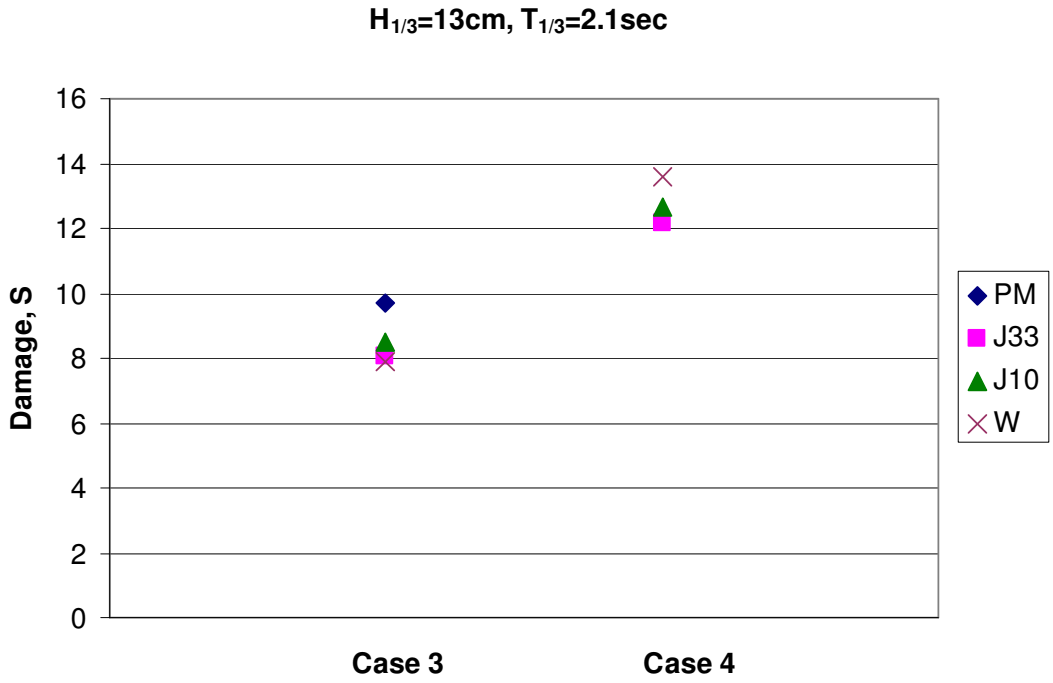

Fig. 3.19 Damage Results of Case 3 and Case 4

3.2.7 Model tests with storms with increasing H_s in steps

In order to check the spectral shape and wave grouping effects during a storm developed by increasing wave heights, a new test series were executed with spectra J33 and J10. For each spectra, wave train with low and high $\alpha_{extreme}$ (0.007 and 0.0105) were generated. In these tests while wave period was kept constant (Ts=1.9s) H_s were increased within the range of 9.5 cm -12 cm in three steps and cumulative damage was measured at the end of each test steps. Each test was repeated twice and presented in Fig.3.20. As it is seen from Fig.3.20, for low wave heights there is insignificant damage difference between J33 and J10 cases. As wave height increases, J33 gives slightly larger damage. Therefore it can be concluded that under the same extreme wave conditions, even if the spectral shape becomes narrower and sharper with a pronounced wave grouping as in J10 spectrum, damage is similar to the J33 spectrum which is in good agreement with the previous findings on the effect of spectral shape and wave grouping.

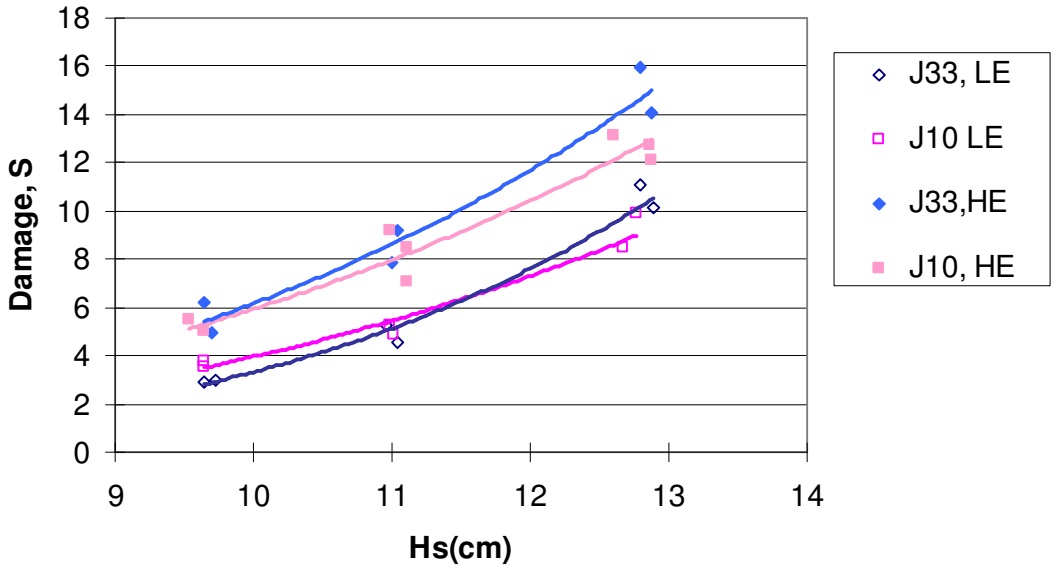

Fig. 3.20 Damage versus wave height for spectral shapes J33 and J10 (LE means Low $\alpha_{extreme}$ and HE means High $\alpha_{extreme}$)

CHAPTER 4

EFFECT OF EXTREME WAVES IN A WAVE TRAIN

Based on the results of experiments given in Chapter 3, it was seen that height of extreme waves was more significant than the situation that they come as a group in a wave train on the stability of rubble mound breakwaters. Therefore, extended experiments were conducted to observe the effect of heights of extreme waves on the stability of rubble mound breakwaters.

4.1 Experimental Set-up

In the experiments, J33 was chosen as spectrum shape and the test program given in Table 4.1 was executed. Two structure slope angles of cotα=1.5 and 3.0 were tested since those are the limits of mostly applied slope angle range. The model cross-section with slope of 1:1.5 was given in Fig. 3.1. After finishing test series with cotα=1.5, new model was constructed with the slope of 1:3. Cross-section of the model was drawn in Fig 4.1. Crest height of the model with the slope of 1:3 is the same with the model with the slope of 1:1.5. Thus, wave overtopping was not allowed for both slopes.

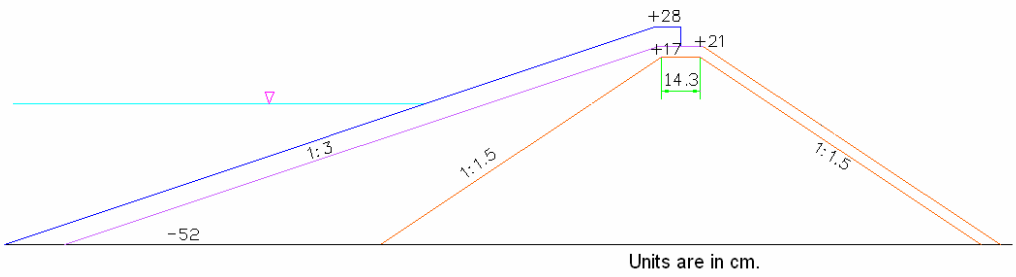

Fig. 4.1 Cross-section of the model with the slope of 1:3

Size of stones were same for both of the slope angles which were $D_{n50(armour)}$=0.034m, $D_{n50(filter)}$=0.021m and $D_{n50(core)}$=0.0148m.

A test series consisted of the tests with same period and $\alpha_{extreme}$, but different significant wave heights in a range given in Table 4.1. Significant wave heights are almost same in the tests of each series with same wave period but different $\alpha_{extreme}$. A water depth of 0.52 m was kept constant for all tests.

Table 4.1 Test Program

Test series no	cotα	H_s(cm)	T_m(s)	$\alpha_{extreme}$	no of tests
1	1.5	7.74-12.93	1.68	0.007	10
2	1.5	7.77-12.89	1.68	0.0105	10
3	1.5	7.67-12.89	1.81	0.007	6
4	1.5	7.63-12.74	1.81	0.0105	6
5	1.5	8.45-13.82	2.04	0.007	6
6	1.5	8.44-13.65	2.04	0.0105	6
7	3	9.01-11.93	1.65	0.007	6
8	3	9.01-12.09	1.65	0.0105	6
9	3	9.25-12.22	1.85	0.007	6
10	3	9.28-12.14	1.85	0.0105	6
11	3	9.28-12.26	2.00	0.007	6
12	3	9.29-12.15	2.00	0.0105	6

4.2. Test Results and Discussions

4.2.1 Damage curves

In the experiments, waves were generated according to the test program given in Table 4.1. Damage level was calculated after each test. After completing each test series, damage curve which is the plot of significant wave height, H_s, versus damage level, S, was drawn. Damage curves for cotα=1.5 are shown in Fig. 4.2, 4.3 and 4.3. and the damage curves for cotα=3 are shown in Fig. 4.5, 4.6 and 4.6. In all of the figures, the curves of test series with $\alpha_{extreme}$=0.007 were called as low $\alpha_{extreme}$,LE, case and the

curves of test series with $\alpha_{extreme}$=0.0105 were called as high $\alpha_{extreme}$, HE, case and they were plotted together on the same figure.

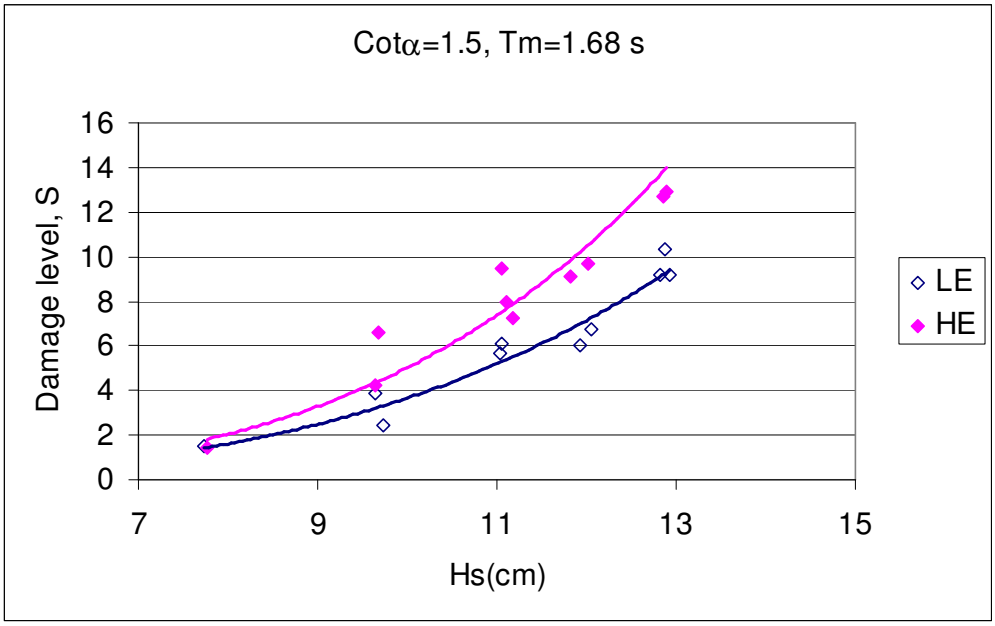

Fig. 4.2 Damage curves of experiment results for cotα=1.5 and T_m=1.68s (LE means low $\alpha_{extreme}$, and HE means high $\alpha_{extreme}$ cases)

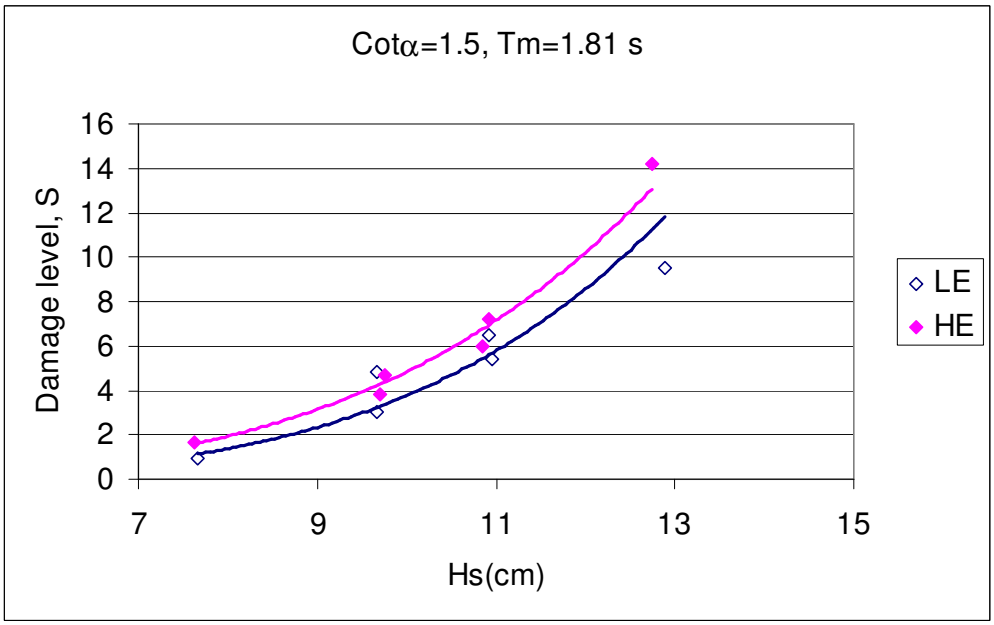

Fig. 4.3 Damage curves of experiment results for cotα=1.5 and T_m=1.81s (LE means low $\alpha_{extreme}$, and HE means high $\alpha_{extreme}$ cases)

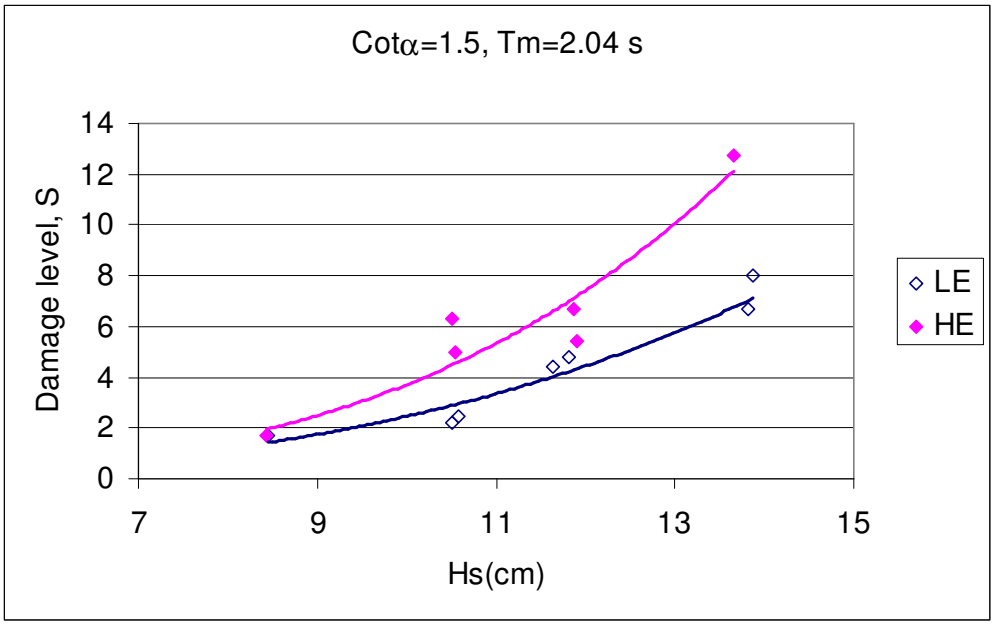

Fig. 4.4 Damage curves of experiment results for cotα=1.5 and T_m=2.04s (LE means low $\alpha_{extreme}$, and HE means high $\alpha_{extreme}$ cases)

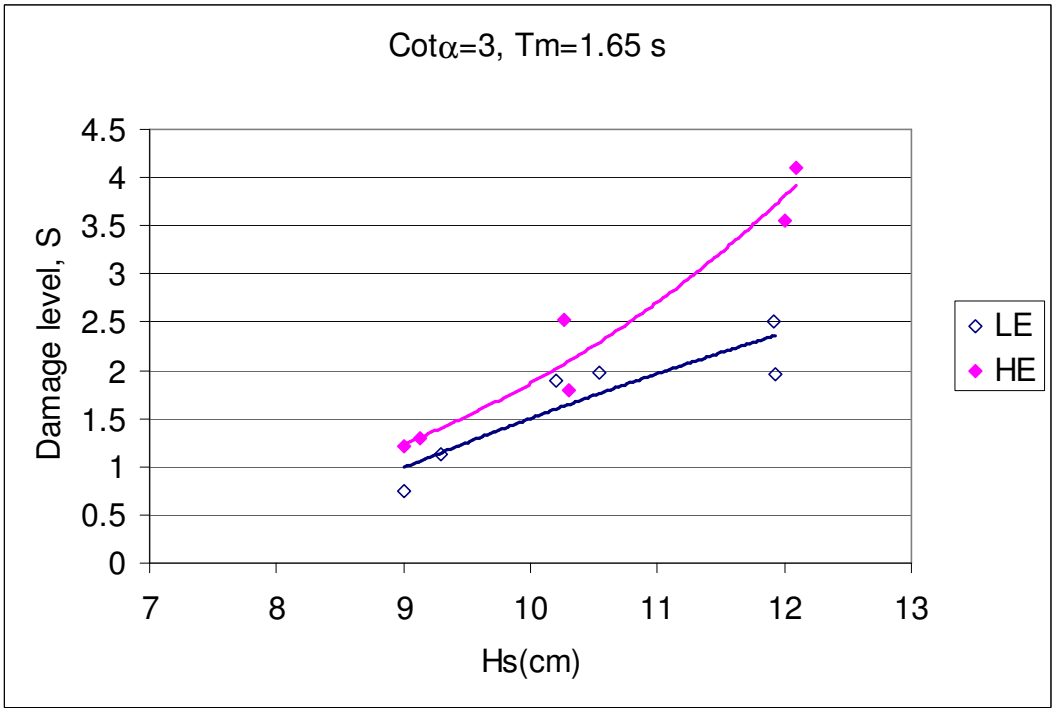

Fig. 4.5 Damage curves of experiment results for cotα=3 and T_m=1.65s (LE means low $\alpha_{extreme}$, and HE means high $\alpha_{extreme}$ cases)

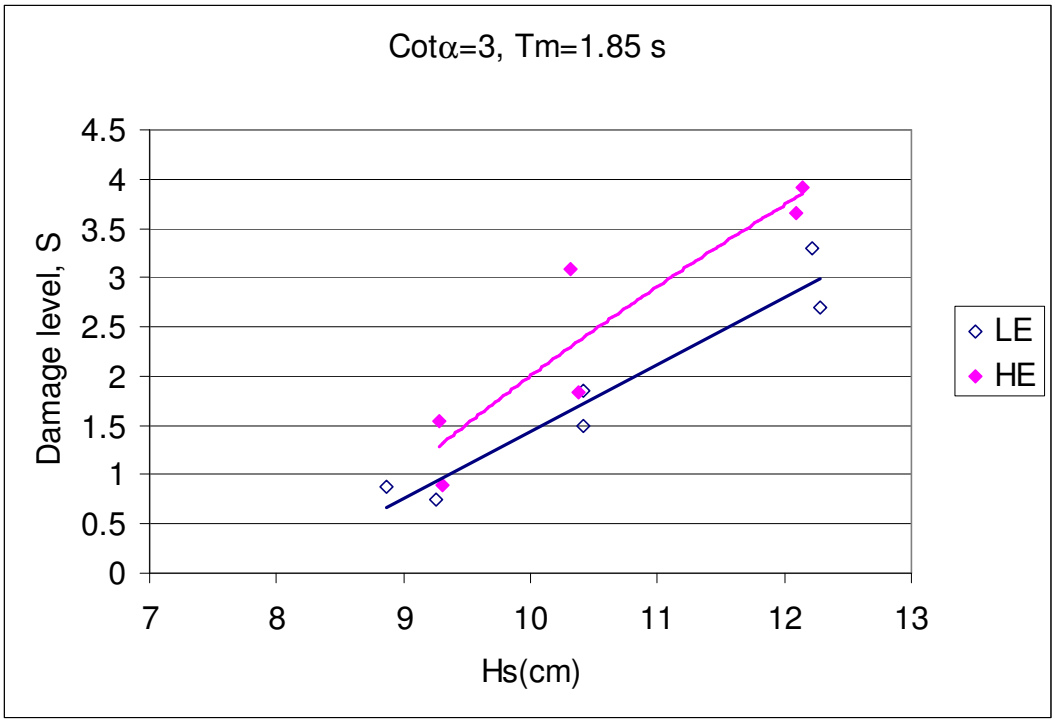

Fig. 4.6 Damage curves of experiment results for cotα=3 and T_m=1.85s (LE means low $\alpha_{extreme}$, and HE means high $\alpha_{extreme}$ cases)

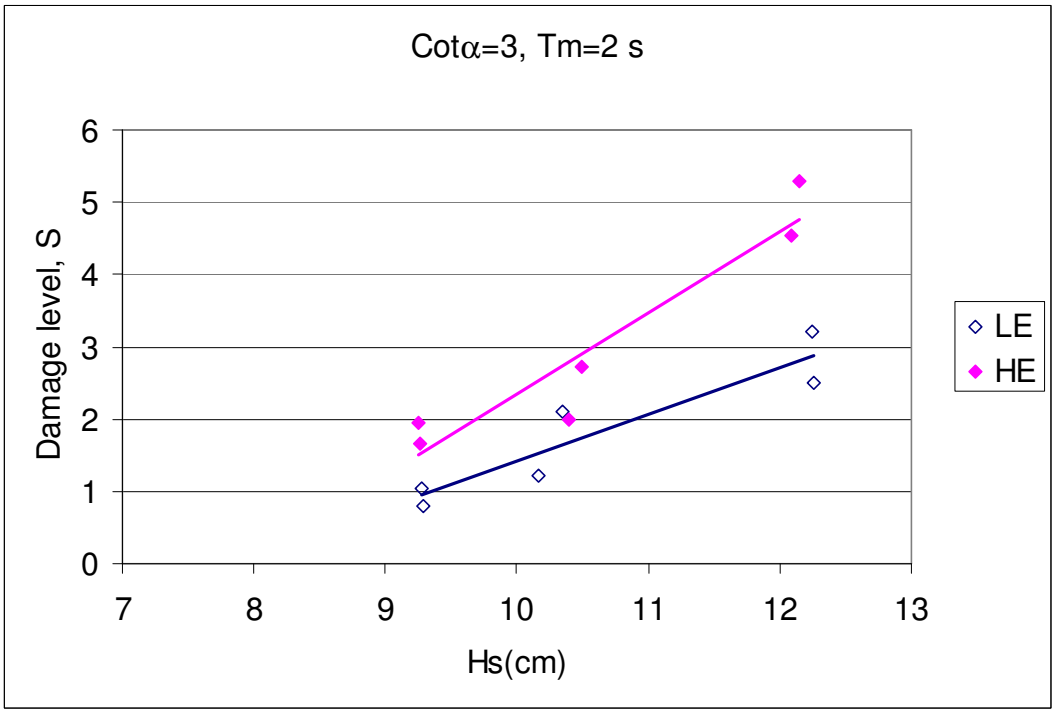

Fig. 4.7 Damage curves of experiment results for cotα=3 and T_m=2.0s (LE means low $\alpha_{extreme}$, and HE means high $\alpha_{extreme}$ cases)

As it can be seen from the Figures 4.2-4.7, for both of the slope angle cotα=1.5 and 3, the wave train with high value of $\alpha_{extreme}$ is more destructive than it is with low $\alpha_{extreme}$. The difference in the damage levels caused by the wave train with low $\alpha_{extreme}$ (LE) and high $\alpha_{extreme}$ (HE) increase as wave height increase except for the case with cotα=1.5 and T_m=1.81 s.

4.2.2 Stability curves

Stability curves are the plots of Irribaren number ($\zeta_m=\tan\alpha/(H_s/L_0)^{0.5}$) versus stability number ($Ns=H_s/\Delta d_{n50}$). Those plots which are the dimensionless demonstration of the test results were used for the stability analysis.

In order to plot stability curves, first, the damage curve is drawn through the measured points as it was shown as an example in Fig. 4.8 for cotα=1.5, T_m=1.81s and LE case. Damage curve was obtained as the best fit curve of experiment points. The equation of the best curve was obtained in this case as:

$$S=0.0001H_s^{4.5208} \qquad (4.1)$$

In order to plot stability curves, the H_s values are taken from the damage curves corresponding to the different fixed damage levels. Damage levels for cotα=1.5 were chosen as S=2, 3, 5 and 8. After H_s values corresponding to chosen damage levels were taken from the damage curve, N_s and ζ_m values were calculated with Δ=1.64, D_{n50}= 0.034m as used in the experiments. Relative mass density Δ and nominal 50% diameter of armour stone,$D_{n50,}$ were defined in Eq. 2.20. Results are given in Table 4.2 as an example for cotα=1.5, T_m=1.81s and LE case. Equations of best curves with correlation coefficient, R^2 and the tables of calculated Ns and ζ_m for the other cases of cotα=1.5 were given in Appendix A.

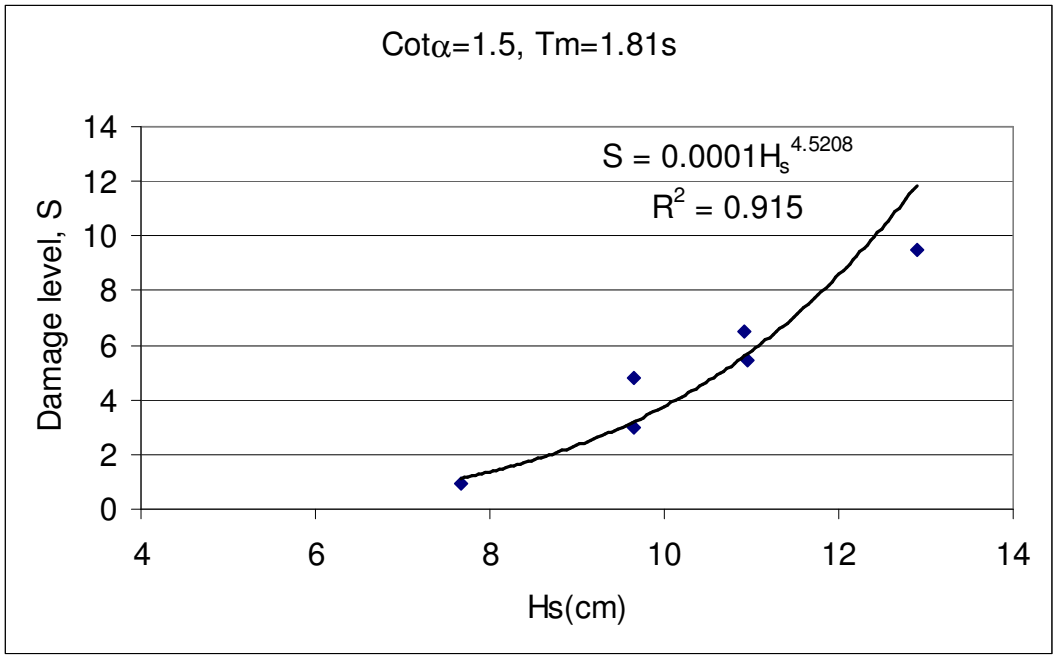

Fig. 4.8 Example damage curve for Cotα=1.5, T_m=1.83 s, and LE case

Table 4.2 Extracted H_s values and calculated N_s and ζ_m for cotα=1.5, T_m=1.83 s, and LE case

Damage level, S	H_s(m) (Eq. 4.1)	$N_s=H_s/\Delta*Dn_{50}$	T_m(s)	L_{0m}(m)	Irribaren no, ζ_m
2	0.0894	1.603	1.83	5.224	5.096
3	0.0978	1.754	1.83	5.224	4.873
5	0.1095	1.964	1.83	5.224	4.605
8	0.1215	2.179	1.83	5.224	4.372

Stability curves of ζ_m versus N_s, were firstly plotted for cotα=1.5 and for chosen damage levels, S=2,3,5 and 8, and demonstrated in Figs. 4.9, 4.10, 4.11 and 4.12. Meer's formula with permeability coefficient, P=0.4 and 0.45 were also drawn on the same figure to compare the experimental results. In Van der Meer's stability formulae, permeability coefficient P is defined by P=0.1 for the impermeable core, 0.5 for the permeable core and 0.6 for the homogenous structure. The other structure with filter layer between armour and core layers is represented by P=0.4. When P is equal to 0.4, the

condition is given as $D_{n50armour}/D_{n50filter}=2$ and $D_{n50armour}/D_{n50core}=4$. Experiment model has a filter layer as it is shown in Fig.3.7 and Fig. 4.1, so P=0.4 may be a suitable value for permeability parameter. But in the model $D_{n50armour}/D_{n50filter}=1.62$ and $D_{n50armour}/D_{n50core}=2.33$ as given in Section 3.2.1. This means that the model may be more permeable than P=0.4. To cover the difference between the permeability parameter of Meer's formulae and the experiment model, Meer's formulae were plotted for both P=0.4 and P=0.45.

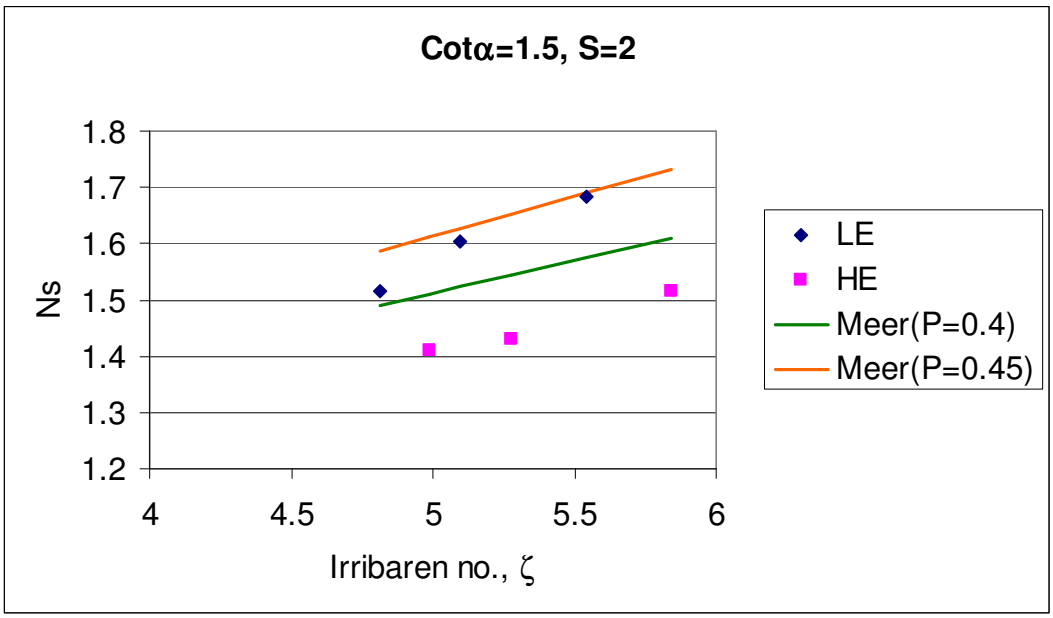

Fig. 4.9 Result for cotα=1.5 and Damage level S=2 (LE means Low $\alpha_{extreme}$ and HE means High $\alpha_{extreme}$)

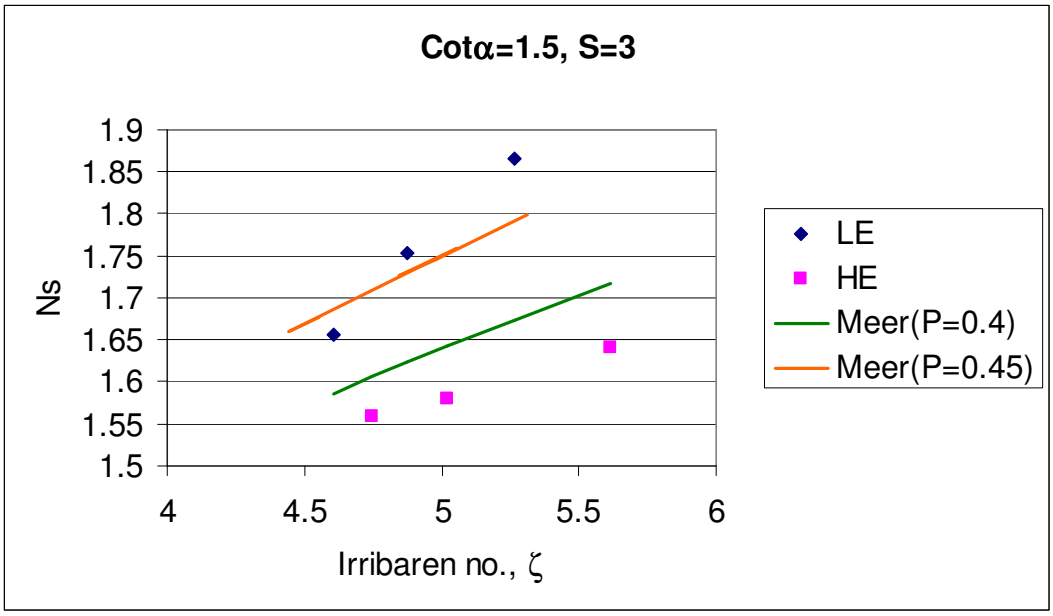

Fig. 4.10 Result for cotα=1.5 and Damage level S=3 (LE means Low $\alpha_{extreme}$ and HE means High $\alpha_{extreme}$)

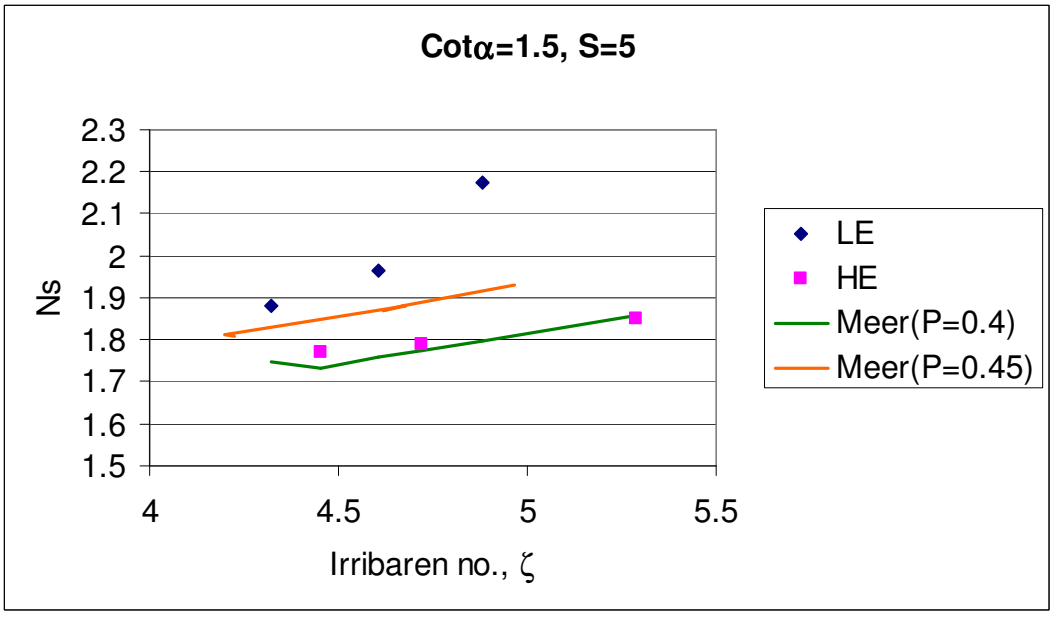

Fig. 4.11 Result for Cotα=1.5 and Damage level S=5 (LE means Low $\alpha_{extreme}$ and HE means High $\alpha_{extreme}$)

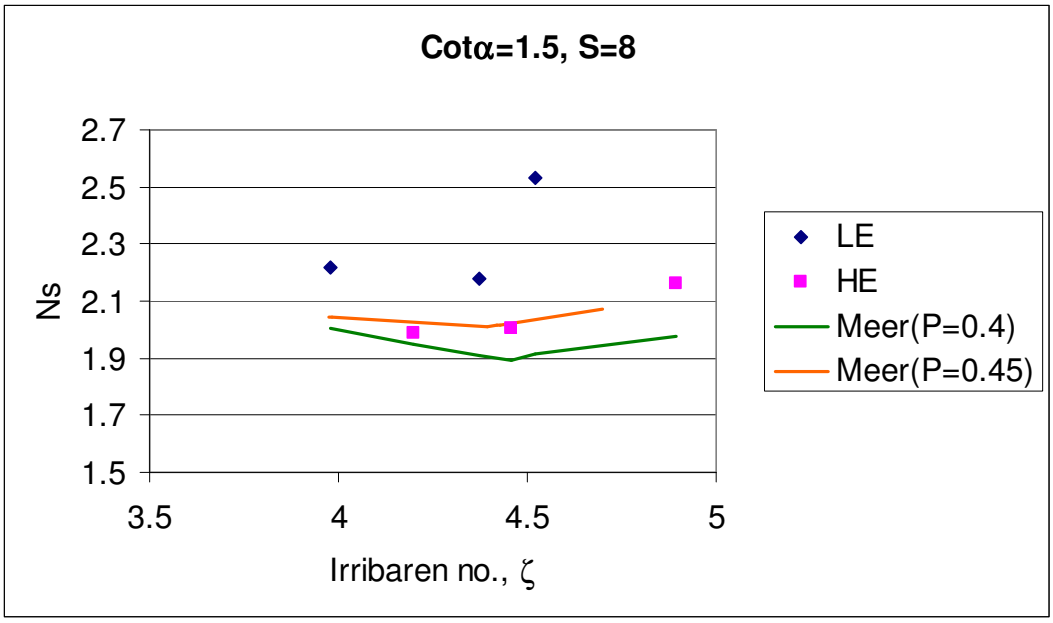

Fig. 4.12 Result for cotα=1.5 and Damage level S=8 (LE means Low $\alpha_{extreme}$ and HE means High $\alpha_{extreme}$)

From the Figs. 4.9 – 4.12 plotted for cotα=1.5, it is seen that stability decreases in high $\alpha_{extreme}$ (HE) cases. Minimum stability is found near ζ_m=4.5 which is the transition from surging to plunging waves for cotα=1.5. Calculated Irribaren numbers, ζ_m, of the test series with T_m=1.81s for the damage level S= 8 are very close to ζ_m=4.5. Therefore, the difference in the damage levels of the case (LE) and the case (HE) did not increase as wave height increase for the cases with cotα=1.5 and T_m=1.81 s.

The difference in the stability numbers of the wave train with low $\alpha_{extreme}$ (LE) and high $\alpha_{extreme}$ (HE) decrease while approaching to this transition zone. This result may be attributed to the fact that while wave run-down is effective on the stability in the surging region, in the transition zone, both wave run-up and run-down forces become effective due to plunging and surging waves, respectively, which causes decrease in the stability even extreme waves are low.

HE case for S=2,3,5 and 8 may be assumed almost parallel to Meer's curves even there is small deflection as ζ_m increase.

Meer's curve with P=0.4 has lower stability than it is with P=0.45 as permeability increase the stability.

As it can be seen from Figs. 4.10 and 4.11, Meer's stability curve with P=0.4 is between experiment curves of low $\alpha_{extreme}$ (LE) and high $\alpha_{extreme}$ (HE) at the start of damage (S=2 and 3). Meer's stability curve with P=0.45 has similar values of experiment curves of low $\alpha_{extreme}$ (LE). These are expected results since Meer's formula does not include the effect of extreme waves in a wave train. But for higher damages, this trend changes. For S=5 as it can be seen in Fig 4.11, Meer's curve with P=0.4 has similar stability number values with the experiment curve of high $\alpha_{extreme}$ (HE) and Meer's curve with P=0.45 is between experiment curves of low $\alpha_{extreme}$ (LE) and high $\alpha_{extreme}$ (HE). For S=8 as given in Fig. 4.12, while Meer's formula for P=0.45 gives similar stability values with HE case, for P=0.4, stability values of Meer are even lower than the experiment curve of high $\alpha_{extreme}$ (HE). This result may be due to the reason that Meer's formula emphasizes the effect of the damage level and so formula covers the effect of extreme waves on the stability for higher damages.

Stability curves belonging to cotα=3 were plotted by applying same procedure given as an example in Fig. 4.8 and Table 4.2. Equations of best curves with correlation coefficient, R^2 and the tables of calculated N_s and ζ_m for the cases of cotα=3 were given in Appendix A.

For cotα=3, damage level were chosen as S=2 and 3 to obtain stability curves because the fact that on slope cotα=3, wave heights tested similar to cotα=1.5 caused damage level only up to 3 as it was shown in the damage curves of Figs. 4.5-4.7. To obtain higher damage levels for slope cotα=3 could only be possible with larger of the wave height distribution

which would bring the breaking case into the problem. Since breaking was out of scope of this work, these tests were kept as for future studies.

ζ_m versus N_s curves for cotα=3 were plotted and demonstrated in Figs. 4.13 and 4.14. Meer's stability curves with permeability coefficient, P=0.4 and 0.45 were also drawn on the same figure to compare the results.

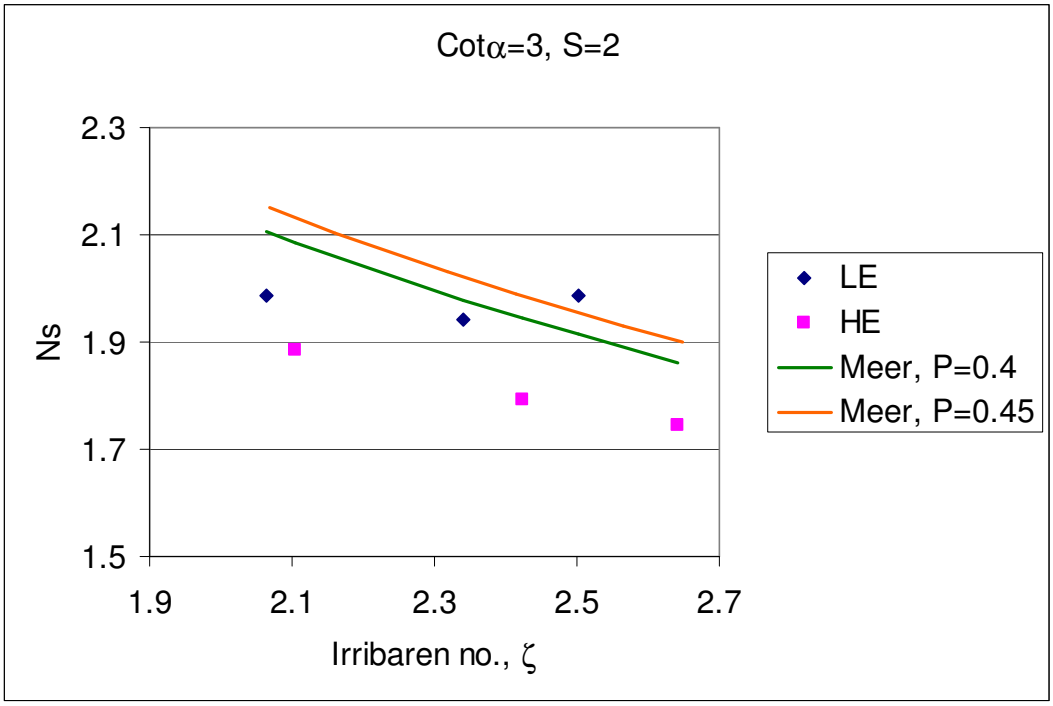

Fig. 4.13 Result for cotα=3 and Damage level S=2 (LE means Low $\alpha_{extreme}$ and HE means High $\alpha_{extreme}$)

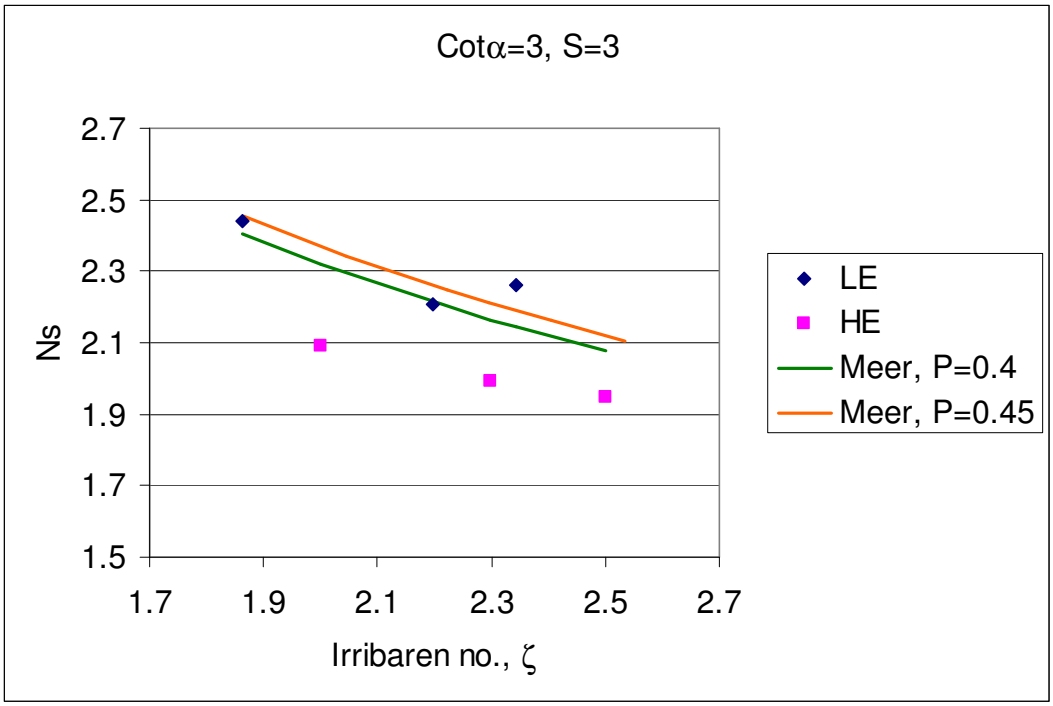

Fig. 4.14 Result for cotα=3 and Damage level S=3

According to Figs. 4.13 and Fig 4.14, stability decreases in high $\alpha_{extreme}$ cases as it was in cotα=1.5 case. Moreover, stability decrease as ζ_m increase because, as ζ_m increase, it is approached to the transition zone of plunging to surging which is almost at ζ_m=3.

As it is in cotα=1.5 cases, the difference in the stability numbers of the wave train by low $\alpha_{extreme}$ (LE) and high $\alpha_{extreme}$ (HE) decreases as it is approached to this transition zone. Fig 4.13 and 4.14 show that while Meer's stability curve with P=0.4 is between experiment curves of low $\alpha_{extreme}$ (LE) and high $\alpha_{extreme}$ (HE), Meer's stability curve with P=0.45 has similar values of experiment curves of low $\alpha_{extreme}$ (LE) for both damage levels of S=2 and 3.

Stability curves of experimental case HE for both damage level and case LE for S=3 may be assumed almost parallel to Meer's curves even there is deflection as ζ_m decrease. But for S=2, stability curve of experimental case LE is inconsistent with this general trend.

Meer's curve with P=0.4 has lower stability than it is with P=0.45 but the difference between the curves is considerably less for cotα=3 than it is for cotα=1.5.

Therefore it can be stated that high extreme waves in a wave train decrease stability without dependency to slope angle. Meer's stability curves which does not include the effect of extreme waves in a wave train, give higher stability values than experiment curves of high $\alpha_{extreme}$ (HE) for start of the damage i.e. S=2 and 3.

4.3 Design Considerations

When a statically stable rubble mound breakwater is designed with a two diameter thick armour layer, initial damage (no damage) criterion is taken into account. The initial damage criterion is 0-5% where the damage is given in terms of displaced units. When damage is defined in terms of eroded area, initial damage corresponds to damage level, S=2 (CEM, 2003). Therefore the stability curves of damage level, S=2 were used in order to see the effect of extreme waves in a wave train on the stability of rubble mound structures for the design. For the slope angle cotα=1.5, Fig. 4.8 was redrawn as it is in Fig. 4.15 with the equations of stability curves of LE and HE cases to compare N_s values for experiment results and Meer's results corresponding to ζ_m values. Hudson equation is also plotted on this figure since it is a widely used formula even it depends on regular wave experiments' results. Hudson formula has a constant value of N_s for each ζ_m value because, according to the formula:

$$Ns = (K_D Cot\alpha)^{1/3} \qquad (4.2)$$

N_s is equal to 1.82 for K_D=4 and cotα=1.5. The resulted N_s values are given in Table 4.3.

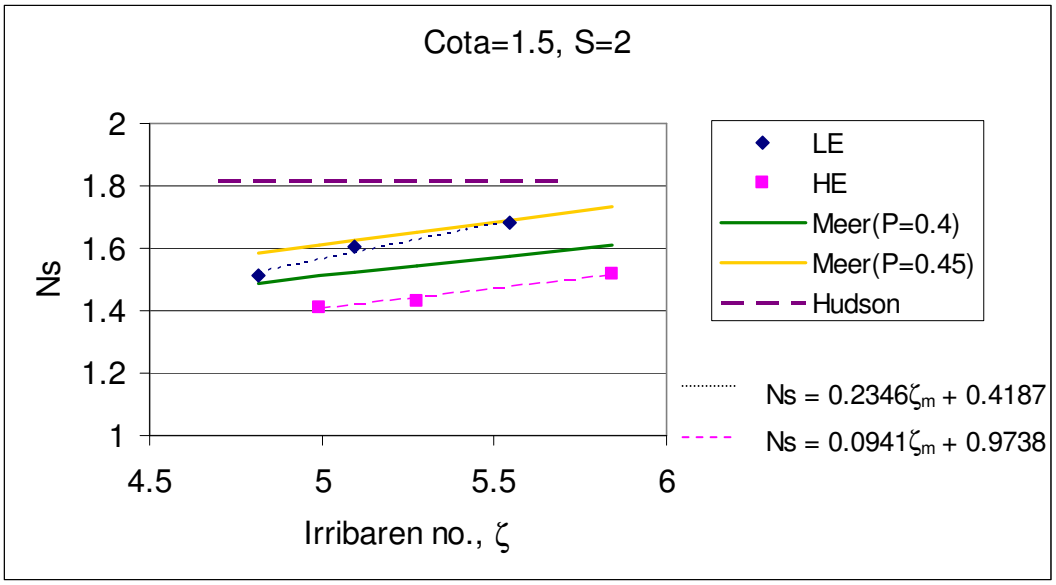

Fig. 4.15 Stability Curves for cotα=1.5 and Damage level S=2 with Hudson formula and experiment equations

Table 4.3 The N_s values of experiment results, Meer and Hudson's equations for cotα=1.5 and S=2

	Ns				
Irribaren no, ζ	LE	HE	Meer(P=0.4)	Meer (P=0.45)	Hudson
4.7	1.498	1.366	1.475	1.570	1.817
4.9	1.544	1.392	1.500	1.599	1.817
5.1	1.589	1.418	1.524	1.628	1.817
5.3	1.634	1.443	1.548	1.657	1.817
5.5	1.680	1.469	1.571	1.685	1.817
5.7	1.725	1.495	1.593	1.712	1.817
5.9	1.770	1.521	1.616	1.739	1.817

As it was given before N_s is defined as $N_s=H_s/\Delta d_{n50}$. Rewriting the equation gives:

$$W = D_{n50}^3 \gamma_s = \left(\frac{H_s}{N_s \Delta}\right)^3 = \left(\frac{1}{N_s^3}\right)\left(\frac{H_s}{\Delta}\right)^3 \qquad (4.2)$$

When γ_s,Δ and H_s are constant, W is proportional to $1/N_s^3$ which is called as weight coefficient here. Weight coefficients of experiment cases LE and HE, Meer's formula and Hudson formula with corresponding ζ_m were given in Table 4.4.

Table 4.4 Weight coefficients of experiment cases LE and HE, Meer's formula and Hudson formula (cotα=1.5)

	Weight Coefficients				
Irribaren no, ζ	LE	HE	Meer(P=0.4)	Meer (P=0.45)	Hudson
4.7	0.297	0.392	0.312	0.259	0.167
4.9	0.272	0.371	0.296	0.244	0.167
5.1	0.249	0.351	0.282	0.232	0.167
5.3	0.229	0.333	0.270	0.220	0.167
5.5	0.211	0.315	0.258	0.209	0.167
5.7	0.195	0.299	0.247	0.199	0.167
5.9	0.180	0.284	0.237	0.190	0.167

As it can be seen from Table 4.4, HE case of experiment results has the highest weight coefficients for all ζ_m values. While weight coefficients of Meer's formula with P=0.4 are between HE and LE cases, weight coefficients of Meer's formula with P=0.45 are very similar to experimental LE case. Hudson formula has the lowest weight coefficients.

The experimental results of LE and HE cases together with Meer's and Hudson's results for weight coefficients given in Table 4.4 were re-evaluated by dividing all weight coefficients to the weight coefficient of Meer with P=0.4 to obtain the weight ratios for corresponding ζ_m and given in Table 4.5. Re-evaluation results were plotted in Fig. 4.16.

Table 4.5 Weight ratios of experiment cases LE and HE, Meer's equation with P=0.4 ($\cot\alpha$=1.5)

	Weight ratios			
Irribaren no, ζ	LE/Meer	HE/Meer	Hudson/Meer	Meer(P=0.4)
4.7	0.954	1.260	0.535	1
4.9	0.917	1.252	0.562	1
5.1	0.882	1.243	0.590	1
5.3	0.849	1.233	0.618	1
5.5	0.818	1.222	0.646	1
5.7	0.788	1.211	0.674	1
5.9	0.760	1.199	0.703	1

According to the Table 4.5 and Fig. 4.16, structure may need 26% heavier weight for the armour layer in order to stand high extreme waves with a damage level not more than S=2 for ζ_m=4.7. As ζ_m increases, weight difference decreases to 20%. Hudson formula underestimates the necessary weight comparing to experiment cases and Meer's formula. As ζ_m increase (away from transition zone), result of Hudson starts to approach to experiment, LE, results.

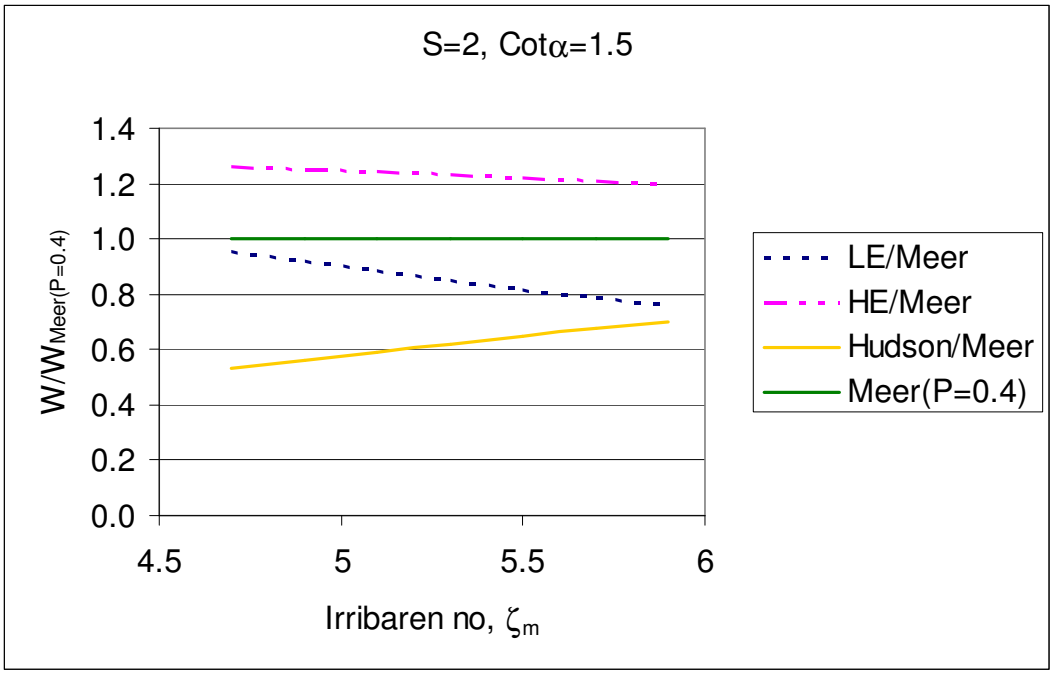

Fig. 4.16 Weight ratios of experiment cases of LE and HE and Hudson formula to Meer's formula with P=0.4 (cotα=1.5)

As it can be seen from Fig. 4.16, weight ratio of experimental case HE slightly changes 1.26 to 1.20 with corresponding ζ_m. Therefore, if HE curve is assumed almost parallel to Meer's curve for practical purposes, then $W/W_{Meer(P=0.4)}$ can be given as 1.23 for HE case, for all ζ_m in the range of 4.7-5.9.

The similar re-evaluation of Table 4.4 was done by dividing all weight coefficients to the weight coefficient of Meer with P=0.45 to obtain the weight ratios for corresponding ζ_m and given in Table 4.6. Re-evaluation results were plotted in Fig. 4.17.

Table 4.6 Weight ratios of experiment cases LE and HE, Meer's equation with P=0.45 (cotα=1.5)

	Weight ratios			
Irribaren no, ζ	LE/Meer	HE/Meer	Hudson/Meer	Meer (P=0.45)
4.7	1.150	1.518	0.644	1
4.9	1.112	1.518	0.682	1
5.1	1.076	1.516	0.720	1
5.3	1.042	1.512	0.758	1
5.5	1.009	1.507	0.797	1
5.7	0.977	1.501	0.836	1
5.9	0.947	1.494	0.876	1

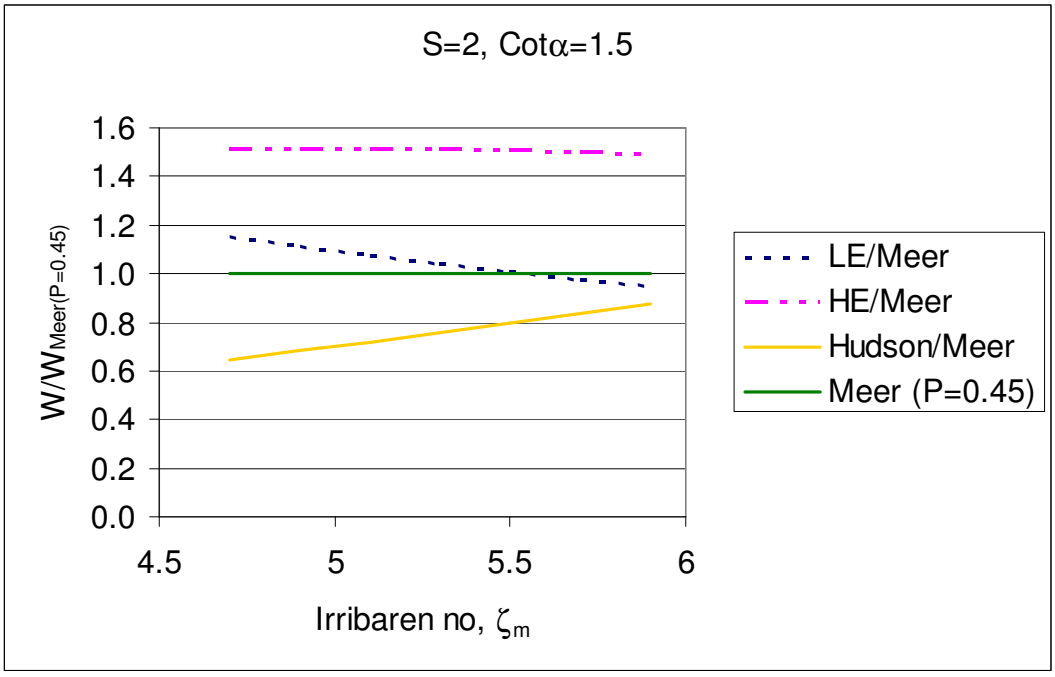

Fig. 4.17 Weight ratios of experiment cases of LE and HE and Hudson formula to Meer's formula with P=0.45 (cotα=1.5)

According to Table 4.6 and Fig.4.17, weight difference between experiment case of HE and Meer's equation increase to 52%. It was 26% when experiment case HE is compared with Meer's result for P=0.4. The reason is the effect of permeability coefficient in Meer's formula. When permeability

factor P increase, stability also increase and Meer's formula gives less weight.

Weight ratio decreases to 49% as ζ_m increases. Therefore it can be said that stability curve of experiment case HE is almost parallel to Meer's curve with P=0.45. If it is assumed that stability curves of experimental cases HE and LE are parallel to Meer's curve with P=0.45 for practical purposes, then it is calculated that $W/W_{Meer(P=0.45)}$=1.5 for HE and it is 1.05 for LE for all ζ_m in the range of 4.7-5.9.

Hudson formula underestimates the necessary weight but weight ratio $W_{Hudson}/W_{Meer(P=0.45)}$ is higher than the weight ratio $W_{Hudson}/W_{Meer(P=0.4)}$. It means Hudson formula gives closer values to Meer's formula since Meer's weight coefficients decreased due to increase in permeability coefficient, P=0.45.

For the slope angle of cotα=3, similar analysis performed for the slope angle of cotα=1.5 were done considering design of the rubble mound breakwaters. Initial damage level was taken as S=2 for cotα=1.5 cases. It is also S=2 for cotα=3 according to Meer (1988). But it is also stated that the extent of damage depends on the slope angle. More stones have to be displaced or moved for gentler slopes before the 'no damage' criterion is reached. This is due to larger amount of stones around the water level for a gentler slope (Meer, 1988). Considering this fact and since the ζ_m versus N_s curves of experiment results for S=3 given in Fig 4.14, seems more stable, it was decided to use the stability curves belongs to both S=2 and 3 to make a comment about design.

For the slope angle cotα=3, Fig. 4.13 which is the stability curve of S=2, was redrawn, as it was given in Fig. 4.18 with the equations of stability curves of LE and HE cases to compare N_s values for experiment results and Meer's results corresponding to ζ_m values. Hudson equation is also plotted on this figure.

Hudson formula has a constant value of N_s for each ζ_m value and it is equal to 2.29 for K_D=4 and cotα=3. The resulted N_s values are given in Table 4.7 for S=2.

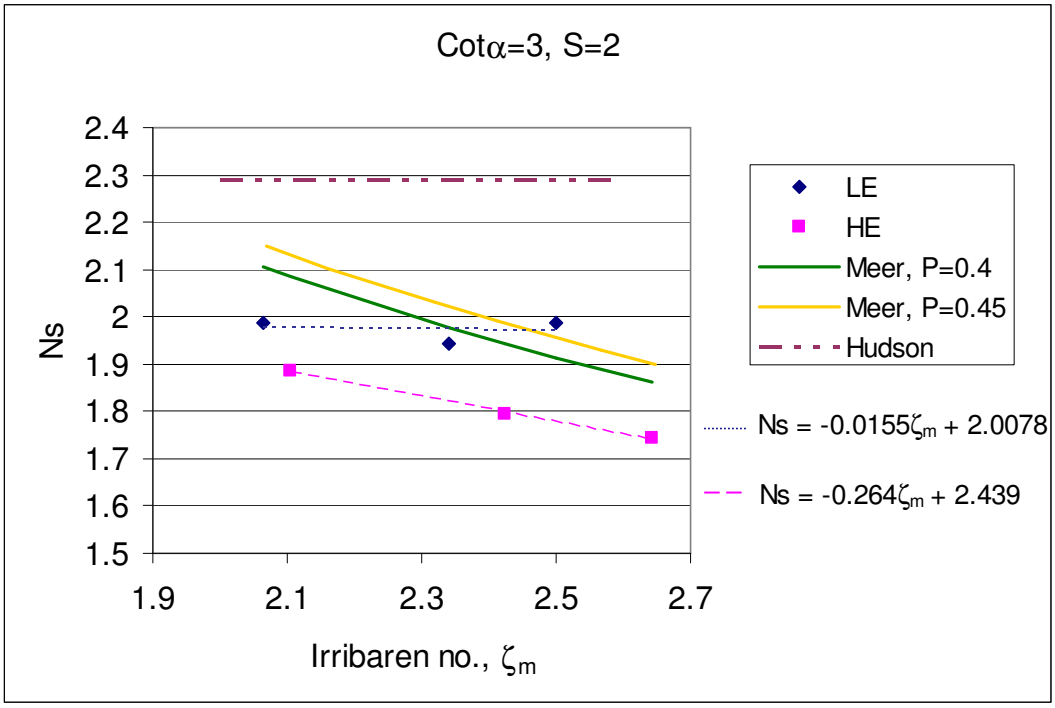

Fig. 4.18 Stability Curves for cotα=3 and Damage level S=2 with Meer and Hudson formulae and equations of experimental result

Table 4.7 The N_s values of experiment results, Meer and Hudson's formulae for cotα=3 and S=2

	Ns				
Irribaren no, ζ	LE	HE	Meer(P=0.4)	Meer (P=0.45)	Hudson
2	1.977	1.911	2.140	2.186	2.289
2.2	1.974	1.858	2.041	2.084	2.289
2.4	1.971	1.805	1.954	1.996	2.289
2.6	1.968	1.753	1.877	1.917	2.289

As it was given in Eq.4.2, weight of armour layer stone, W is proportional to $1/N_s^3$. Therefore it is possible to obtain weight ratios of experiment cases LE and HE, Meer's equation and Hudson equation. The result was given in Table 4.8.

Table 4.8 Weight coefficients of experiment cases LE and HE, Meer's equation and Hudson equation (cotα=3, S=2)

	Weight coefficients				
Irribaren no, ζ	LE	HE	Meer(P=0.4)	Meer (P=0.45)	Hudson
2	0.129	0.143	0.102	0.075	0.083
2.2	0.130	0.156	0.118	0.089	0.083
2.4	0.131	0.170	0.134	0.103	0.083
2.6	0.131	0.186	0.151	0.118	0.083

The experimental results of LE and HE cases together with Meer's and Hudson's results for weight coefficients given in Table 4.8 were re-evaluated by dividing all weight coefficients to the weight coefficient of Meer with P=0.4 to obtain the weight ratios for corresponding ζ_m and given in Table 4.9. Re-evaluation results were plotted in Fig. 4.19.

Table 4.9 Weight ratios of experiment cases LE and HE, Meer's equation with P=0.4 (cotα=3, S=2)

	Weight ratios			
Irribaren no, ζ	LE/Meer	HE/Meer	Hudson/Meer	Meer(P=0.4)
2	1.269	1.405	0.817	1
2.2	1.105	1.324	0.708	1
2.4	0.975	1.267	0.621	1
2.6	0.868	1.229	0.551	1

According to the Table 4.9 and Fig. 4.19, structure may need 40.5% heavier weight for the armour layer comparing with Meer's result for P=0.4 in order to stand high extreme waves with a damage level not more than S=2. Weight difference between experiment case HE and Meer with P=0.4 was

26-20% for cotα=1.5 cases. The reason may be the under prediction of Meer's formula for the necessary diameter of armour stone for flatter slopes (Hald and Burcharth 2000). Therefore it can be said that effect of extreme waves in a wave train gains more importance for the slope of cotα=3 when the armour layer design is made by using Meer's formulas.

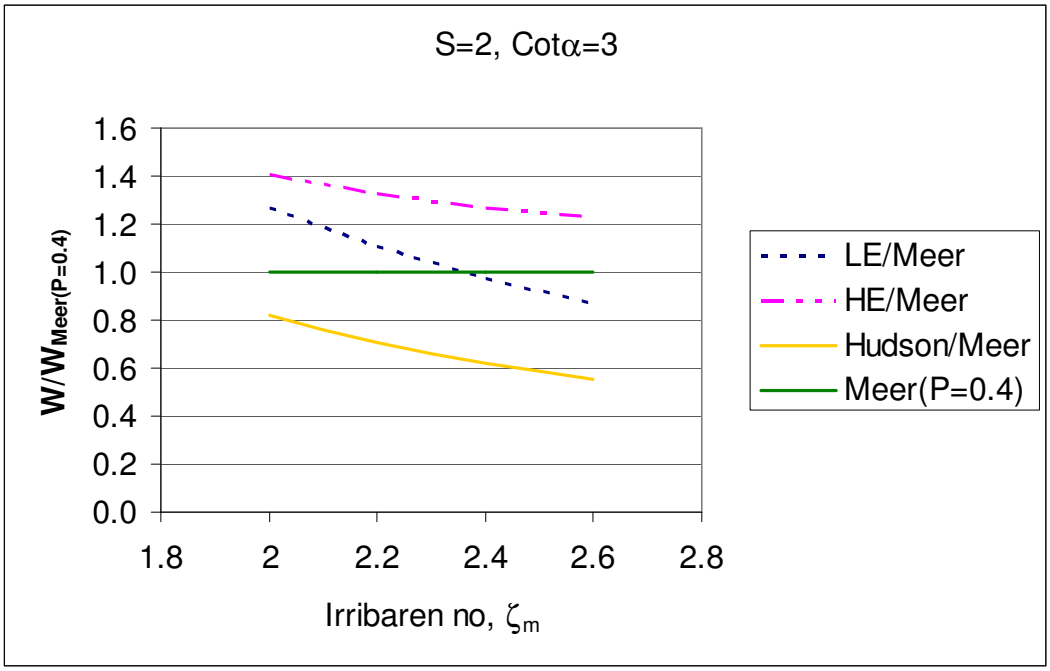

Fig. 4.19 Weight ratios of experiment cases of LE and HE and Hudson formula to Meer's formula with P=0.4 (cotα=3)

As ζ_m increase (approaches to transition zone), weight difference decreases from 40.5% to 23%. If it is assumed that stability curves of experimental cases are parallel to Meer's curve with P=0.4, then it is calculated that $W/W_{Meer(P=0.4)}$=1.32 for HE and it is 1.07 for LE for all ζ_m in the range of 2-2.6.

Hudson formula underestimates the necessary weight. As being away from transition zone, result of Hudson starts to approach to experiment LE case.

The similar re-evaluation of Table 4.8 was done by dividing all weight coefficients to the weight coefficient of Meer with P=0.45 to obtain the weight ratios for corresponding ζ_m and given in Table 4.10. Re-evaluation results were plotted in Fig. 4.20.

Table 4.10 Weight ratios of experiment cases LE and HE, Meer's equation with P=0.45 (cotα=3, S=2)

Irribaren no, ζ	LE/Meer	HE/Meer	Hudson/Meer	Meer (P=0.45)
2	1.352	1.497	1.111	1
2.2	1.178	1.411	0.940	1
2.4	1.039	1.350	0.809	1
2.6	0.925	1.309	0.706	1

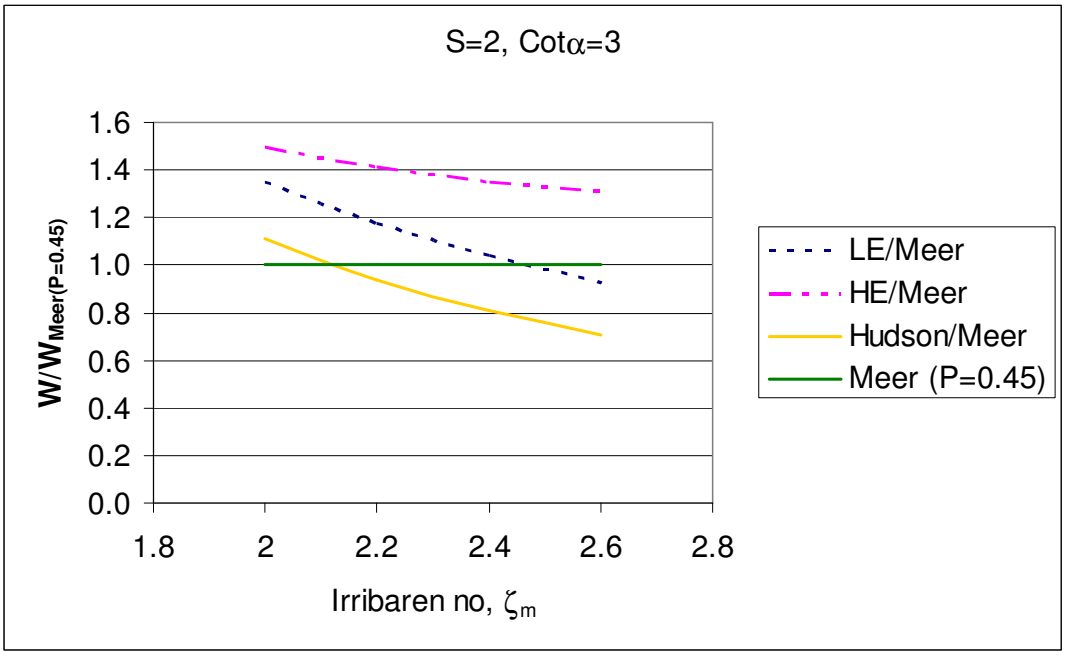

Fig. 4.20 Weight ratios of experiment cases of LE and HE and Hudson formula to Meer's formula with P=0.45 (cotα=3)

According to Table 4.10 and Fig.4.20, weight ratio of experiment case of HE and Meer's equation increase to 50% for ζ_m=2 as maximum. It was 40.5%

when comparing experiment LE case to Meer's equation with P=0.4. The reason is the effect of permeability coefficient of Meer's formula. When permeability factor P increase, stability also increase and Meer's formula gives less weight. But the difference in weight ratio due to permeability is lower for the slope of cotα=3 (50-40.5=9.5%) than the slope of cotα=1.5 (52-26=26%). The reason may be that the permeability is more effective in surging region (ζ_m>3.5) than plunging region in Meer's equations since water can dissipate into the core easily and flow becomes less violent as permeability increase in the surging region where run down is the dominant force (Meer,1988). Experiment cases with the slope of cotα=1.5 are in surging region at S=2 and the experiment cases with the slope of cotα=3 are in plunging region at S=2 and 3.

As ζ_m increase, weight ratio difference decreases from 50% to 30%. If it is assumed that stability curves of experimental cases are parallel to Meer's curve with P=0.45 for practical purposes, then it is calculated that $W/W_{Meer(P=0.45)}$=1.4 for HE and it is 1.14 for LE for all ζ_m in the range of 2-2.6.

Hudson formula underestimates the necessary weight for ζ_m>2.1 comparing with Meer's formula. Weight ratio Hudson/Meer(P=0.45) is higher than the weight ratio Hudson/Meer(P=0.4) since Meer's weight coefficients decreased due to increase in permeability coefficient, P=0.45.

Then, Fig. 4.14 which is the stability curve of S=3 for cotα=3, was redrawn, as it is in Fig. 4.21 with the equations of stability curves of LE and HE cases to compare N_s values for experiment results and Meer's results with P=0.4 and Hudson formula corresponding to ζ_m values. The result was given in Table 4.11.

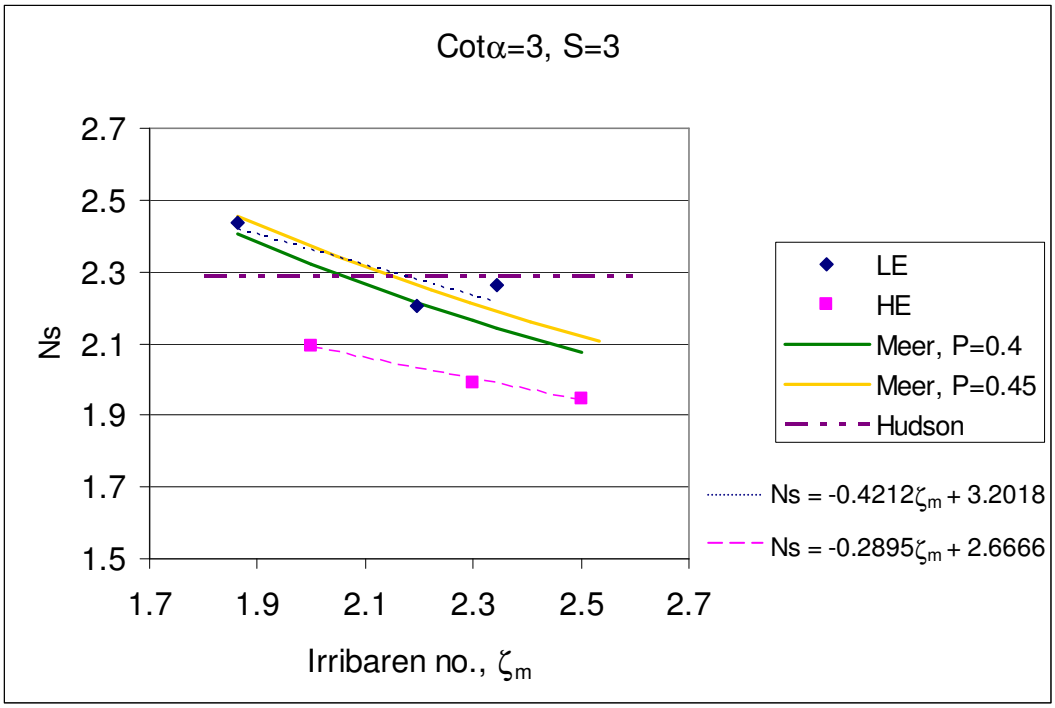

Fig. 4.21 Stability Curves of experimental cases, Meer and Hudson formula and equations of experiment results for cotα=3 and Damage level S=3

Table 4.11 N_s values for cotα=3 and S=3 belong to experiment results, Meer and Hudson's formulae

	Ns				
Irribaren no, ζ	LE	HE	Meer(P=0.4)	Meer(P=0.45)	Hudson
1.9	2.402	2.116	2.381	2.432	2.289
2.1	2.317	2.058	2.265	2.314	2.289
2.3	2.233	2.000	2.164	2.211	2.289
2.5	2.149	1.942	2.076	2.120	2.289
2.7	2.065	1.884	1.998	2.040	2.289

Weight coefficients, $1/N_s^3$, of experiment cases LE and HE, Meer's formula and Hudson formula was given in Table 4.12.

Table 4.12 Weight Coefficients of experiment cases LE and HE, Meer's equation and Hudson equation

	Weight coefficients				
Irribaren no, ζ	LE	HE	Meer(P=0.4)	Meer(P=0.45)	Hudson
1.9	0.072	0.106	0.074	0.069	0.083
2.1	0.080	0.115	0.086	0.081	0.083
2.3	0.090	0.125	0.099	0.093	0.083
2.5	0.101	0.136	0.112	0.105	0.083
2.7	0.114	0.149	0.125	0.118	0.083

Re-evaluation of Table 4.12 were done by dividing all weight coefficients to the weight coefficient of Meer with P=0.4 to obtain the weight ratios for corresponding ζ_m and given in Table 4.13. Re-evaluation results were plotted in Fig. 4.22.

Table 4.13 Weight ratios of experiment cases LE and HE, Meer's equation with P=0.4 ($\cot\alpha$=3, S=3)

	Weight ratios			
Irribaren no, ζ	LE/Meer	HE/Meer	Hudson/Meer	Meer(P=0.4)
1.9	0.975	1.425	1.125	1
2.1	0.934	1.333	0.968	1
2.3	0.910	1.267	0.845	1
2.5	0.902	1.221	0.746	1
2.7	0.906	1.191	0.664	1

According to the Table 4.13 and Fig. 4.22, structure may need 42.5% heavier weight for the armour layer in order to stand high extreme waves with a damage level not more than S=3. Increase of weight due to high extreme waves was 40.5% for S=2. Therefore $W/W_{Meer(P=0.4)}$ is almost same for S=2 and S=3. As ζ_m increase (approaches to transition zone), weight ratio decreases to 19%. If it is assumed that stability curves of experimental cases are parallel to Meer's curve with P=0.4 for practical purposes, then it is calculated that W/W_{Meer}=1.31 for HE and it is 0.94 for LE for all ζ_m in the range of 1.9-2.7.

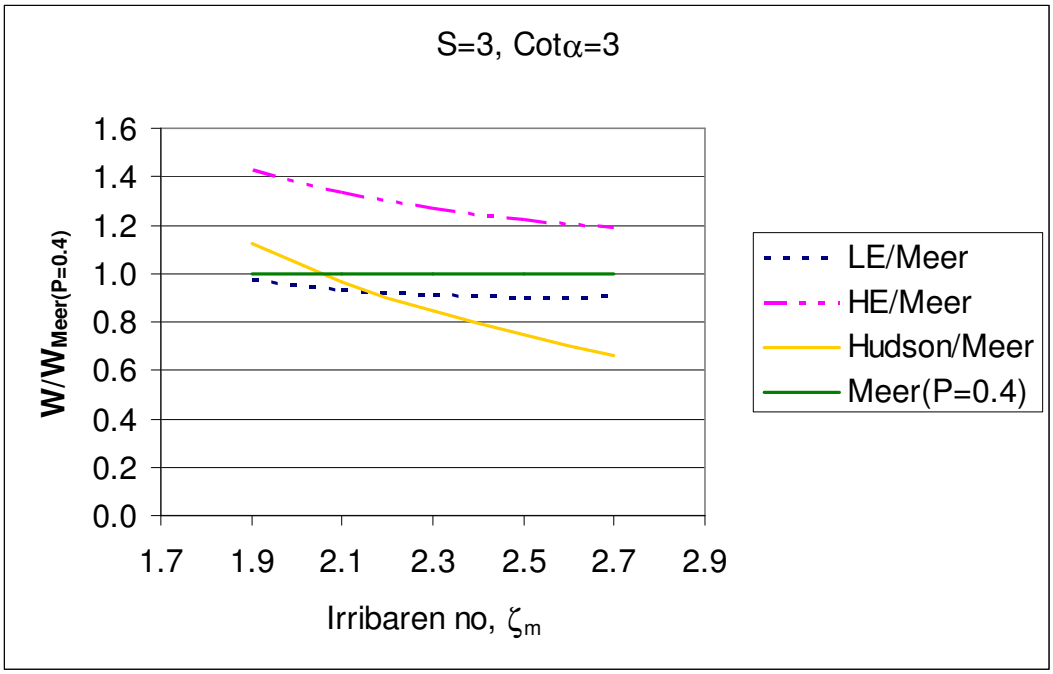

Fig. 4.22 Weight ratios of experiment cases LE and HE, Meer's equationd with P=0.4

Hudson formula underestimates the necessary weight for ζ_m>2 comparing with Meer's formula. Underestimation increase as ζ_m increase (approaching to transition zone).

The same comparison was done for Meer's equation with P=0.45. The results are demonstrated in Table 4.14. Tabulated values were plotted in Fig. 4.23.

Table 4.14 Weight ratios of experiment cases LE and HE and Meer's equation with P=0.45 (cotα=3, S=3)

Irribaren no, ζ	LE/Meer	HE/Meer	Hudson/Meer	Meer (P=0.45)
1.9	1.039	1.519	1.199	1
2.1	0.995	1.421	1.032	1
2.3	0.970	1.350	0.900	1
2.5	0.961	1.301	0.794	1
2.7	0.965	1.270	0.708	1

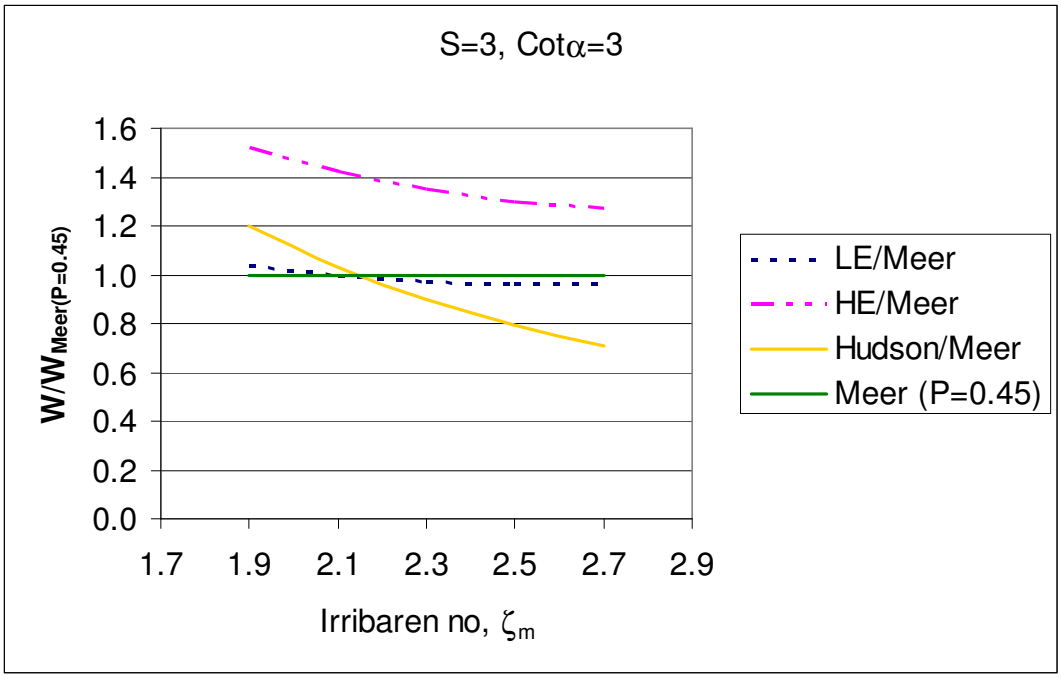

Fig. 4.23 Weight ratios of experiment cases LE and HE,and Hudson formula to Meer's formula with P=0.45

According to Table 4.14 and Fig. 4.23, weight difference between experiment case of HE and Meer's equation increased to 51.9% from 42.5%. Therefore, increase of permeability factor P from 0.4 to 0.45 caused almost 10% more increase in the weight.

If it is assumed that stability curves of experimental cases are parallel to Meer's curve with P=0.45, then it is calculated that W/WMeer=1.39 for HE and it is 1 for LE for all ζ_m.

Hudson formula underestimates the necessary weight for ζ_m>2.15 comparing with Meer's formula. For ζ_m<2.15, values of Hudson are between the experiment case HE and Meer's results.

Results on weight ratios of experimental cases LE and HE to Meer's formula are summarised in Table 4.15 under the assumption of that stability curves of experimental cases are parallel to Meer's curve with P=0.4 and 0.45. Weight ratio range corresponding to ζ_m values were also given in brackets.

Table 4.15 Summary of the results on weight ratios of experimental cases LE and HE to Meer's formula

	W_{LE}/W_{Meer}	W_{HE}/W_{Meer}	W_{LE}/W_{Meer}	W_{HE}/W_{Meer}	
P	0.4	0.4	0.45	0.45	ζ_m
cotα=1.5 S=2	0.86 (0.95-0.76)	1.23 (1.26-1.20)	1.05 (1.15-0.95)	1.5 (1.52-1.49)	all (4.7-5.9)
cotα=3 S=2	1.07 (0.87-1.27)	1.32 (1.23-1.4)	1.14 (0.92-1.36)	1.4 (1.31-1.5)	all (2-2.6)
cotα=3 S=3	0.94 (0.9-0.98)	1.31 (1.19-1.42)	1 (0.96-1.04)	1.39 (1.27-1.52)	all (1.9-2.7)

As it can be seen from Table 4.15, considering the slope of cotα=3, weight ratios of experimental case HE to Meer's formula is very similar for both the damage level of S=2 and S=3. This result is valid for both of the permeability factors P=0.4 and 0.45. For the case LE, weight ratios belong the damage level of S=2 and S=3 are different. The reason may be due to inconsistent trend of LE case for S=2. Therefore it may be meaningful to take W_{LE}/W_{Meer} ratio obtained from S=3 curve into account.

If the experiment cases are compared with Meer's formula with P=0.4, then it may be necessary to increase weight of armour layer stone 23% for cotα=1.5 and 30% for cotα=3 on the average for all ζ_m in the range given in Table 4.1 in the last column. On the other hand, Meer's formula overestimates the weight 14% for cotα=1.5 and 6% for cotα=3 according to the Table 4.1.

If the experiment cases are compared with Meer's formula with P=0.45, then increase in weight of armour layer stone may be 40-50% on the average for all ζ_m in the range given in Table 4.1 for cotα=1.5 and cotα=3, respectively. Weight ratios of W_{LE}/W_{Meer} are almost equal to 1 that indicates the underestimation of Meer's formula when permeability increases.

4.3.1. Comparison between experiment cases and Hudson formula

In order to make a better comparison between the experiment cases LE, HE and Hudson formula, weight ratios were calculated by dividing weight coefficients of experiment cases to the weight coefficient of Hudson formula given in Table 4.4. The results were tabulated in Table 4.16 and plotted in Fig.4.24 for cotα=1.5.

Table 4.16 Weight ratios of experiment cases LE, HE and Hudson Formula (cotα=1.5)

	Weight ratios		
Irribaren no, ζ_m	LE/Hudson	HE/Hudson	Hudson
4.7	1.784	2.355	1
4.9	1.631	2.226	1
5.1	1.496	2.107	1
5.3	1.375	1.995	1
5.5	1.266	1.892	1
5.7	1.169	1.796	1
5.9	1.081	1.706	1

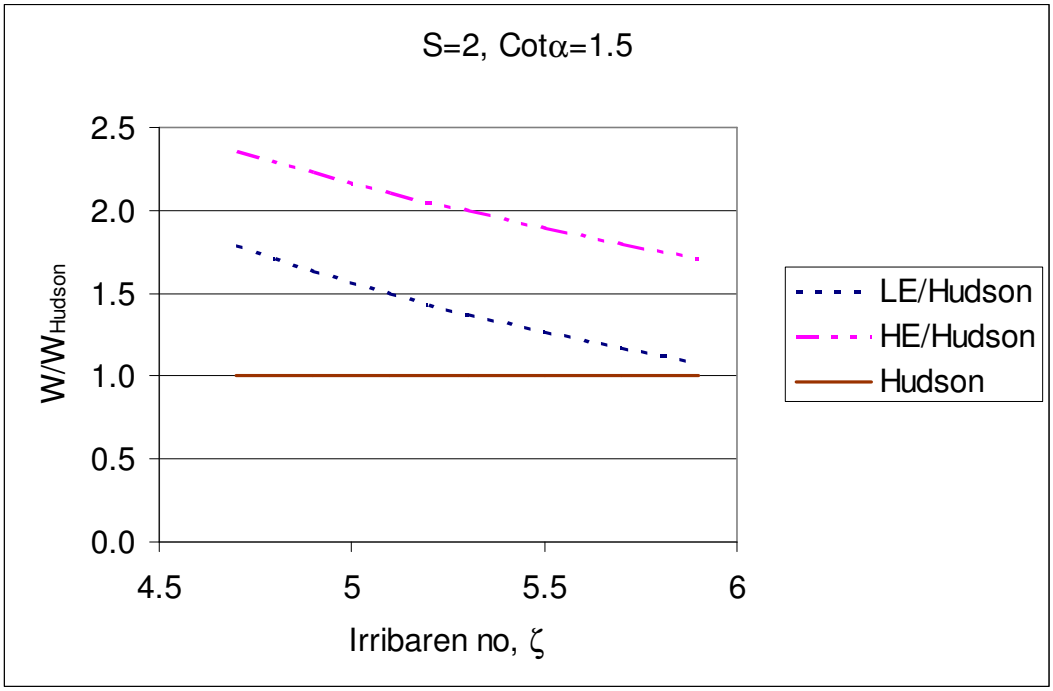

Fig.4.24 Weight ratios of experiment cases LE, HE and Hudson Formula (cotα=1.5)

As it can be seen from Table 4.16 and Fig.4.24, Hudson formula underestimates the necessary weight as almost half of the weight resulted from experiment cases. As ζ_m increase (away from transition zone), result of Hudson starts to approach to experiment, LE, results. This may be due to that Hudson formula does not include the effect of wave period and so there is not a decrease in the stability while approaching to transition zone.

For the slope cotα=3, weight comparison results for S=2 were tabulated in Table 4.17 and plotted in Fig.4.25.

Table 4.17 Weight ratios of experiment cases LE, HE and Hudson Formula (cotα=3, S=2)

	Weight ratios		
Irribaren no, ζ_m	LE/Hudson	HE/Hudson	Hudson
2	1.553	1.719	1
2.2	1.561	1.870	1
2.4	1.568	2.039	1
2.6	1.576	2.229	1

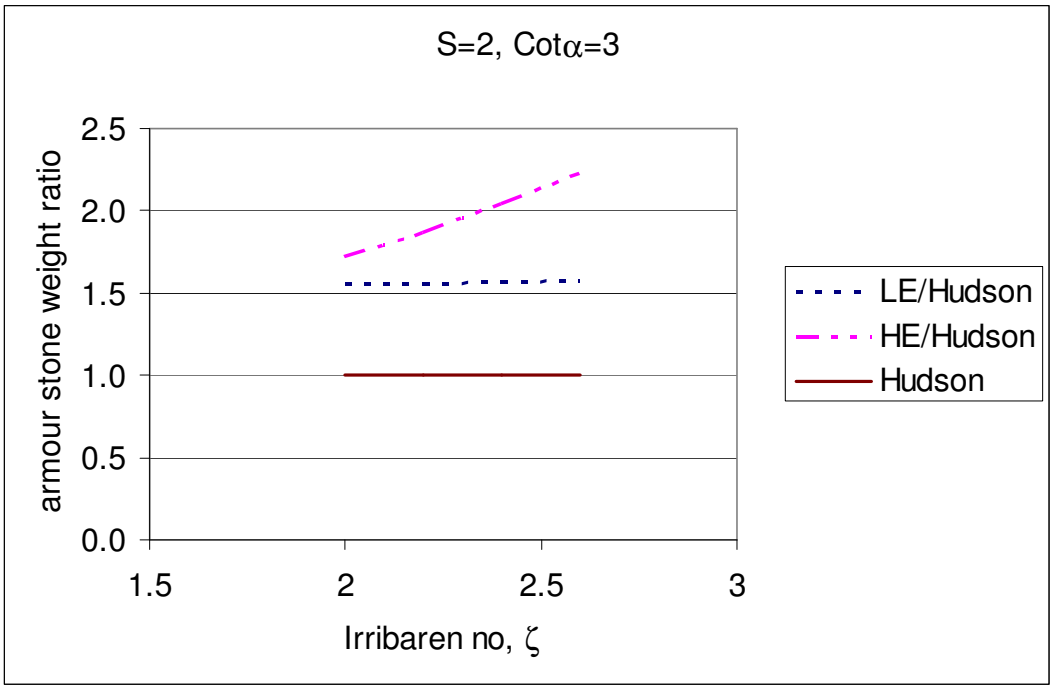

Fig.4.25 Weight ratios of experiment cases LE, HE and Hudson Formula (cotα=3, S=2)

According to Table 4.17 and Fig.4.25, similar to the slope of cotα=1.5, Hudson formula underestimates the necessary weight. Underestimation is almost half of the experiment cases. As being away from transition zone, result of Hudson starts to approach to experiment LE case.

If no damage definition is corresponded to S=3 for cotα=3, then weight ratios were obtained using Table 4.12. The results were given in table 4.18

Table 4.18 Weight ratios of experiment cases LE, HE and Hudson Formula (cotα=3, S=3)

	Weight ratios		
Irribaren no, ζ_m	LE/Hudson	HE/Hudson	Hudson
1.9	0.866	1.267	1
2.1	0.964	1.377	1
2.3	1.078	1.500	1
2.5	1.209	1.638	1
2.7	1.364	1.793	1

As Table 4.18 indicates, Hudson formula underestimates the necessary weight for ζ_m>2.2 comparing with experiment cases. For ζ_m<2.2, Hudson's result is between experiment LE and HE cases. Underestimation increase as ζ_m increase (approaching to transition zone).

CHAPTER 5

OCCURANCE PROBABILITY OF EXTREME WAVES IN A WAVE TRAIN

In Chapter 4, it was demonstrated that waves which have higher $\alpha_{extreme}$ are more destructive comparing with having lower $\alpha_{extreme}$. Moreover, when the analysis was carried into design conditions, it was calculated that structure may need 26% heavier weight for the armour layer in order to stand high extreme waves comparing Meer's formula with P=0.4 cotα=1.5 and it may increase up to 42.5% for cotα=3. Therefore it was concluded that extreme wave heights in a wave train is important considering the stability of rubble mound breakwaters. It seems that one characteristic wave height like mostly used $H_{1/3}$ or $H_{1/10}$ is not enough to represent the effect of extreme waves in a sea state. But designers generally can get information only about significant wave height and period. It is also possible to fit spectrum of any sea state to a standard spectrum by using field measurements. Therefore, if a relation between spectral shape and extreme waves in a wave train is set up, it might be a useful tool to a designer who has the information about the spectral shape of design waves.

5.1. Relation between Spectral Shape and Extreme Waves in a Wave Train

In order to investigate the relation between spectral shape and extreme waves in a wave train a numerical simulation study was done. In the simulation, time series were generated for different shapes of energy spectrum by Deterministic Spectral Amplitude (DSA) model. DSA model was explained in Chapter 3. Spectral shapes used in this study are the same ones given in Table 3.1, Chapter 3. After time series were generated,

$\alpha_{extreme}$ value was calculated for each series and then average values and probability density functions (pdf) of $\alpha_{extreme}$ are obtained for each spectral shape.

But first of all, the sensitivity of pdf to the selection of significant wave height and period, data number, simulation realization number, was checked by changing these parameters. N=16384 data points with Δt=0.5 seconds interval, $H_{1/3}$= 4 m and $T_{1/3}$= 8 sec were taken for one simulation as an initial step and the number of simulation realizations was changed from 50 to 10000. The result is shown in Fig. 5.1 (a) and (b). The figures belong to Spectral Shape J10 as an example, but other Spectral Shapes have the same tendency. According to the Fig. 5.1 (a), after 100 simulations result becomes statistically stable. In order to be safe side, it was decided to use 1000 simulations for each spectral shape. Then the effect of significant wave height and period on the probability densities was investigated. As it was expected, the change in wave height or period does not have significant influence on pdf as a result of linear simulation. After then, keeping the number of simulation realizations (1000), data interval (0.5sec), significant wave height (4m) and period (8sec) constant, the number of data points was changed from 1024 to 65536. The result is shown in Fig. 5.1 (b).

It is seen from the figures that small number of data points that is, small number of wave carries serious statistical variations. After 32768 data (approximately 2000 waves) the probability densities becomes statistically stable.

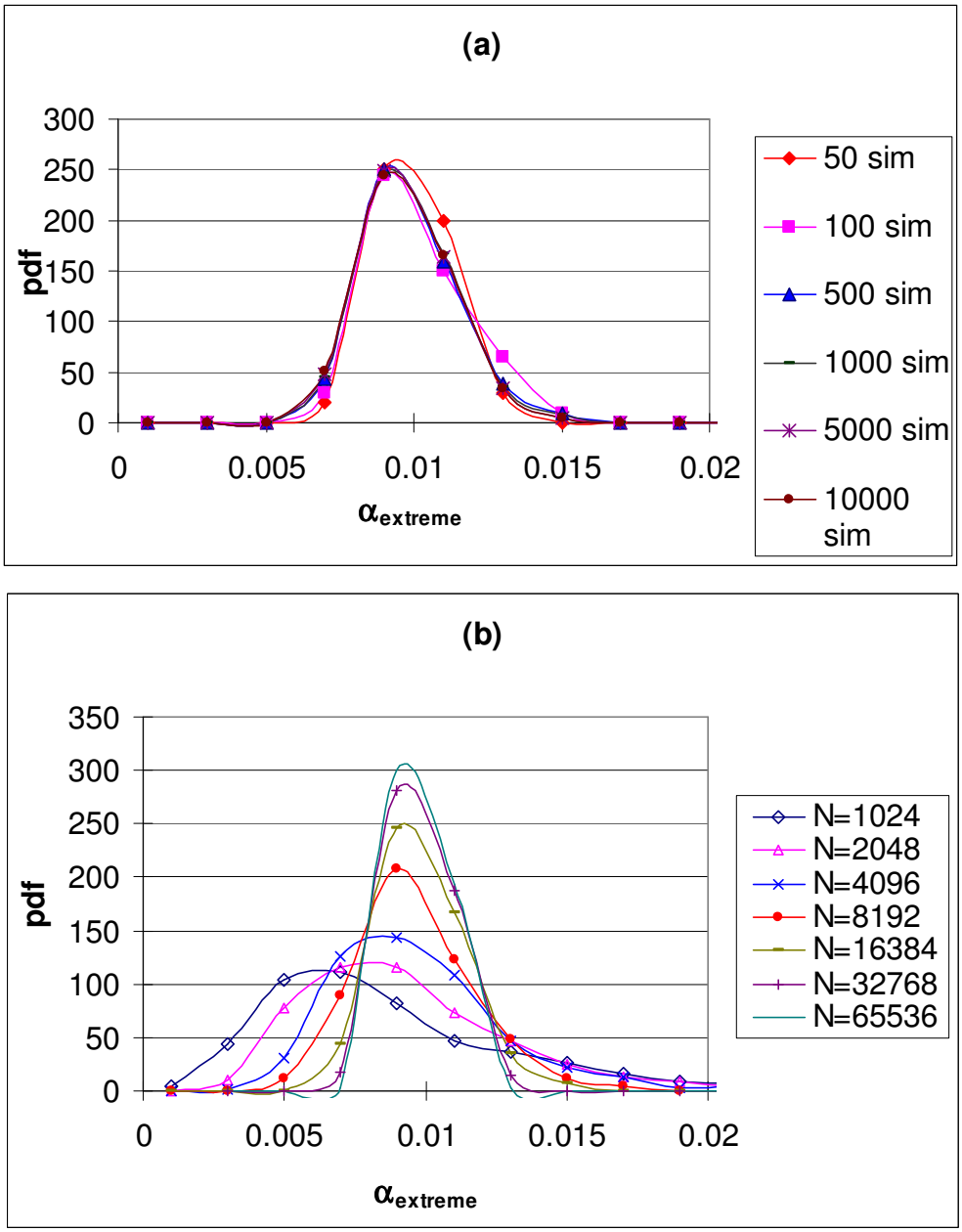

Fig. 5.1 Sensitivity of pdf of mean run length and exceedance parameter: (a) effect of simulation realization number (N=16384, Δt=0.5 sec, $H_{1/3}$=4m, T1/3=8sec); (b) effect of data points' number in one simulation (Δt=0.5sec, $H_{1/3}$=4m, $T_{1/3}$=8sec, 1000 simulations)

Therefore, 32768 data is chosen as suitable number for probability density analysis of wave grouping. In the Fig. 5.1, ordinates were normalized in order to get the area under the curve as unity.

After getting appropriate values of numerical simulations' parameters to obtain a stable statistics, 1000 simulations were realized for each shape of the spectrum. The parameter, $\alpha_{extreme}$, was calculated for every realization and probability densities were calculated using 1000 simulation results. The most probable $\alpha_{extreme}$ and standard deviation of it for each shape of the spectrum is given in Table 5.1. According to Table 5.1, as mean value increase standard deviation and the variation coefficient, v, also increase for extreme wave parameter, $\alpha_{extreme}$. In fact, it is found that there is a linear relationship between average of $\alpha_{extreme}$, μ, and standard deviation, σ, and variation coefficient, v. Equations of linearity are as follows:

$$\frac{\sigma}{\mu} = 41.084\mu - 0.2934 \tag{5.1}$$

Table 5.1 Average, μ, Standard Deviation, σ, and Variation Coefficient, v, of $\alpha_{extreme}$ for Different Spectral Shapes

Spectral Shape	μ	σ	v=σ/μ
PM	0.0089	0.0007	0.075
J33	0.0093	0.0008	0.086
J10	0.0098	0.0010	0.107
W	0.0103	0.0014	0.132

According to Table 5.1, the narrower and sharper the spectrum shape is, the higher the expected $\alpha_{extreme}$ is.

Probability density functions and exceedance probabilities of $\alpha_{extreme}$ were plotted in Fig. 5.2 and 5.3, respectively. In Fig 5.2, ordinate pdf represents probability density which is relative frequency divided by the dx which is class interval of $\alpha_{extreme}$. Then, probability of $\alpha_{extreme}$ taking the value between x and x+dx is obtained by the product pdf value (p(x)dx. According to the Figs 5.2 and 5.3, it is more probable to get high $\alpha_{extreme}$ parameter for narrow spectrum comparing to broad one.

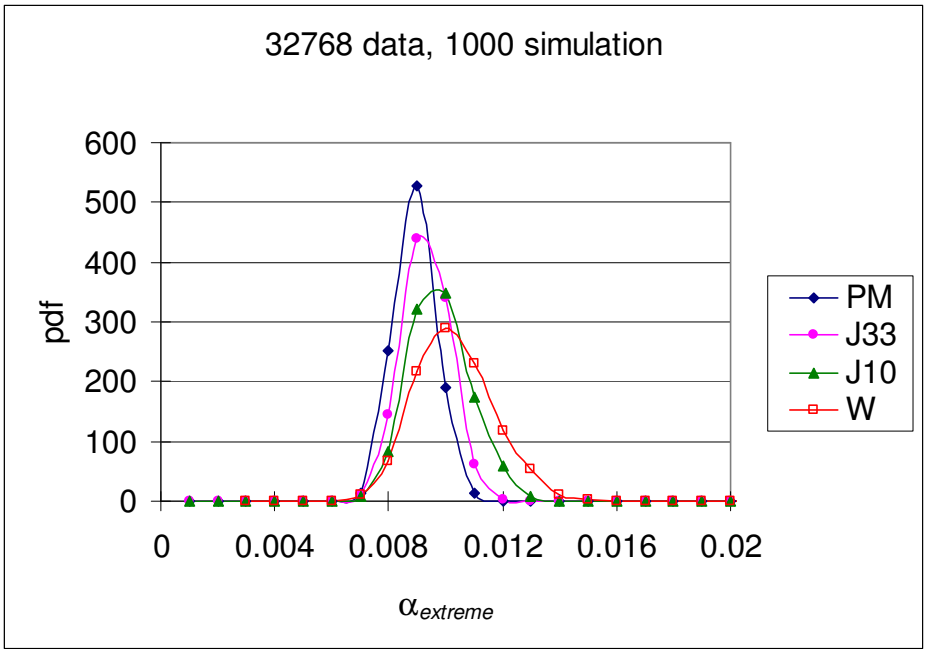

Fig. 5.2 Probability density of extreme wave parameter, $\alpha_{extreme}$, for each of the spectral shape

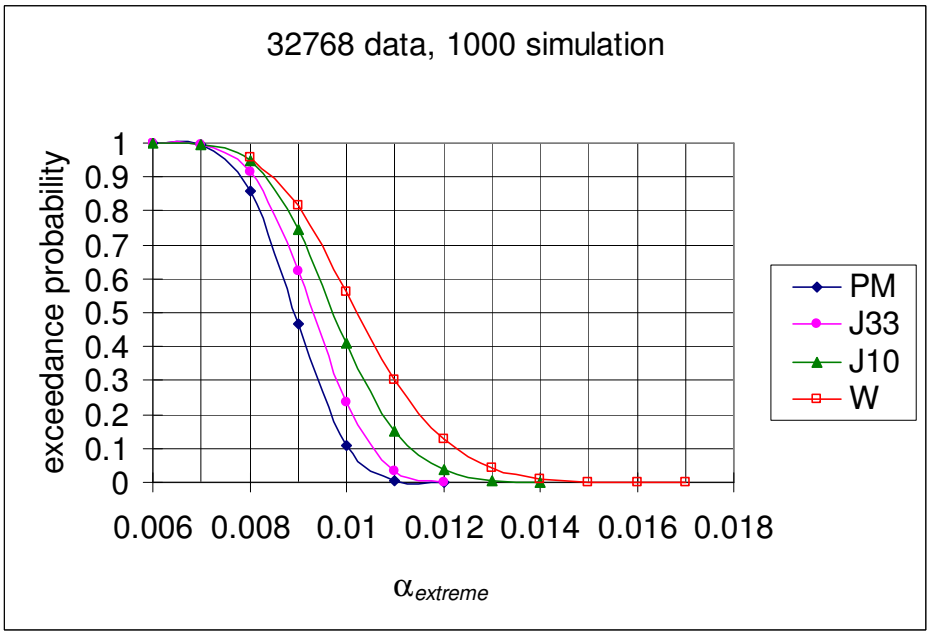

Fig. 5.3 Exceedance Probability of extreme wave parameter, $\alpha_{extreme}$, for Each of the Spectral Shape

As it can be seen in Fig. 5.3 the probability of having $\alpha_{extreme}$ more than 0.009 is 48% for PM spectrum, 62% for J33 spectrum, 75% for J10 and 81% for W spectrum.

5.2. Engineering Application

In the present study, it was shown by hydraulic model experiments that wave train with high $\alpha_{extreme}$ may affect the design weight of armour layer stone. Also, by numerical simulations, occurrence probability of $\alpha_{extreme}$ under different spectral shapes has been obtained. These results will be used together in an afford to achieve more practical tools for engineering applications.

As a result of experimental work carried out, weight ratios were obtained from the evaluation of the effect of $\alpha_{extreme}$ on the stability of armour layer of rubble mound breakwaters and suggested to be used in the engineering applications. These results will now be given together with the occurrence probability of $\alpha_{extreme}$ for cotα=1.5 and 3 and for weight ratios of experiment result to Meer 's formula with P=0.4 and 0.45.

As it was stated before, during the hydraulic model experiments, $\alpha_{extreme}$ is 0.007 in the test series called as low $\alpha_{extreme}$ case (LE) and it is 0.0105 in the test series called as high $\alpha_{extreme}$ (HE). Using these values it is possible to obtain occurrence probabilities of LE and HE cases for different spectral shapes from Fig. 5.3. In his work, Van der Meer (1988) used PM spectrum while deriving his formulae. Since there is not any information about $\alpha_{extreme}$ in his tests and he was not interested in extreme waves in his test series, the value of $\alpha_{extreme}$ was assumed to be a median value of $\alpha_{extreme}$ belonging to PM spectrum which is almost 0.089.

5.2.1 Computation for cotα=1.5 and P=0.4

Using the values of $\alpha_{extreme}$ for the cases LE, Meer and HE, exceedance probabilities of $\alpha_{extreme}$ were taken from Fig 5.3 for each spectral shape. Those probabilities were matched with the weight ratios of experiment cases LE and HE to Meer's equation with P=0.4 for the corresponding ζ_m

values given in Table 4.5, Chapter 4. As a result, exceedance probabilities of weight ratios for different spectral shapes were obtained and tabulated in Table 5.2 for cotα=1.5.

Table 5.2 Exceedance probabilities of weight ratios ($W/W_{Meer(P=0.4)}$) for different spectral shapes (cotα=1.5)

ζ=4.7

Case	$W/W_{Meer(P=0.4)}$	PM	J33	J10	W
LE	0.954	0.995	0.995	0.995	0.995
Meer	1.000	0.500	0.624	0.747	0.815
HE	1.260	0.058	0.135	0.282	0.431

ζ=4.9

Case	$W/W_{Meer(P=0.4)}$	PM	J33	J10	W
LE	0.917	0.995	0.995	0.995	0.995
Meer	1.000	0.500	0.624	0.747	0.815
HE	1.252	0.058	0.135	0.282	0.431

ζ=5.1

Case	$W/W_{Meer(P=0.4)}$	PM	J33	J10	W
LE	0.882	0.995	0.995	0.995	0.995
Meer	1.000	0.500	0.624	0.747	0.815
HE	1.243	0.058	0.135	0.282	0.431

ζ=5.3

Case	$W/W_{Meer(P=0.4)}$	PM	J33	J10	W
LE	0.849	0.995	0.995	0.995	0.995
Meer	1.000	0.500	0.624	0.747	0.815
HE	1.233	0.058	0.135	0.282	0.431

ζ=5.5

Case	$W/W_{Meer(P=0.4)}$	PM	J33	J10	W
LE	0.818	0.995	0.995	0.995	0.995
Meer	1.000	0.500	0.624	0.747	0.815
HE	1.222	0.058	0.135	0.282	0.431

ζ=5.7

Case	$W/W_{Meer(P=0.4)}$	PM	J33	J10	W
LE	0.788	0.995	0.995	0.995	0.995
Meer	1.000	0.500	0.624	0.747	0.815
HE	1.211	0.058	0.135	0.282	0.431

ζ=5.9

Case	$W/W_{Meer(P=0.4)}$	PM	J33	J10	W
LE	0.760	0.995	0.995	0.995	0.995
Meer	1.000	0.500	0.624	0.747	0.815
HE	1.199	0.058	0.135	0.282	0.431

The weight ratio versus exceedance probability plots for different spectral shapes were given in Fig. 5.4. This figure is just example for cotα=1.5 and ζ_m=4.7. Plots for other ζ_m values were given in Appendix B.

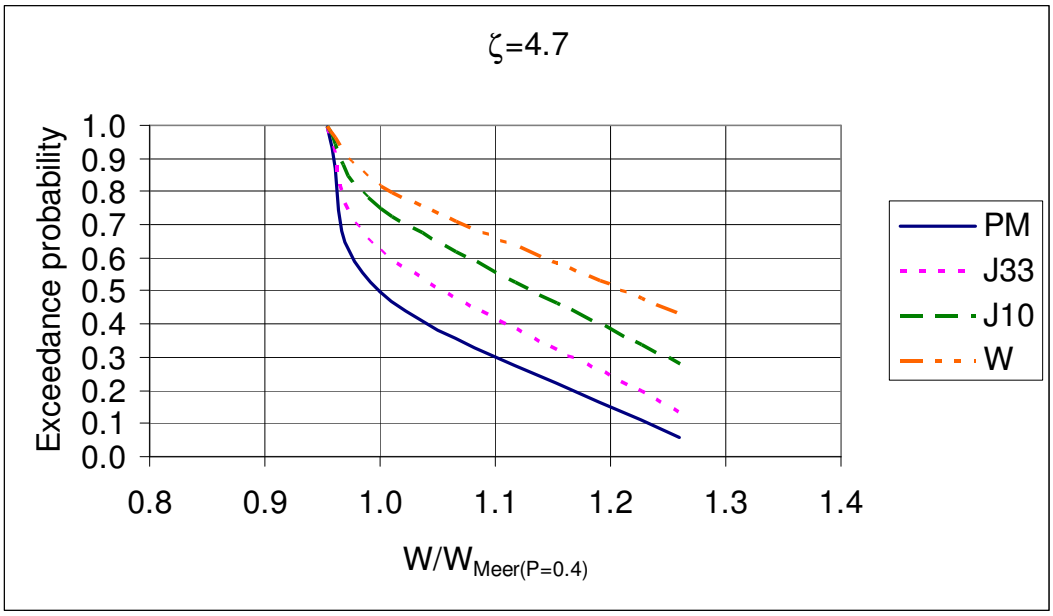

Fig. 5.4 Weight ratio versus exceedance probability for different spectral shapes (cotα=1.5, P=0.4)

As it can be seen from the Fig. 5.4, possibility of need for heavier armour stone than the calculated weight from Meer's equation with P=0.4 increases as spectral shape becomes narrower. For example considering the most probable (average) case, $W/W_{Meer(P=0.4)}$ =1 for PM, 1.06 for J33, 1.13 for J10 and 1.21 for W spectrum. It means that for the condition of ζ_m=5.7 and structure slope, cotα=1.5, necessary weight of armour stone calculated by Meer formula with P=0.4 will be enough if the spectrum is PM. But if spectrum is narrower than PM, then up to 21% increase of weight may be needed.

Among the spectrum types, PM and J33 are the most widely used spectrums. Because, it is known from the extensive field measurements that PM and J33 spectrums are good representatives of fully developed and

developing sea states, respectively. Therefore it would be more practical to see occurrence probability of weight ratios for PM and J33 spectrums. Weight ratios versus exceedance probability plot of PM spectrum for different ζ_m and cotα=1.5 was given in Fig 5.5. In the Fig. 5.5, levels belong to the most probable 20% (50%±10) and 60% (50%±30) of occurrence were drawn, also. From pdf of $\alpha_{extreme}$ for PM spectrum given in Fig 5.3, it was calculated that the most probable 60% of occurrence of $\alpha_{extreme}$ corresponds to $\mu_{\alpha extreme} \pm \sigma_{\alpha extreme}$ where $\mu_{\alpha extreme}$ =0.0089 and $\sigma_{\alpha extreme}$ =0.0007 as given in Table 5.1. The most probable 20% of occurrence of $\alpha_{extreme}$ corresponds to $\mu_{\alpha extreme} \pm 0.3\sigma_{\alpha extreme}$.

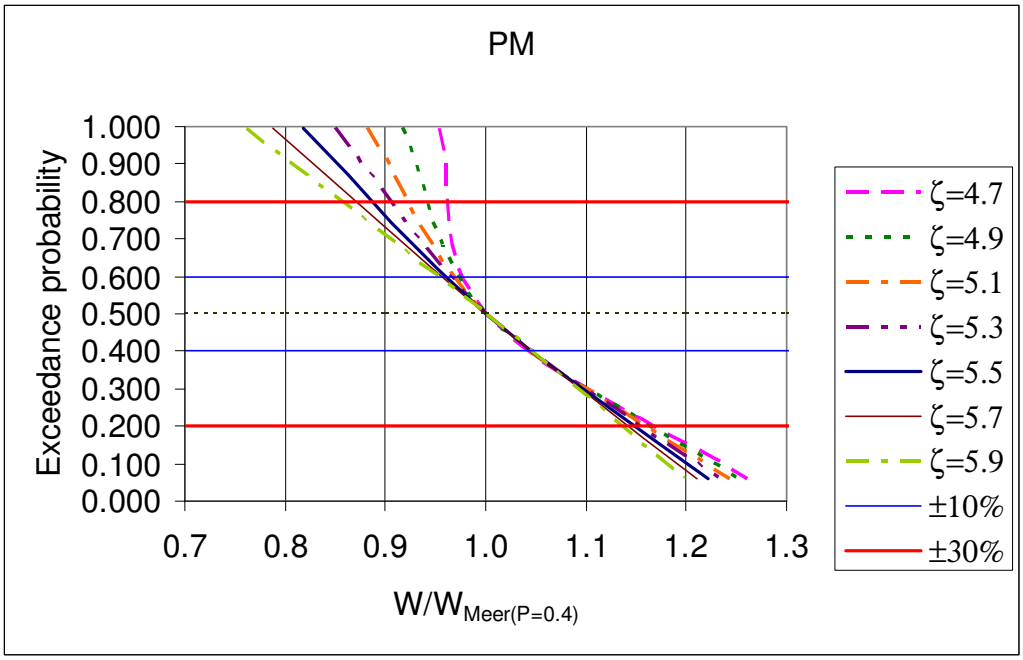

Fig. 5.5 Exceedance probability of weight ratios for PM spectrum (cotα=1.5, P=0.4)

Weight ratios of PM spectrum belonging to these probability levels shown in Fig 5.5 were tabulated for each ζ_m in Table 5.3. Finally, ζ_m versus weight ratios taken from Table 5.3 was plotted in Fig. 5.6.

Table 5.3 Weight ratios for PM spectrum (cotα=1.5, P=0.4)

PM	30%	10%	median	-10%	-30%
4.7	1.160	1.040	1.000	0.980	0.960
4.9	1.155	1.040	1.000	0.975	0.940
5.1	1.150	1.040	1.000	0.970	0.920
5.3	1.145	1.040	1.000	0.965	0.900
5.5	1.140	1.040	1.000	0.960	0.880
5.7	1.135	1.040	1.000	0.955	0.860
5.9	1.130	1.040	1.000	0.950	0.840

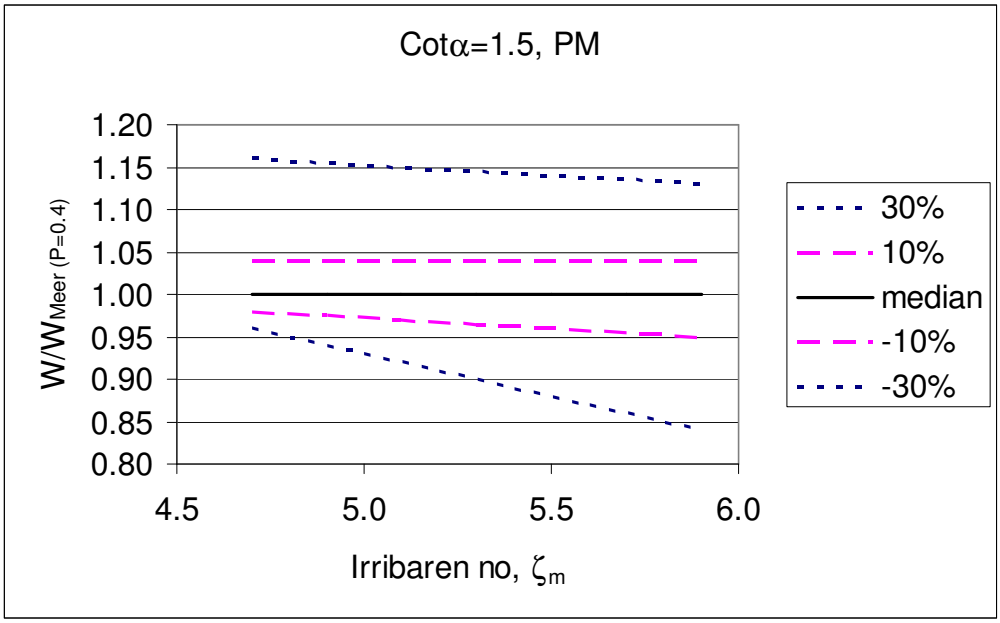

Fig. 5.6 Weight ratios of PM spectrum for each ζ_m in a range of 4.7-5.7 (cotα=1.5, P=0.4)

According to Table 5.3 and Fig. 5.6 Meer's equations estimates well the weight of armour stone on the average (median) for the spectrum PM. For the most probable 20% of occurrence of $\alpha_{extreme}$, the necessary weight has a maximum range of 0.95-1.04 times of Meer's result for ζ_m=5.9. When the occurance probability of $\alpha_{extreme}$ increases to 60%, that is the possibility of having $\alpha_{extreme}$ within $\mu\pm\sigma$, then weight ratio is between (0.96-1.16) for ζ_m=4.7 and it is between (0.84-1.13) for ζ_m=5.9. Therefore necessary

weight may increase to 1.16 times of Meer's result due to high extreme waves.

Repeating the procedure for the spectrum J33, weight ratios versus exceedance probability plot of J33 spectrum for different ζ_m and cotα=1.5 was drawn in Fig 5.7. In the Fig. 5.7, levels belongs to the most probable 20% (50%±10) and 60% (50%±30) of occurrence were drawn, also. From pdf of $\alpha_{extreme}$ for J33 spectrum given in Fig 5.3, it was calculated that the most probable 60% of occurrence of $\alpha_{extreme}$ corresponds to $\mu_{\alpha extreme} \pm \sigma_{\alpha extreme}$ where $\mu_{\alpha extreme}$ =0.0093 and $\sigma_{\alpha extreme}$ =0.0008 as given in Table 5.1. The most probable 20% of occurrence of $\alpha_{extreme}$ corresponds to $\mu_{\alpha extreme} \pm 0.3\sigma_{\alpha extreme}$.

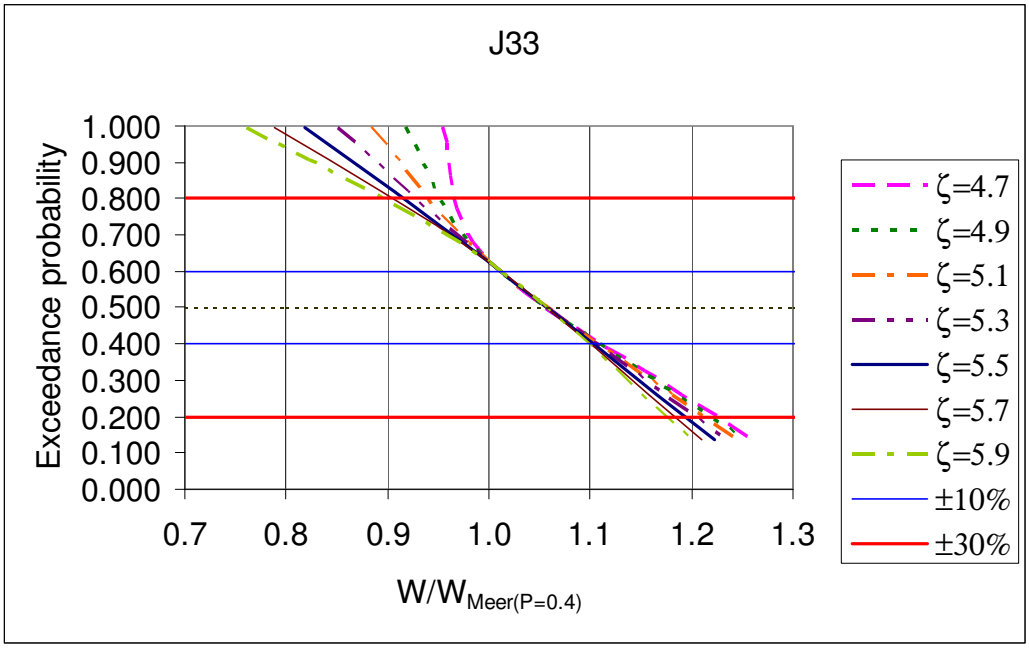

Fig. 5.7 Exceedance probability of weight ratios for J33 spectrum (cotα=1.5, P=0.4)

Weight ratios of J33 spectrum belonging to these probability levels shown in Fig 5.7 were tabulated for each ζ_m in Table 5.4. Then, ζ_m versus weight ratios taken from Table 5.4 was plotted in Fig. 5.8.

Table 5.4 Weight ratios of J33 spectrum (cotα=1.5, P=0.4)

J33	30%	10%	median	-10%	-30%
4.7	1.220	1.090	1.050	1.010	0.965
4.9	1.212	1.094	1.052	1.010	0.950
5.1	1.204	1.098	1.054	1.010	0.935
5.3	1.196	1.102	1.056	1.010	0.920
5.5	1.188	1.106	1.058	1.010	0.905
5.7	1.180	1.110	1.060	1.010	0.890
5.9	1.172	1.114	1.062	1.010	0.875

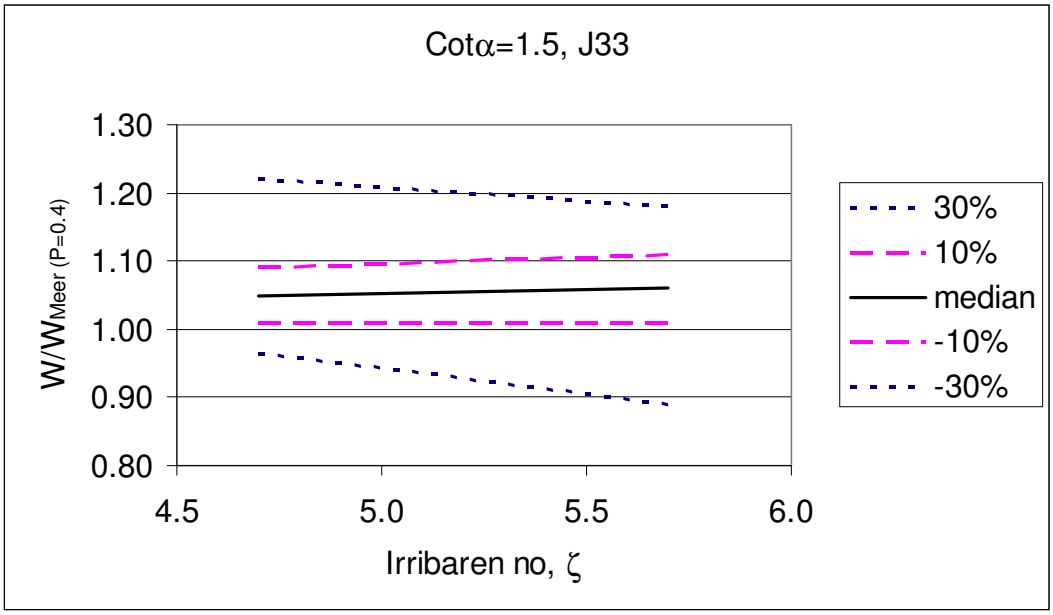

Fig. 5.8 Weight ratios of J33 spectrum (cotα=1.5, P=0.4)

As it can be seen in Table 5.4 and Fig. 5.8, Meer's equation underestimates the weight 5%-6% when the spectrum is J33 on the average. Underestimation can increase to 22%, if the range of occurrence probability of $\alpha_{extreme}$ is the most probable 60%. Weight ratio difference of PM and J33 spectrums come from that the possibility of having high $\alpha_{extreme}$ is higher for J33 spectrum than it is for PM spectrum.

5.2.2 Computation for cotα=1.5 and P=0.45

Using the values of $\alpha_{extreme}$ for the cases LE, Meer and HE, exceedance probabilities of $\alpha_{extreme}$ were taken from Fig 5.3 for each spectral shape. Those probabilities were matched with the weight ratios of experiment cases LE and HE to Meer's equation with P=0.45 for the corresponding ζ_m values given in Table 4.6, Chapter 4. As a result, exceedance probabilities of weight ratios for different spectral shapes were obtained and tabulated in Table C.1 in Appendix C for cotα=1.5.

Weight ratios versus exceedance probability plot of PM spectrum for different ζ_m and cotα=1.5 was given in Fig. C.1, Appendix C. In the Fig. C.1, levels belong to the most probable 20% (50%±10) and 60% (50%±30) of occurrence were drawn, also.

Weight ratios of PM spectrum belong to these probability levels shown in Fig C.1 were tabulated for each ζ_m in Table 5.5. Finally, ζ_m versus weight ratios taken from Table 5.5 was plotted in Fig. 5.9.

Table 5.5 Weight ratios of PM spectrum (cotα=1.5, P=0.45)

PM	30%	10%	median	-10%	-30%
4.7	1.340	1.110	1	1	1
4.9	1.340	1.110	1	1	1
5.1	1.340	1.110	1	1	1
5.3	1.340	1.110	1	1	1
5.5	1.340	1.110	1	1	1
5.7	1.340	1.110	1	0.995	0.985
5.9	1.340	1.110	1	0.990	0.970

According to Table 5.5 and Fig. 5.9 Meer's equation estimates well the weight of armour stone on the average (median) for the spectrum PM. For the most probable 20% of occurrence of $\alpha_{extreme}$, the necessary weight increase up to 1.11 times of Meer's result. When the occurrence probability

of $\alpha_{extreme}$ increases to 60%, that is the possibility of having $\alpha_{extreme}$ within $\mu\pm\sigma$, then necessary weight is 34% more than of Meer's result. It was 13-16% in the case of P= 0.4. The difference comes from the permeability effect on the Meer's formula which is more effective for the slope $\cot\alpha$=1.5 due to surging waves. Weight ratio is almost same for all ζ_m since the experiment curves, especially HE curve, are almost parallel to Meer's stability curve with P=0.45.

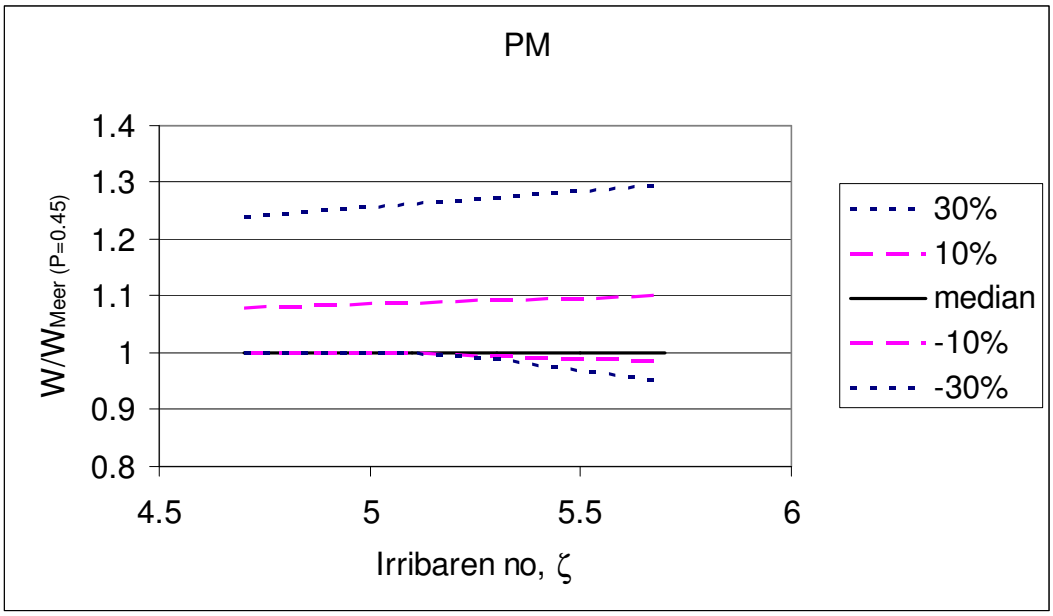

Fig. 5.9 Weight ratios of PM spectrum ($\cot\alpha$=1.5, P=0.45)

Repeating the procedure for the spectrum J33, weight ratios versus exceedance probability plot of J33 spectrum for different ζ_m and $\cot\alpha$=1.5 was drawn in Fig C.2, Appendix C. In the Fig. C.2, levels belongs to the most probable 20% (50%±10) and 60% (50%±30) of occurrence were drawn, also. Weight ratios of J33 spectrum belong to these probability levels shown in Fig C.2 were tabulated for each ζ_m in Table 5.6. Then, ζ_m versus weight ratios taken from Table 5.6 were plotted in Fig. 5.10.

Table 5.6 Weight ratios of J33 spectrum (cotα=1.5, P=0.45)

J33	30%	10%	median	-10%	-30%
4.7	1.430	1.230	1.130	1.020	1
4.9	1.430	1.230	1.130	1.020	1
5.1	1.430	1.230	1.130	1.020	1
5.3	1.430	1.230	1.130	1.020	1
5.5	1.430	1.230	1.130	1.020	1
5.7	1.430	1.230	1.130	1.020	0.990
5.9	1.430	1.230	1.130	1.020	0.975

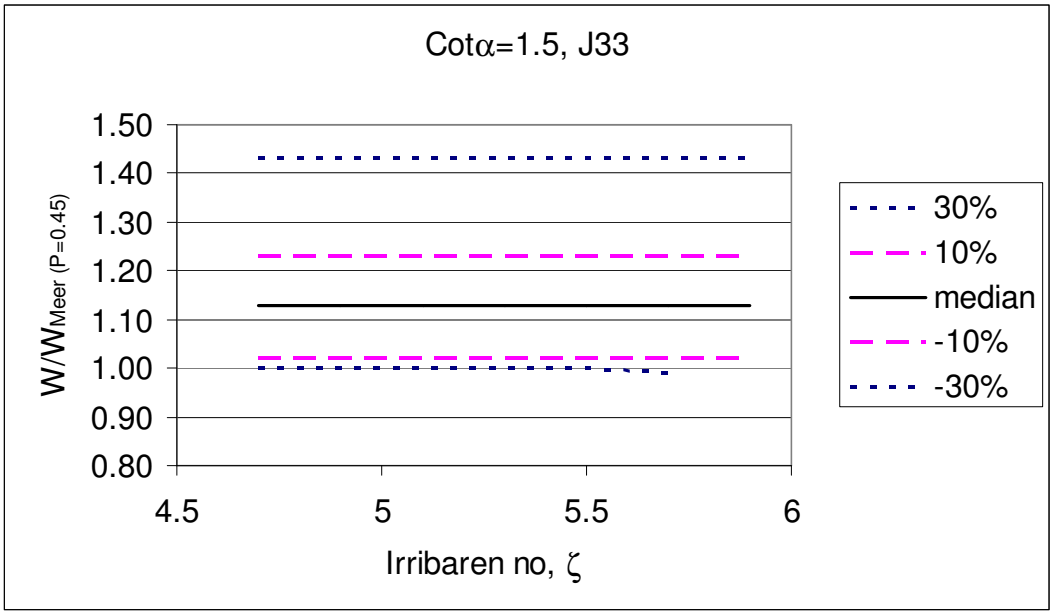

Fig. 5.10 Weight ratios of J33 spectrum (cotα=1.5, P=0.45)

As it can be seen in Table 5.6 and Fig. 5.10, Meer's equation underestimates the weight 13% when the spectrum is J33 on the average. Underestimation can increase to 23%, if the range of occurrence probability of $\alpha_{extreme}$ is the most probable 20% for all ζ_m. When the occurance probability of $\alpha_{extreme}$ increases to 60%, that is the possibility of having $\alpha_{extreme}$ within $\mu\pm\sigma$, then necessary weight is 43% more than of Meer's result for all ζ_m. It was 34% for the spectrum PM. Weight ratio difference of PM and J33 spectrums come from that the possibility of having high $\alpha_{extreme}$ is

higher for J33 spectrum than it is for PM spectrum. Weight ratio increase was 17-22% in the case where experiment case is compared with Meer's formula for P=0.4. The reason is that Meer's formula predicts less weight when permeability increase and this makes the weight difference between experiment result and Meer's formula to increase.

5.2.3 Computation for cotα=3 and P=0.4

Using the values of $\alpha_{extreme}$ for the cases LE, Meer and HE, exceedance probabilities of $\alpha_{extreme}$ were taken from Fig 5.3 for each spectral shape. Those probabilities were matched with the weight ratios of experiment cases LE and HE to Meer's equation with P=0.4 for the corresponding ζ_m values given in Table 4.13. Table 4.13 is the result of weight ratios for cotα=3 and S=3. It is chosen since it was demonstrated in Chapter 4 that weight ratios of experimental case HE to Meer's formula is very similar for both the damage level of S=2 and S=3 and further, for the case LE, it was said that it might be meaningful to take W_{LE}/W_{Meer} ratio obtained from S=3 curve into account because of its consistent trend. As a result, exceedance probabilities of weight ratios for different spectral shapes were obtained and tabulated in Table 5.7 for cotα=3.

Table 5.7 Exceedance probabilities of weight ratios ($W/W_{Meer(P=0.4)}$) for different spectral shapes ($\cot\alpha$=1.5)

	ζ=1.9	Exceedance Probabilities			
Case	$W/W_{Meer(P=0.4)}$	PM	J33	J10	W
LE	0.975	0.995	0.995	0.995	0.995
Meer	1.000	0.5	0.624	0.746	0.814
HE	1.425	0.058	0.135	0.282	0.431
	ζ=2.1				
	$W/W_{Meer(P=0.4)}$	PM	J33	J10	W
LE	0.934	0.995	0.995	0.995	0.995
Meer	1.000	0.5	0.624	0.746	0.814
HE	1.333	0.058	0.135	0.282	0.431
	ζ=2.3				
	$W/W_{Meer(P=0.4)}$	PM	J33	J10	W
LE	0.910	0.995	0.995	0.995	0.995
Meer	1.000	0.5	0.624	0.746	0.814
HE	1.267	0.058	0.135	0.282	0.431
	ζ=2.5				
	$W/W_{Meer(P=0.4)}$	PM	J33	J10	W
LE	0.902	0.995	0.995	0.995	0.995
Meer	1.000	0.5	0.624	0.746	0.814
HE	1.221	0.058	0.135	0.282	0.431
	ζ=2.7				
	$W/W_{Meer(P=0.4)}$	PM	J33	J10	W
LE	0.906	0.995	0.995	0.995	0.995
Meer	1.000	0.5	0.624	0.746	0.814
HE	1.191	0.058	0.135	0.282	0.431

Weight ratios versus exceedance probability plot of PM and J33 spectrum for different ζ_m within a range of 1.9-2.7 and $\cot\alpha$=3 was given in Fig 5.13 and Fig. 5.14, respectively. In the Figs. 5.11 and 5.12, levels belong to the most probable 20% (50%±10) and 60% (50%±30) of occurrence were drawn, also.

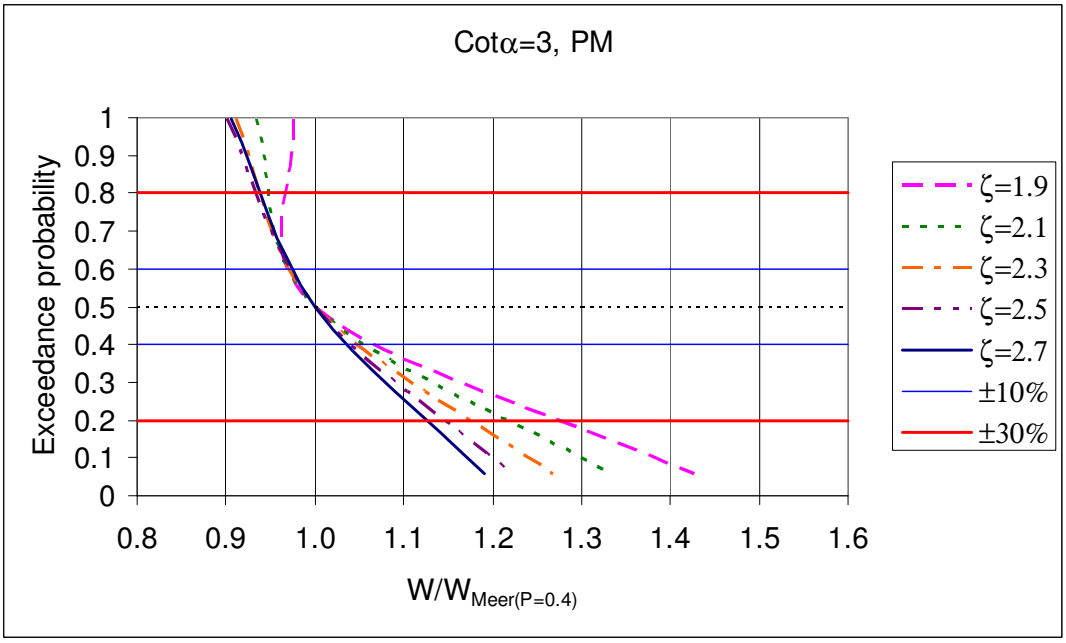

Fig. 5.11 Exceedance probability of weight ratios for PM spectrum (P=0.4)

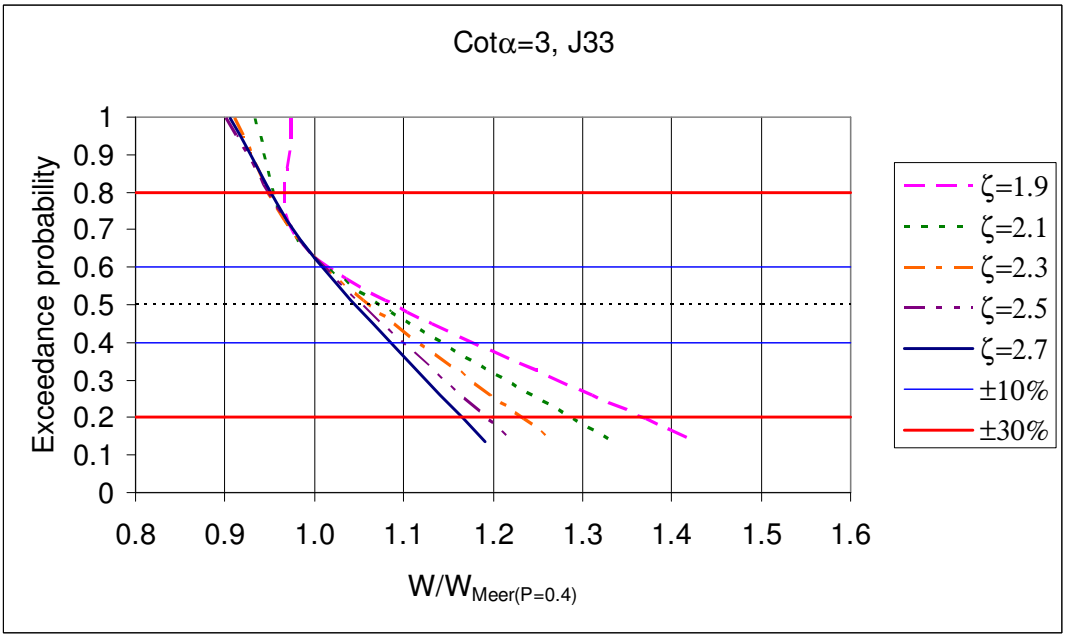

Fig. 5.12 Exceedance probability of weight ratios for J33 spectrum (P=0.4)

Weight ratios of PM spectrum belong to these probability levels shown in Fig 5.11 were tabulated for each ζ_m in Table 5.8. Finally, ζ_m versus weight ratios taken from Table 5.8 were plotted in Fig. 5.13.

Table 5.8 Weight ratios of PM spectrum (cotα=3, P=0.4)

PM			$W/W_{Meer(P=0.4)}$		
ζ_m	30%	10%	median	-10%	-30%
1.9	1.28	1.062	1	0.97	0.97
2.1	1.24	1.054	1	0.97	0.96
2.3	1.2	1.046	1	0.97	0.95
2.5	1.16	1.038	1	0.97	0.94
2.7	1.12	1.030	1	0.97	0.93

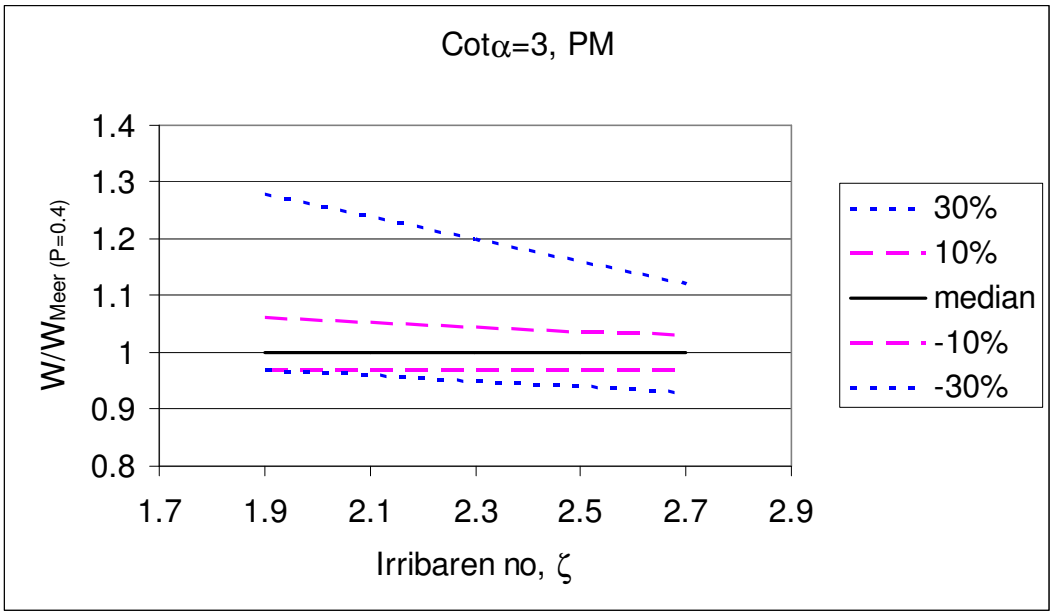

Fig. 5.13 Weight ratios of PM spectrum (cotα=3, P=0.4)

According to Table 5.8 and Fig. 5.13, Meer's equations estimate well the weight of armour stone on the average (median) for the spectrum PM. For the most probable 20% of occurrence of $\alpha_{extreme}$, the necessary weight has a maximum range of (0.97-1.06) times of Meer's result for ζ_m=1.9. When the occurance probability of $\alpha_{extreme}$ increases to 60%, that is the possibility of having $\alpha_{extreme}$ within $\mu\pm\sigma$, then weight ratio is between (0.93-1.12) for ζ_m=2.7 and it is between (0.97-1.28) for ζ_m=1.9. Therefore necessary weight may be %28 more than of Meer's result due to high extreme waves.

İt was 13-16% for the slope of cotα=1.5. The reason may be due to the under prediction of Meer's formula for cotα=3. Weight ratio decreases as ζ_m increases.

Weight ratios of J33 spectrum belonging to the probability levels of ±10%, median and ±30% shown in Fig 5.12 were tabulated for each ζ_m in Table 5.9. Then, ζ_m versus weight ratios taken from Table 5.4 was plotted in Fig. 5.14.

Table 5.9 Weight ratios of J33 spectrum (cotα=3, P=0.4)

J33			$W/W_{Meer(P=0.4)}$		
ζ_m	30%	10%	median	-10%	-30%
1.9	1.36	1.18	1.08	1.01	0.97
2.1	1.31	1.155	1.07	1.01	0.965
2.3	1.26	1.13	1.06	1.01	0.96
2.5	1.21	1.105	1.05	1.01	0.955
2.7	1.16	1.08	1.04	1.01	0.95

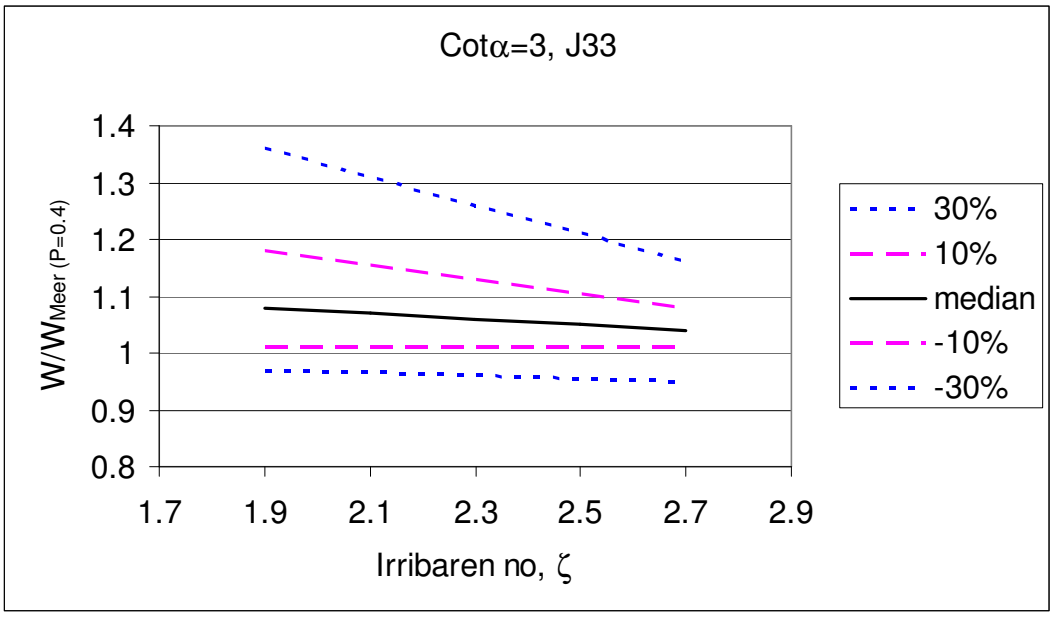

Fig. 5.14 Weight ratios of J33 spectrum (cotα=3, P=0.4)

Table 5.9 and Fig. 5.16 indicate that Meer's equation underestimates the weight 4%-8% when the spectrum is J33 on the average. Underestimation can increase to 36% for ζ_m= 1.9, if the range of occurrence probability of $\alpha_{extreme}$ is the most probable 60%. Weight increase was 28% for PM spectrum and ζ_m= 1.9. Weight ratio difference of PM and J33 spectrums comes from that the possibility of having high $\alpha_{extreme}$ is higher for J33 spectrum than it is for PM spectrum. The maximum weight ratio was 1.22 for the slope of cotα=1.5 and spectrum J33. The reason may be again due to the under prediction of Meer's formula for cotα=3. Weight ratio decreases as ζ_m increases.

5.2.4 Computation for cotα=3 and P=0.45

For the computation belongs to cotα=3 and P=0.45, exceedance probabilities taken from Fig 5.3 were matched with the weight ratios of experiment cases LE and HE to Meer's equation with P=0.45 for the corresponding ζ_m values given in Table 4.14. As a result, exceedance probabilities of weight ratios for different spectral shapes were obtained and tabulated in Table C.2 in Appendix C for cotα=3 and P=0.45.

Weight ratios versus exceedance probability plot of PM and J33 spectrums for different ζ_m within a range of 1.9-2.7 and cotα=3 were given in Fig. C.3 and Fig C.4, in Appendix C. In Figs. C.3 and C4, levels belong to the most probable 20% (50%±10) and 60% (50%±30) of occurrence were drawn, also.

Then, weight ratios of PM spectrum belong to these probability levels shown in Fig C.3 were tabulated for each ζ_m in Table 5.10. Finally, ζ_m versus weight ratios taken from Table 5.10 was plotted in Fig. 5.15.

Table 5.10 Weight ratios of PM spectrum (cotα=3, P=0.45)

PM			$W/W_{Meer(P=0.45)}$		
ζ_m	30%	10%	median	-10%	-30%
1.9	1.33	1.08	1	0.98	1
2.1	1.29	1.07	1	0.98	0.99
2.3	1.25	1.06	1	0.98	0.98
2.5	1.21	1.05	1	0.98	0.97
2.7	1.17	1.04	1	0.98	0.96

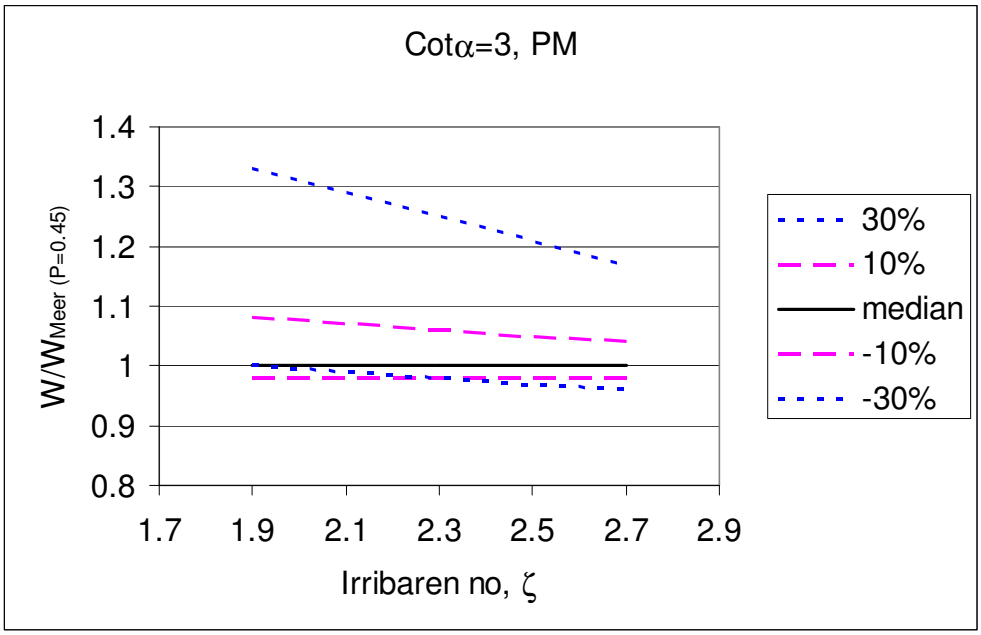

Fig. 5.15 Weight ratios of PM spectrum (cotα=3, P=0.45)

According to Table 5.10 and Fig. 5.17, Meer's equations estimates well the weight of armour stone on the average (median) for the spectrum PM. For the most probable 20% of occurrence of $\alpha_{extreme}$, the necessary weight increase up to 1.08 times of Meer's result for ζ_m=1.9. When the occurance probability of $\alpha_{extreme}$ increases to 60%, that is the possibility of having $\alpha_{extreme}$ within $\mu\pm\sigma$, then necessary weight is 33% more than of Meer's result at ζ_m=1.9. It was 28% in the case of P= 0.4. This small difference of 5% is

due to permeability effect on the Meer's formula which is not much effective for the slope cotα=3. Increase in weight was 34% for the slope of cotα=1.5.

Therefore, it can be said that there is not much difference in the weight ratios for both of the slopes if P=0.45.

Weight ratios of J33 spectrum belong to these probability levels shown in Fig C.4 were tabulated for each ζ_m in Table 5.11. Then, ζ_m versus weight ratios taken from Table 5.11 were plotted in Fig. 5.16.

Table 5.11 Weight ratios of J33 spectrum (cotα=3, P=0.45)

J33			$W/W_{Meer(P=0.45)}$		
ζ_m	30%	10%	median	-30%	-20%
1.9	1.438	1.18	1.08	1.01	0.99
2.1	1.386	1.155	1.07	1.01	0.985
2.3	1.334	1.13	1.06	1.01	0.98
2.5	1.282	1.105	1.05	1.01	0.975
2.7	1.23	1.08	1.04	1.01	0.97

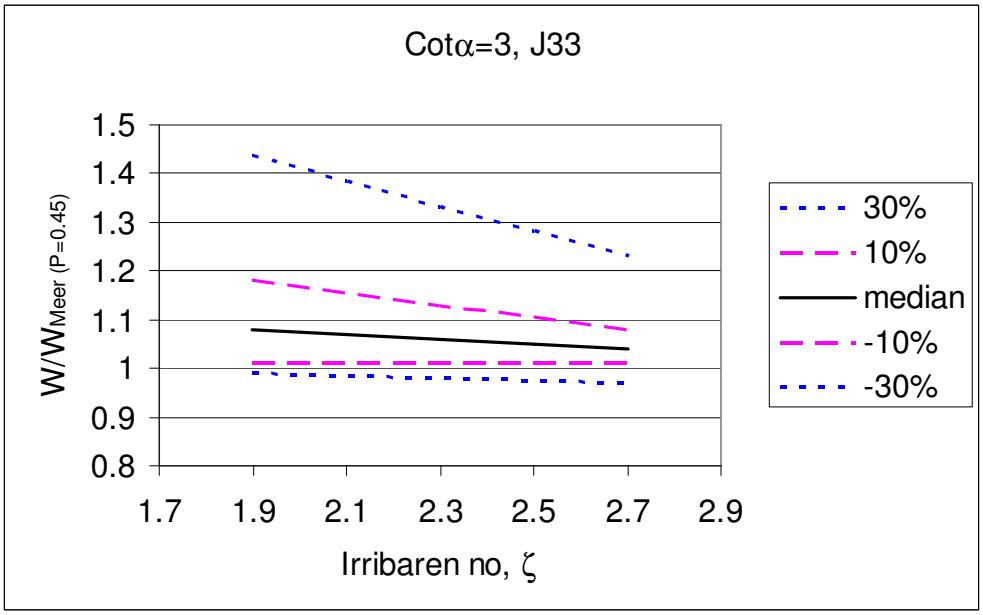

Fig. 5.16 Weight ratios of J33 spectrum (cotα=3, P=0.45)

Table 5.11 and Fig. 5.16 demonstrate that Meer's equation underestimates the weight 4%-8% on the average when the spectrum is J33. Underestimation can increase to 18%, if the range of occurrence probability of $\alpha_{extreme}$ is the most probable 20% for ζ_m=1.9. When the occurance probability of $\alpha_{extreme}$ increases to 60%, that is the possibility of having $\alpha_{extreme}$ within $\mu\pm\sigma$, then necessary weight is 43.8% more than of Meer's result at ζ_m=1.9. It was 33% when the spectrum was PM. Weight ratio difference of PM and J33 spectrums comes from that the probability of having high $\alpha_{extreme}$ is higher for J33 spectrum than it is for PM spectrum. Weight ratio increase was 36% when P=0.4, spectrum was J33 and the slope was 1:3. The reason is that Meer's formula predicts less weight when permeability increase and this makes the weight difference between experiment result and Meer's formula to increase. The maximum weight ratio increase is almost same for both of the slopes cotα=1.5 (%43) and cotα=3 (43.8%) when the permeability factor P=0.45 for J33 spectrum as it was in the case of PM spectrum.

5.2.5 Computation for practical purposes

In Chapter 4, for practical purposes, the weight ratios of experimental cases LE and HE to Meer's formula were also calculated under the assumption of that stability curves of experimental cases are parallel to Meer's curve with P=0.4 and 0.45. Results were summarised in Table 4.15 for both of the slopes. These results can be called as average results corresponding to all ζ_m within a defined range according to the slope. Exceedance probabilities taken from Fig 5.3 were matched with these average results given in Table 4.15 and using these results:

Tables of exceedance probabilities of weight ratios for different spectral shapes,

Plots of weight ratios versus exceedance probability of PM and J33 spectrums for all ζ_m within a determined range,

Tables and figures of weight ratios of PM and J33 spectrum belonging to the

probability levels of ±10%, median and ±30% for each ζ_m within a determined range were prepared and presented in Appendix D.

Only the summary of the results was given in Table 5.12 for cotα=1.5 and Table 5.13 for cotα=3 with weight ratio range corresponding to change in ζ_m values given in brackets.

Table 5.12 Summary of the results on weight ratios of $W_{experiment}/W_{Meer}$ correspond to median (50%), ±10% and ±30% probabilities of $\alpha_{extreme}$ (cotα=1.5, ζ_m=4.7-5.9)

Case	Weight Ratios ,$W_{experiment}/W_{Meer}$				
	30%	10%	median	-10%	-30%
PM, P=0.4	1.15 (1.16-1.13)	1.05 (1.04)	1.00 (1)	0.97 (0.95-0.98)	0.92 (0.84-0.96)
PM, P=0.45	1.33 (1.34)	1.12 (1.11)	1.00 (1)	1.00 (0.99-1)	1.00 (0.97-1.0)
J33, P=0.4	1.19 (1.22-1.17)	1.10 (1.11-1.09)	1.06 (1.06-1.05)	1.02 (1.01)	0.94 (0.88-0.96)
J33, P=0.45	1.43 (1.43)	1.23 (1.23)	1.13 (1.13)	1.03 (1.02)	1.00 (0.98-1.0)

Table 5.13 Summary of the results on weight ratios of $W_{experiment}/W_{Meer}$ correspond to median (50%), ±10% and ±30% probabilities of $\alpha_{extreme}$ (cotα=3, ζ_m=1.9-2.7)

Case	Weight Ratios ,$W_{experiment}/W_{Meer}$				
	30%	10%	median	-10%	-30%
PM, P=0.4	1.20 (1.28-1.12)	1.06 (1.06-1.03)	1.00 (1)	0.98 (0.97)	0.96 (0.97-0.93)
PM, P=0.45	1.25 (1.33-1.17)	1.09 (1.08-1.04)	1.00 (1)	1.00 (0.98)	1.00 (1-0.96)
J33, P=0.4	1.27 (1.36-1.16)	1.14 (1.18-1.08)	1.08 (1.08-1.04)	1.00 (1.01)	0.97 (0.97-0.99)
J33, P=0.45	1.34 (1.44-1.23)	1.17 (1.18-1.2)	1.10 (1.08-1.04)	1.00 (1.01)	1.00 (0.99-0.97)

From Tables 5.12 ad 5.13, for cotα=1.5, if the weight coefficient of experiment case is compared to weight coefficient of Meer with P=0.4, it is resulted that 15% and 19% of weight increase may be necessary for the spectrum PM and J33 respectively in the case of possibility of having $\alpha_{extreme}$ within $\mu\pm\sigma$. This result is valid for all ζ_m in the range of as 4.7-5.9. For cotα=3, the weight increase for the spectrum PM and J33 are 20% and 27%, respectively, in the same conditions. That result is valid for all ζ_m in the range of as 1.9-2.7. Therefore it can be said that effect of extreme waves in a wave train gains more importance for the slope of cotα=3 when the armour layer design is made by using Meer's formulas with permeability coefficient, P=0.4.

If the weight coefficients of the experiment cases are compared to weight coefficient of Meer with P=0.45, for cotα=1.5, it is resulted that 33% and 43% of weight increase may be necessary for the spectrum PM and J33 respectively in the case of possibility of having $\alpha_{extreme}$ within $\mu\pm\sigma$. This result is valid for all ζ_m in the range of as 4.7-5.9. For cotα=3, the weight increase for the spectrum PM and J33 are 33-17% and 44-23%, respectively, in the same conditions. That result is valid for ζ_m in the range of as 1.9-2.7, respectively. Therefore it may be concluded that effect of extreme waves in a wave train is almost similar for both the slope of cotα=1.5 and 3 when the armour layer design is made by using Meer's formulas with permeability coefficient, P=0.45.

From the stability side of view underestimated weight of armour layer stone is critical. On the other hand, designers also try to avoid overestimating the weight from the economical side of view. In the tables 5.13 and 5.14 weight ratios less than 1 show the overestimation zone of Meer's formula. For the slope of cotα=1.5, overestimation may increase to 8% for P=0.4 cases. It decreases to 6% for the slope of cotα=3. The overestimation of Meer's formula is insignificant for P=0.45 cases for both of the slopes.

An engineering application is carried out as a real case in Trabzon, Turkey. Following wave and structure information is given for Trabzon Harbour:

Hs_0=7m (significant wave height in deep water)
ds=18m (construction depth)
Hs_{ds}=6m (significant wave height at the construction depth of the structure)
T_m=11 sec
Slope:1/3
γ_s=2.65t/m3
Nonbreaking wave condition (design wave is not breaking at the toe of the structure)

Under the given design conditions, if the armour layer stone weight is calculated by Hudson formula (Eq. 2.19) with H= Hs and K_D=4, it is 10.6t.

If the armour layer stone weight is calculated by Meer's formula (Eq. 2.21 and 2.22) with S=2, N=1000, P=0.4, ζ_m=1.9, it is 11.75t.

If the effect of extreme waves is taken into consideration and in the case of possibility of having $\alpha_{extreme}$ within $\mu \pm \sigma$, weight is between 11.3t-14.1t for the spectrum PM and it is between 11.4t-14.9t for the spectrum JONSWAP.

If the armour layer stone weight is calculated by Hudson formula by using $H_{1/10}$ as recommended by SPM (1984) for the wave height, weight increases to 21.7t. ($H_{1/10}$ is assumed as 1.27 times of Hs according to Rayleigh distribution, i.e. 1.27x6=7.62m)

Therefore, it is shown by this example that for nonbreaking wave condition, Hudson formula underestimates the armour layer weight when H=Hs. But when H=$H_{1/10}$, then formula overestimates the weight. Meer's formula gives armour stone weight between possible range of 11.3-14.9t, however, there is a possibility of Meer's formula to underestimates the necessary weight in case of high extreme wave cases.

CHAPTER 6

SUMMARY AND CONCLUSIONS

It has remained as a question up to now that a decrease in the armour stability is due to grouping of high waves which may be related to narrow banded spectrum or due to only high waves in a wave train called as extreme waves in this study, even they come alone. This thesis tried to find an answer to that question by means of hydraulic model experiments.

First of all, experiments were conducted to investigate the wave grouping and spectral shape effect on the stability of rubble mound breakwaters. A model of rubble mound breakwater with 1:1.5 slope was installed inside the wave channel of hydraulic laboratory of the Disaster Prevention Research Institute of Kyoto University. Time series, approximately equal to 1000 waves, with similar wave height statistics but different degrees of wave grouping and spectral shape were generated. The test program given in Table 3.2 was executed.

Based on the results of experiments, extended experiments were conducted to observe the effect of heights of extreme waves on the stability of rubble mound breakwaters. In the experiments, J33 was chosen as spectrum shape and the test program given in Table 4.1 was executed. Two rubble mound breakwater models with slope angles of $\cot\alpha$=1.5 and 3.0 which were installed inside the wave channel of hydraulic laboratory of the Disaster Prevention Research Institute of Kyoto University structure were tested since those are the limits of mostly applied slope angle range. The Damage Curves which are the plot of significant wave height, H_s, versus

damage level, S, and Stability Curves which are the plots of Irribaren number ($\zeta_m=\tan\alpha/(H_s/L_0)^{0.5}$) versus stability number ($N_s=H_s/\Delta d_{n50}$) were drawn by using the results of the experiments. While stability curves of the slope $\cot\alpha$=1.5 were plotted for the damage levels of S=2,3,5 and 8, those of $\cot\alpha$=3 were plotted for S=2 and 3.

In order to carry the test results into the design conditions, stability curves belong the initial damage level of S=2 for $\cot\alpha$=1.5 and initial damage levels of S=2 and 3 for $\cot\alpha$=3 were re-analysed and weight ratios of experiment cases LE and HE to Meer's equation with permeability coefficient P=0.4 and 0.45 were obtained corresponding to Irribaren number ζ_m within a range. The ζ_m range is 4.7-5.9 for $\cot\alpha$=1.5 and 1.9-2.7 for $\cot\alpha$=3 tests.

Moreover, for practical purposes, the weight ratios of experimental cases LE and HE to Meer's formula were also calculated under the assumption of that stability curves of experimental cases are parallel to Meer's curve with P=0.4 and 0.45. These results can be called as average results corresponding to all ζ_m within a defined range given above for each slope.

Finally, in order to achieve more practical tools for engineering applications, occurrence probabilities of extreme waves under four different spectral shapes of PM, J33 J10, W were obtained by a numerical simulation. Probability density functions and exceedance probabilities of $\alpha_{extreme}$ for each spectral shape were plotted using the results of numerical study.

As a result of experimental work carried out, weight ratios were obtained from the evaluation of the effect of $\alpha_{extreme}$ on the stability of armour layer of rubble mound breakwaters and suggested to be used in the engineering applications. Exceedance probabilities of $\alpha_{extreme}$ for the cases LE, Meer and HE were matched with the weight ratios of experiment cases LE and HE to Meer's equation with P=0.4 and P=0.45 for the corresponding ζ_m values and for both slopes of $\cot\alpha$=1.5 and 3. As a result, exceedance probabilities of weight ratios for different spectral shapes were obtained.

Since, PM and J33 are the widely used spectrums for wind waves, weight ratios versus exceedance probability plots of PM and J33 spectrums for different ζ_m and for both of the slopes $\cot\alpha$=1.5 and 3 were drawn. From the plots, weight ratios of $W_{experiment}/W_{Meer}$ correspond to median (50%), ±10% and ±30% probabilities of $\alpha_{extreme}$ were determined for the corresponding ζ_m values. ±30% probability (the most probable 60% of occurrence of $\alpha_{extreme}$) corresponds to $\mu_{\alpha extreme}\pm\sigma_{\alpha extreme}$ and ±10% probability (the most probable 20% of occurrence of $\alpha_{extreme}$) corresponds to $\mu_{\alpha extreme}\pm0.3\sigma_{\alpha extreme}$.

Moreover, this procedure was repeated for average weight ratios calculated for practical purposes under the assumption of that stability curves of experimental cases are parallel to Meer's curve with P=0.4 and 0.45. As a result, weight ratios of $W_{experiment}/W_{Meer}$ correspond to median (50%), ±10% and ±30% probabilities of $\alpha_{extreme}$ were determined for all ζ_m values within a defined range and for both slopes of $\cot\alpha$=1.5 and 3

The followings are the important results and conclusions of the present dissertation:

According to the result of the hydraulic model experiments, the damage to breakwater armour layer is almost same even the spectrum shape is different and the wave grouping is pronounced under the condition of similar extreme waves in the train i.e. similar $\alpha_{extreme}$ parameter.

Experiments also indicated that the wave trains with same significant wave height, $H_{1/3}$, but with different extreme waves i.e. different $\alpha_{extreme}$ cause different damage levels. The higher the value of $\alpha_{extreme}$ is, the more destructive the wave train is. Therefore it is concluded that height of the extreme waves in a wave train is more important point rather than the situation that they come as a group considering the stability of rubble mound breakwaters.

According to the damage curves given in Figs. 4.2-4.7 of extended experiments conducted to observe the effect of heights of extreme waves, for both of the slope angle cotα=1.5 and 3, the wave train with high value of $\alpha_{extreme}$ is more destructive than it is with low $\alpha_{extreme}$. The difference in the damage levels caused by the wave train with low $\alpha_{extreme}$ (LE) and high $\alpha_{extreme}$ (HE) increase as wave height increase.

it can be stated from stability curves (Figs.4.8-4.13) which are the dimensionless demonstration of the test results used for the stability analysis, that high extreme waves in a wave train decrease stability without dependency to slope angle.

Meer's stability curves which does not include the effect of extreme waves in a wave train, give higher stability values than experiment curves of high $\alpha_{extreme}$ (HE) for start of the damage i.e. S=2 and 3. But for higher damages, Meer's stability curves start to result less stability values. This result may mean that Meer's formula emphasizes the effect of the damage level and so formula covers the effect of extreme waves on the stability for higher damages.

Stability decreases in all the cases of HE (wave train with high $\alpha_{extreme}$), LE (wave train with low $\alpha_{extreme}$) and Meer's results as approaching to the transition zone, in which, both wave run-up and run-down forces become effective.

The difference in the stability numbers of the wave train with low $\alpha_{extreme}$ (LE) and high $\alpha_{extreme}$ (HE) decrease while approaching to this transition zone. This result may be attributed to the fact that while wave run-down is effective on the stability in the surging region, in the transition zone, both wave run-up and run-down forces become effective due to plunging and surging respectively, which causes decrease in the stability even extreme waves are low.

According to the results on weight ratios, if the experiment cases are compared with Meer's formula with P=0.4, then it may be necessary to increase weight of armour layer stone 23% for cotα=1.5 and 30% for cotα=3 on the average for all ζ_m in the range given above. On the other hand, Meer's formula overestimates the weight 14% for cotα=1.5 and 6% for cotα=3.

In the case of possibility of having $\alpha_{extreme}$ within $\mu\pm\sigma$, for cotα=1.5, it is resulted that 15% and 19% of weight increase may be necessary for the spectrum PM and J33 respectively. This result is valid for all ζ_m in the range of as 4.7-5.9. For cotα=3, the weight increase for the spectrum PM and J33 are 20% and 27%, respectively, in the same conditions. That result is valid for all ζ_m in the range of as 1.9-2.7. Therefore it can be said that effect of extreme waves in a wave train gains more importance for the slope of cotα=3 when the armour layer design is made by using Meer's formulas with permeability coefficient, P=0.4.

If the experiment cases are compared with Meer's formula with P=0.45, then increase in weight of armour layer stone may be 50 and 40% for all ζ_m in the range given above for cotα=1.5 and 3, respectively. Weight ratios of W_{LE}/W_{Meer} are almost equal to 1 that indicates the underestimation of Meer's formula when permeability increases.

In the case of possibility of having $\alpha_{extreme}$ within $\mu\pm\sigma$, for cotα=1.5, it is resulted that 33% and 43% of weight increase may be necessary for the spectrum PM and J33 respectively. This result is valid for all ζ_m in the range of as 4.7-5.9. For cotα=3, the weight increase for the spectrum PM and J33 are 33-17% and 44-23%, respectively, in the same conditions. That result is valid for ζ_m in the range of as 1.9-2.7, respectively. Therefore it may be concluded that effect of extreme waves in a wave train is almost similar for both the slope of cotα=1.5 and 3 when the armour layer design is made by using Meer's formulas with permeability coefficient, P=0.45.

Weight ratios for J33 spectrum are always higher than those for PM spectrum. The difference comes from that the possibility of having high $\alpha_{extreme}$ is higher for J33 spectrum than it is for PM spectrum. In fact, the possibility of need for heavier armour stone than the calculated weight from Meer's equation increases as spectral shape becomes narrower.

From the stability side of view underestimated weight of armour layer stone is critical. On the other hand, designers also try to avoid overestimating the weight from the economical side of view. For the slope of cotα=1.5, overestimation may increase to 8% for P=0.4 cases. It decreases to 6% for the slope of cotα=3. The overestimation of Meer's formula is insignificant for P=0.45 cases for both of the slopes.

Probability density functions and exceedance probabilities of $\alpha_{extreme}$ plotted using the results of numerical study indicates that it is more probable to get high $\alpha_{extreme}$ parameter for narrow spectrum comparing to broad one. The probability of having $\alpha_{extreme}$ more than 0.009 is 48% for PM spectrum, 62% for J33 spectrum, 75% for J10 and 81% for W spectrum. Therefore it was demonstrated that spectral shape indirectly affects the stability not due to the wave grouping but due to the extreme waves in a wave train since the occurrence probability of the high extreme waves becomes higher as the spectral shape becomes narrower under same significant wave height condition.

As a conclusion, extreme wave heights in a wave train are important considering the stability of rubble mound breakwaters. It seems that one characteristic wave height like mostly used $H_{1/3}$ or $H_{1/10}$ is not enough to represent the effect of extreme waves in a sea state.

Hudson formula has been widely used due to its simplicity and applicability to the wide range of armour units and configurations. But as it was indicated, it underestimates the weight of armour layer stone for non-breaking wave condition. Therefore it may be better to use Meer's formula

with the possible range of weight given by this study considering the effect of extreme waves in a wave train for non-breaking wave condition.

Since wave breaking was out of scope of this work, only non-breaking wave condition was studied. But wave breaking is unavoidable in shallow zone and very important phenomenon from the stability side of view. Wave height distribution and so extreme waves will be totally changed in breaking zone. Therefore effect of extreme waves in breaking zone is still under question and the answer is kept as a future study.

Since the experiments were conducted for only slopes 1:1.5 and 1:3, and for a limited wave heights and periods, results are valid for a given range of Irribaren number ζ_m. Therefore, it will be useful to make experiment with other slopes like 1:2 and 1:2.5 as a future study.

REFERENCES

Arhan, M. and Ezraty, R. **(**1978). 'Statistical Relations Between Successive Wave Heights', Oceanological Acta, Vol: 1 No:2.

Bruun, P. (1985), 'Design and construction of mounds for breakwaters and coastal protection', Elsevier Science Publishers B.V, pp. 238-258.

Burcharth, H.F. (1979), 'The effect of wave grouping on on-shore structures', Coastal Engineering Journal, Elsevier Pub., Vol.2, pp.189-199.

CEM (2003).'Coastal Engineering Manual', Coastal Engineering Research Center, Dept. of Army Corps of Engineers, US, Chapter VI, Part 5.

Elgar, S., Guza, R.T., Seymour,R.J. (1984).'Group of Waves in Shallow Water', J. of Geophysical Research, Vol.89, No.C3,Pg:3623-3634

Funke, E.R. and Mansard, E.P.D. (1979), 'Synthesis of realistic sea states in a laboratory flume', Hydraulics Laboratory Technical Report LTR-HY-66, National Research Council of Canada, Ottowa.

Goda, Y. (1970), 'Numerical Experiments On Wave Statistics With Spectral Simulation' PHRI Report.

Goda, Y. (1976), 'On Wave Groups', BOSS, Vol.1:115-128

Goda, Y., Suzuki, Y. (1976), 'Estimation of Incident and Reflected Waves in random wave experiments', Proc. 15th ICCE, Hawai, pp.828-845.

Goda, Y. (1983), 'Analysis Of Wave Grouping And Spectra Of Long Traveled Swell', PHRI Report. Vol:22 No:1

Goda, Y. (1985), 'Random Seas and Design of Maritime Structures', University of Tokyo Press.

Goda Y. (1998), 'An Overview of Coastal Engineering With Emphasis On Random Wave Approach', Coastal Engineering Journal, vol.40, No:1, pp. 1-21, World Scientific Pub. and JSCE

Hald, T., Burharth, H.F. (2000) 'An alternative stability equation for rock armoured rubble moubd breakwaters', Proc. ICCE, pp1921-1934.

Hall, K.,R. (1994), 'Influence Of Wave Groups On Stability Of Berm Breakwaters', Journal of Waterway, Port, Coastal and Ocean Engineering, ASCE, Vol: 120.

Hedar, P. A. (1986),'Armour layer stability of rubble-mound breakwaters' Journal of Waterway, Port, Coastal and Ocean Engineering, ASCE, Vol: 112, pp.343-350.

Johnson, R. R., Mansard, E.P.D., and Ploeg, J. (1978). 'Effect of wave grouping on breakwater stability', Proc. 10th ICCE, ASCE, pp. 2228-2247.

Kimura, A. (1980), 'Statistical properties of random wave groups', Proc. 17 th ICCE, pp.2955-2973

Liu, Z., Elgar, S., Guza, R.T. (1993). 'Groups Of Ocean Waves: Linear Theory, Approximations To Linear Theory And Observations', Journal of Waterway, Port, Coastal and Ocean Engineering, ASCE, Vol: 119.

Liu, C. P. (2000).' Wavelet transform and new perspective on coastal and ocean engineering data analysis', Advances in Coastal and ocean Engineering, World Scientific Pub., Vol.6, pp. 57-101.

Medina, J.R., Hudspeth, R.T. (1990). ‘A Review Of The Analysis Of Ocean Wave Groups’, Coastal Engineering Vol:14.

Medina, J.R., Hudspeth, R.T., and Fassardi, C. (1994). "Breakwater armor damage due to wave groups", Journal of Waterway, Port, Coastal and Ocean Engineering, ASCE, Vol. 120, pp. 179-197.

Okuno, T., Uji-ie, H., Sawamoto, M. (1989). ‘Effects Of Wave Grouping On The Stability Of Breakwater Armour Units’, Coastal Engineering in Japan, Vol: 32 No:1.

Ozbahceci, B., Takayama T., Mase, H., Ergin A. (2002).’Occurrence probability of wave grouping for different shapes of wave energy spectra’, The Proceedings of 12th ISOPE Conference 2002, Kitakyushu, Japan. Vol.3, pp.37-42

Sawaragi, T., Ryu, C. Ro, Kusumi, M. (1985). ‘Destruction Mechanism And Design Of R. M. Structures By Irregular Waves’, Coastal Engineering in Japan Vol: 28.

Shore Protection Manual (SPM) (1984). Coastal Engineering Research Center, Dept. of Army, Waterways Experiment station, Vicksburg, Miss.

Tuah, H, Hudspeth, RT (1982).”Comparisons of Numerical Random Sea Simulations,” Jour. Waterway, Port, Coastal and Ocean Engineering, Vol. 108, pp 569-584.

Van der Meer, J.W. (1988).’ Rock Slopes and gravel beaches under wave attack’, Ph.D thesis, Netherland.

Van der Meer, J.W. (1993).’ Deterministic and probabilistic design of breakwater armour layers’, Journal of Waterway, Port, Coastal and Ocean Engineering, ASCE, Vol.114, pp.66-79.

Veltcheva, A.D. (2002).' Wave and group transformation by a Hilbert Spectrum', Coastal Eng. Journal, World Scientific Pub. Comp. and JSCE, Vol.44, no.4, pp. 283-300

Vidal, C., Losada, M.A. and Mansard, E.P.D. (1995). 'Suitable wave height parameter for characterizing breakwater stability', Journal of Waterway, Port, Coastal and Ocean Engineering, ASCE, Vol.121, pp.114-130

APPENDIX A

COMPUTATION OF STABILITY NUMBERS

Table A.1 Equation of best fit Damage Curves of the slope cotα=1.5

Test series no	Equation of best fit curve	R^2
1	$S=0.0008H_s^{3.6671}$	0.9421
2	$S=0.0005H_s^{4.0234}$	0.9181
3	$S=0.0001H_s^{4.0259}$	0.9150
3	$S=0.0004H_s^{4.1009}$	0.9824
5	$S=0.1273e^{0.2934Hs}$	0.9263
6	$S=0.0006H_s^{3.8}$	0.8923

Table A.2 Equation of best fit Damage Curves of the slope cotα=3

Test series no	Equation of best fit curve	R^2
7	$S=4.8768Ln(H_s)-9.7283$	0.8129
8	$S=0.0002H_s^{3.9146}$	0.9465
9	$S=0.6797H_s-5.3611$	0.9316
10	$S=9.5243Ln(H_s)-19.928$	0.8470
11	$S=0.6504H_s-5.0844$	0.8691
12	$S=0.0612e^{0.3583Hs}$	0.9195

Table A.3 Computation of N_s and ζ_m for the experiment cases and Meer's formula with P=0.4 and 0.45 ($\cot\alpha$=1.5)

Serie 1										
S	Hs(cm)	N_s	T_m(s)	L_{0m}(m)	$\cot\alpha$	ζ_m	type	$Ns_{MeerP=0.4}$	type	$Ns_{MeerP=0.45}$
2	8.45	1.51	1.68	4.40	1.5	4.81	surging	1.49	surging	1.59
3	9.43	1.69	1.68	4.40	1.5	4.55	surging	1.58	surging	1.67
5	10.84	1.94	1.68	4.40	1.5	4.25	plunging	1.76	plunging	1.81
8	12.32	2.21	1.68	4.40	1.5	3.98	plunging	2.00	plunging	2.04
Serie 2										
S	Hs(cm)	N_s	T_m(s)	L_{0m}(m)	$\cot\alpha$	ζ_m	type	$Ns_{MeerP=0.4}$	type	$Ns_{MeerP=0.45}$
2	7.86	1.41	1.68	4.40	1.5	4.99	surging	1.51	surging	1.61
3	8.69	1.56	1.68	4.40	1.5	4.75	surging	1.61	surging	1.71
5	9.87	1.77	1.68	4.40	1.5	4.45	surging	1.73	surging	1.84
8	11.09	1.99	1.68	4.40	1.5	4.20	plunging	1.95	plunging	1.99
Serie 3										
S	Hs(cm)	N_s	T_m(s)	L_{0m}(m)	$\cot\alpha$	ζ_m	type	$Ns_{MeerP=0.4}$	type	$Ns_{MeerP=0.45}$
2	8.94	1.60	1.83	5.22	1.5	5.10	surging	1.52	surging	1.63
3	9.78	1.75	1.83	5.22	1.5	4.87	surging	1.62	surging	1.73
5	10.95	1.96	1.83	5.22	1.5	4.60	surging	1.76	surging	1.87
8	12.15	2.18	1.83	5.22	1.5	4.37	plunging	1.91	surging	2.00
Serie 4										
S	Hs(cm)	N_s	T_m(s)	L_{0m}(m)	$\cot\alpha$	ζ_m	type	$Ns_{MeerP=0.4}$	type	$Ns_{MeerP=0.45}$
2	7.98	1.43	1.79	5.00	1.5	5.28	surging	1.54	surging	1.65
3	8.81	1.58	1.79	5.00	1.5	5.02	surging	1.64	surging	1.75
5	9.98	1.79	1.79	5.00	1.5	4.72	surging	1.77	surging	1.89
8	11.19	2.01	1.79	5.00	1.5	4.46	surging	1.91	surging	2.02
Serie 5										
S	Hs(cm)	N_s	T_m(s)	L_{0m}(m)	$\cot\alpha$	ζ_m	type	$Ns_{MeerP=0.4}$	type	$Ns_{MeerP=0.45}$
2	9.39	1.68	2.04	6.49	1.5	5.54	surging	1.58	surging	1.69
3	10.68	1.92	2.04	6.49	1.5	5.20	surging	1.67	surging	1.78
5	12.51	2.24	2.04	6.49	1.5	4.80	surging	1.79	surging	1.90
8	14.11	2.53	2.04	6.49	1.5	4.52	surging	1.92	surging	2.02
Serie 6										
S	Hs(cm)	N_s	T_m(s)	L_{0m}(m)	$\cot\alpha$	ζ_m	type	$Ns_{MeerP=0.4}$	type	$Ns_{MeerP=0.45}$
2	8.45	1.52	2.04	6.49	1.5	5.84	surging	1.61	surging	1.73
3	9.41	1.69	2.04	6.49	1.5	5.54	surging	1.71	surging	1.83
5	10.76	1.93	2.04	6.49	1.5	5.18	surging	1.84	surging	1.97
8	12.18	2.18	2.04	6.49	1.5	4.87	surging	1.97	surging	2.10

Table A.4 Computation of N_s and ζ_m for the experiment cases and Meer's formula with P=0.4 and 0.45 (cotα=3)

Serie 7										
S	Hs(cm)	N_s	T_m(s)	L_{0m}(m)	cotα	ζ_m	type	$Ns_{MeerP=0.4}$	type	$Ns_{MeerP=0.45}$
2	11.08	1.99	1.65	4.25	3	2.06	plunging	2.11	plunging	2.15
3	13.60	2.44	1.65	4.25	3	1.86	plunging	2.40	plunging	2.46
Serie 8										
S	Hs(cm)	N_s	T_m(s)	L_{0m}(m)	cotα	ζ_m	type	$Ns_{MeerP=0.4}$	type	$Ns_{MeerP=0.45}$
2	10.52	1.89	1.64	4.20	3	2.11	plunging	2.09	plunging	2.13
3	11.66	2.09	1.64	4.20	3	2.00	plunging	2.32	plunging	2.37
Serie 9										
S	Hs(cm)	N_s	T_m(s)	L_{0m}(m)	cotα	ζ_m	type	$Ns_{MeerP=0.4}$	type	$Ns_{MeerP=0.45}$
2	10.83	1.94	1.85	5.34	3	2.34	plunging	1.98	plunging	2.02
3	12.30	2.21	1.85	5.34	3	2.20	plunging	2.21	plunging	2.26
Serie 10										
S	Hs(cm)	N_s	T_m(s)	L_{0m}(m)	cotα	ζ_m	type	$Ns_{MeerP=0.4}$	type	$Ns_{MeerP=0.45}$
2	10.00	1.79	1.84	5.28	3	2.42	plunging	1.94	plunging	1.99
3	11.10	1.99	1.84	5.28	3	2.30	plunging	2.16	plunging	2.21
Serie 11										
S	Hs(cm)	N_s	T_m(s)	L_{0m}(m)	cotα	ζ_m	type	$Ns_{MeerP=0.4}$	type	$Ns_{MeerP=0.45}$
2	11.08	1.99	2.00	6.24	3	2.50	plunging	1.91	plunging	1.95
3	12.62	2.26	2.00	6.24	3	2.34	plunging	2.14	plunging	2.19
Serie 12										
S	Hs(cm)	N_s	T_m(s)	L_{0m}(m)	cotα	ζ_m	type	$Ns_{MeerP=0.4}$	type	$Ns_{MeerP=0.45}$
2	9.73	1.75	1.98	6.12	3	2.64	plunging	1.86	plunging	1.90
3	10.86	1.95	1.98	6.12	3	2.50	plunging	2.08	plunging	2.12

APPENDIX B

WEIGHT RATIO CHANGE FOR DIFFERENT SPECTRAL SHAPES AND ζ_m

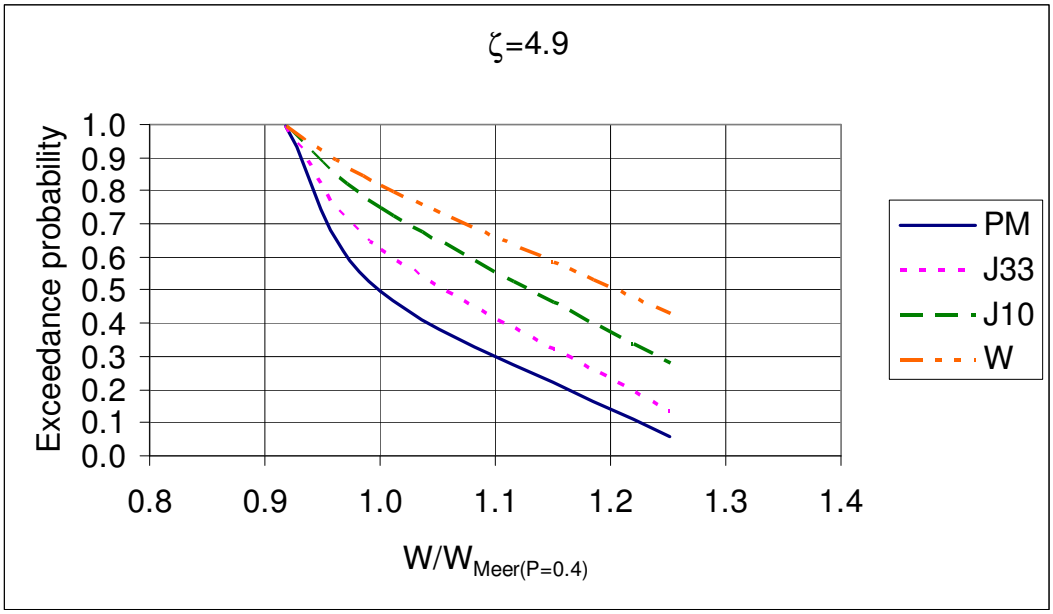

Fig. B.1 Weight ratio versus exceedance probability for different spectral shapes ($\cot\alpha$=1.5, P=0.4, ζ_m=5.5)

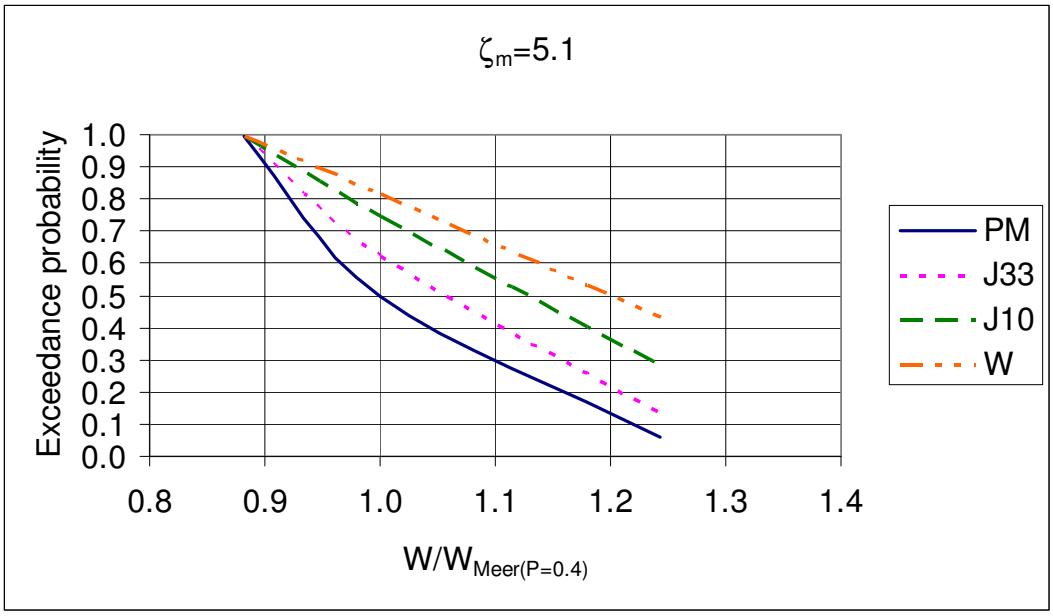

Fig. B.2 Weight ratio versus exceedance probability for different spectral shapes (cotα=1.5, P=0.4, ζ_m=5.1)

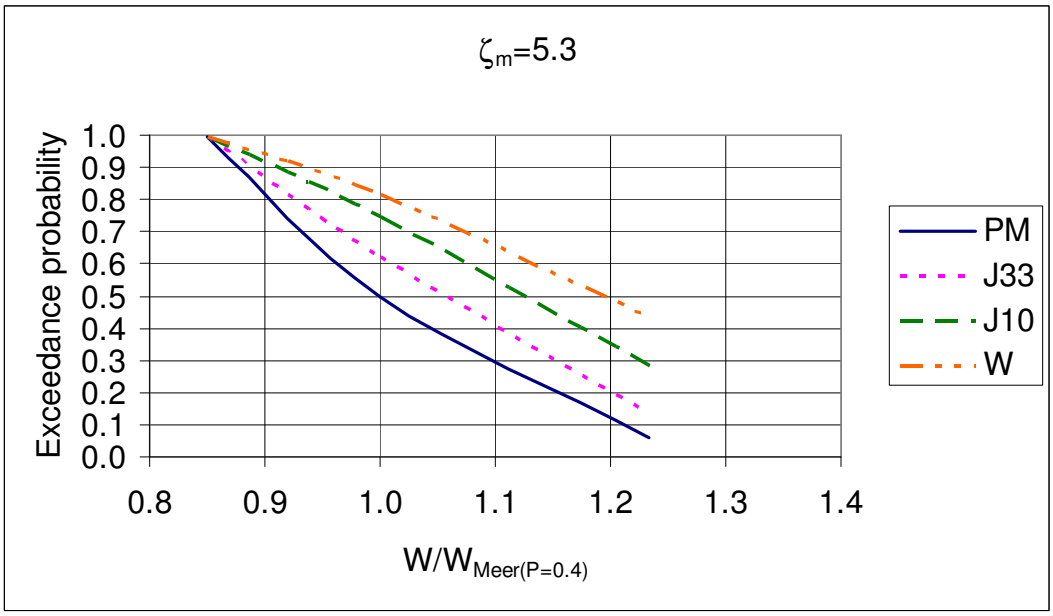

Fig. B.3 Weight ratio versus exceedance probability for different spectral shapes (cotα=1.5, P=0.4, ζ_m=5.3)

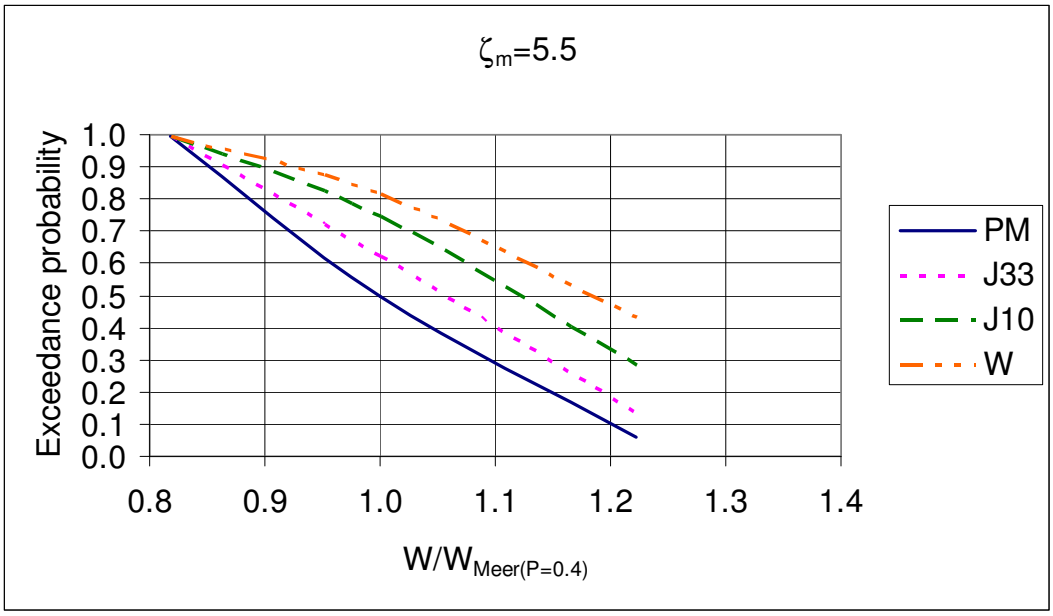

Fig. B.4 Weight ratio versus exceedance probability for different spectral shapes (cotα=1.5, P=0.4, ζ_m=5.5)

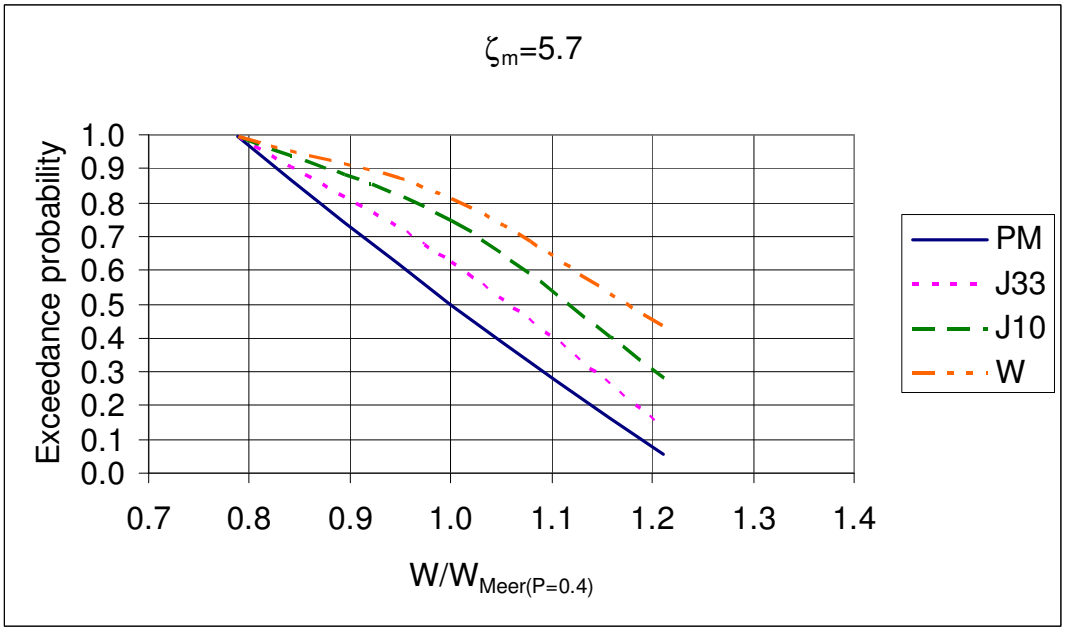

Fig. B.5 Weight ratio versus exceedance probability for different spectral shapes (cotα=1.5, P=0.4, ζ_m=5.7)

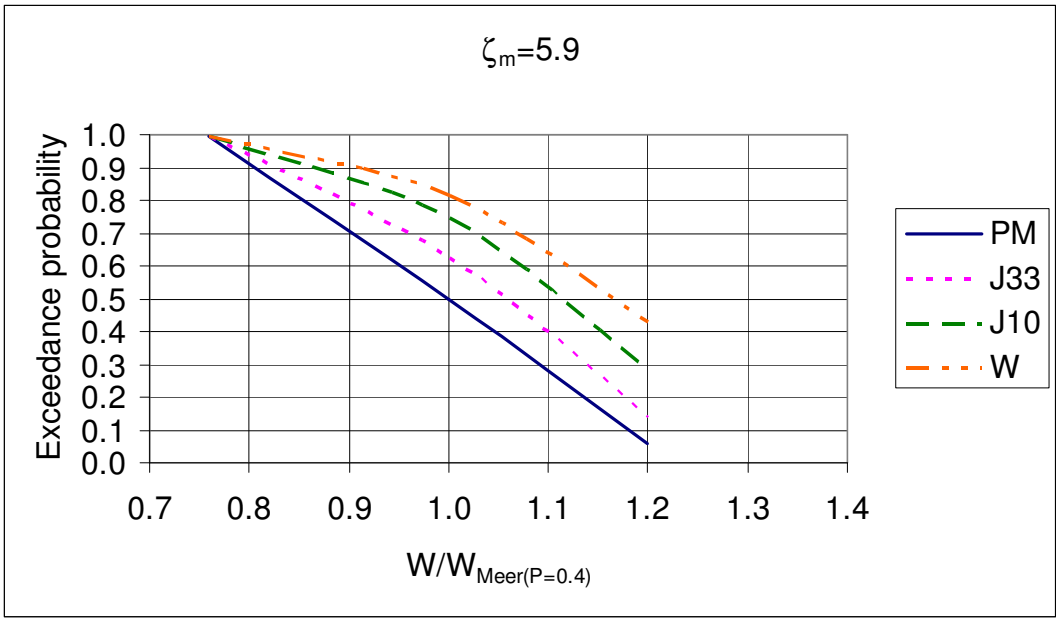

Fig. B.6 Weight ratio versus exceedance probability for different spectral shapes ($\cot\alpha$=1.5, P=0.4, ζ_m=5.9)

APPENDIX C

EXCEEDANCE PROBABILITIES OF WEIGHT RATIOS FOR P=0.45

Table C.1 Exceedance probabilities of weight ratios ($W/W_{Meer(P=0.45)}$) for different spectral shapes ($\cot\alpha$=1.5)

ζ=4.7

Case	$W/W_{Meer(P=0.45)}$	PM	J33	J10	W
LE	1.000	0.995	0.995	0.995	0.995
Meer	1.000	0.5	0.624	0.747	0.815
HE	1.518	0.058	0.135	0.282	0.431

ζ=4.9

Case	$W/W_{Meer(P=0.45)}$	PM	J33	J10	W
LE	1.000	0.995	0.995	0.995	0.995
Meer	1.000	0.5	0.624	0.747	0.815
HE	1.518	0.058	0.135	0.282	0.431

ζ=5.1

Case	$W/W_{Meer(P=0.45)}$	PM	J33	J10	W
LE	1.000	0.995	0.995	0.995	0.995
Meer	1.000	0.5	0.624	0.747	0.815
HE	1.516	0.058	0.135	0.282	0.431

ζ=5.3

Case	$W/W_{Meer(P=0.45)}$	PM	J33	J10	W
LE	1.000	0.995	0.995	0.995	0.995
Meer	1.000	0.5	0.624	0.747	0.815
HE	1.512	0.058	0.135	0.282	0.431

ζ=5.5

Case	$W/W_{Meer(P=0.45)}$	PM	J33	J10	W
LE	1.000	0.995	0.995	0.995	0.995
Meer	1.000	0.5	0.624	0.747	0.815
HE	1.507	0.058	0.135	0.282	0.431

ζ=5.7

Case	$W/W_{Meer(P=0.45)}$	PM	J33	J10	W
LE	0.977	0.995	0.995	0.995	0.995
Meer	1.000	0.5	0.624	0.747	0.815
HE	1.501	0.058	0.135	0.282	0.431

Table C.1. (Continued)

ζ=5.9

Case	$W/W_{Meer(P=0.45)}$	PM	J33	J10	W
LE	0.947	0.995	0.995	0.995	0.995
Meer	1.000	0.5	0.624	0.747	0.815
HE	1.494	0.058	0.135	0.282	0.431

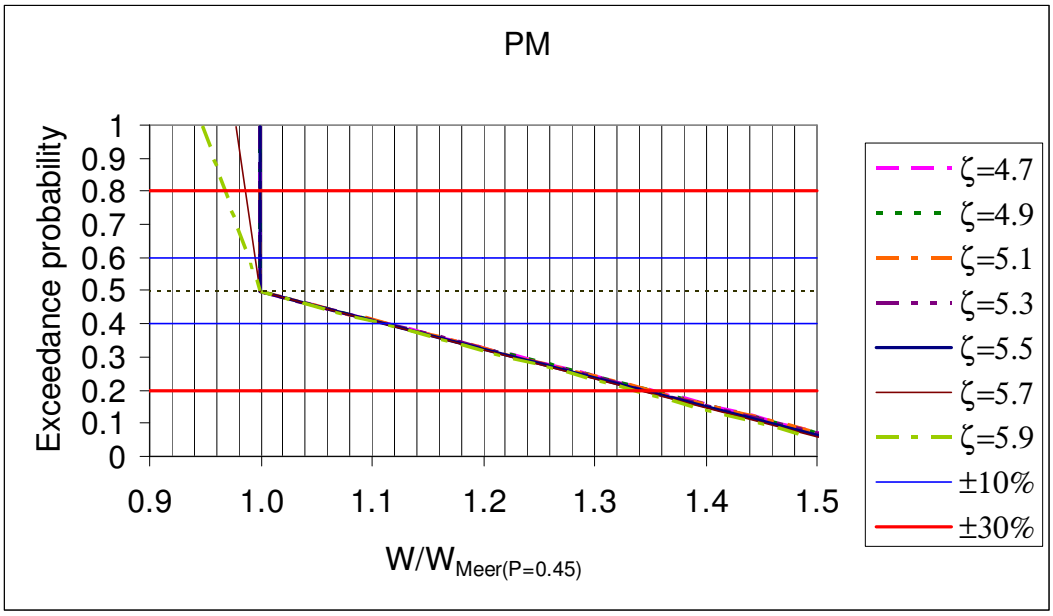

Fig. C.1 Exceedance probability of weight ratios for PM spectrum (cotα=1.5, P=0.45)

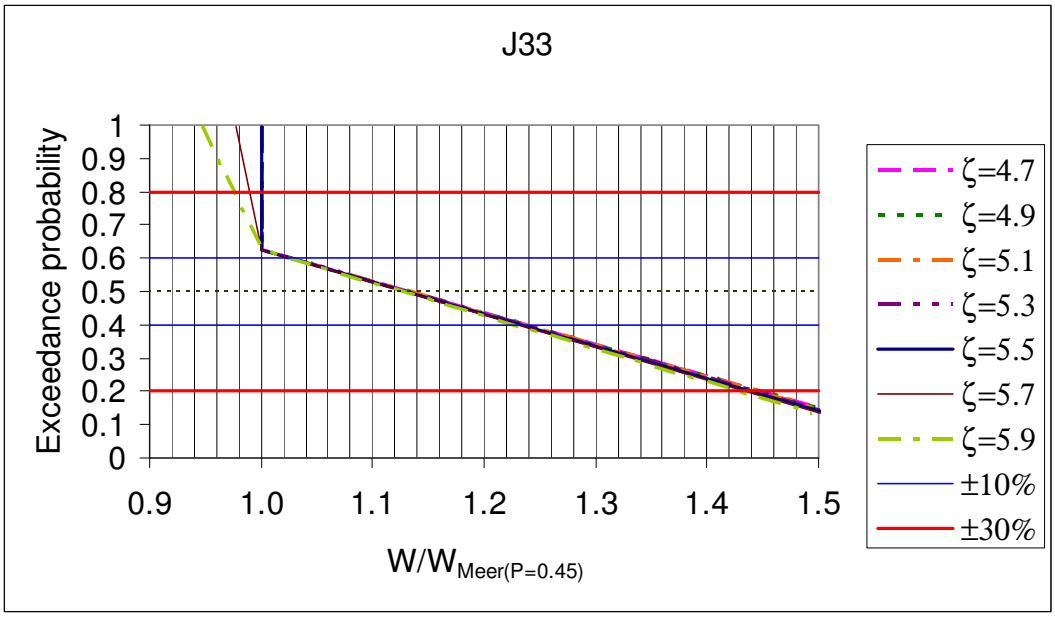

Fig. C.2 Exceedance probability of weight ratios for J33 spectrum (cotα=1.5, P=0.45)

Table C.2 Exceedance probabilities of weight ratios ($W/W_{Meer(P=0.45)}$) for different spectral shapes ($\cot\alpha=3$)

	$\zeta=1.9$	Exceedance Probabilities			
Case	$W/W_{Meer(P=0.45)}$	PM	J33	J10	W
LE	1.039	0.995	0.995	0.995	0.995
Meer	1.000	0.5	0.624	0.746	0.814
HE	1.519	0.058	0.135	0.282	0.431
	$\zeta=2.1$				
	$W/W_{Meer(P=0.45)}$	PM	J33	J10	W
LE	0.995	0.995	0.995	0.995	0.995
Meer	1.000	0.5	0.624	0.746	0.814
HE	1.421	0.058	0.135	0.282	0.431
	$\zeta=2.3$				
	$W/W_{Meer(P=0.45)}$	PM	J33	J10	W
LE	0.970	0.995	0.995	0.995	0.995
Meer	1.000	0.5	0.624	0.746	0.814
HE	1.350	0.058	0.135	0.282	0.431
	$\zeta=2.5$				
	$W/W_{Meer(P=0.45)}$	PM	J33	J10	W
LE	0.961	0.995	0.995	0.995	0.995
Meer	1.000	0.5	0.624	0.746	0.814
HE	1.301	0.058	0.135	0.282	0.431
	$\zeta=2.7$				
	$W/W_{Meer(P=0.45)}$	PM	J33	J10	W
LE	0.965	0.995	0.995	0.995	0.995
Meer	1.000	0.5	0.624	0.746	0.814
HE	1.270	0.058	0.135	0.282	0.431

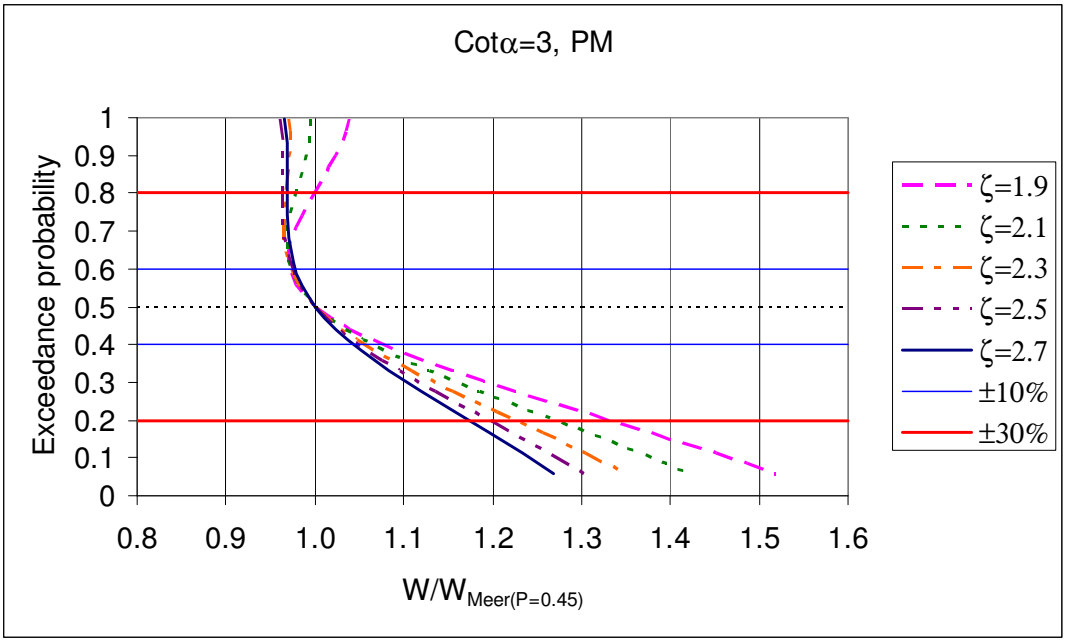

Fig. C.3 Exceedance probability of weight ratios for PM spectrum (cotα=3, P=0.45)

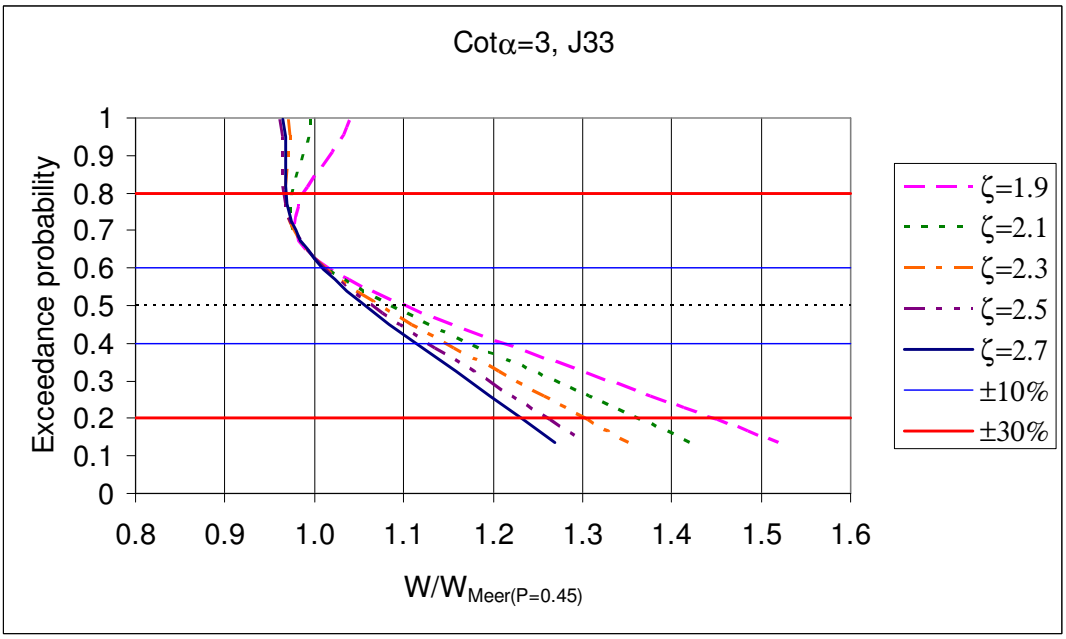

Fig. C.4 Exceedance probability of weight ratios for J33 spectrum (cotα=3, P=0.45)

APPENDIX D

RESULTS ON WEIGHT RATIOS OF EXPERIMENTAL CASES LE AND HE TO MEER'S FORMULA FOR ALL ζ_m WITHIN A RANGE

D.1 Computation for cotα=1.5 and P=0.4

Using the values of $\alpha_{extreme}$ for the cases LE, Meer and HE, exceedance probabilities of $\alpha_{extreme}$ were taken from Fig 5.3 for each spectral shape. Those probabilities were matched with results on weight ratios of experimental cases LE and HE to Meer's formula based on the assumption that stability curves of experimental cases are parallel to Meer's curve with P=0.4 for all ζ_m in a range given in Table 4.14. As a result, exceedance probabilities of weight ratios for different spectral shapes were obtained and tabulated in Table D.1 for cotα=1.5.

Table D.1 Exceedance probabilities of weight ratios for different spectral shapes (cotα=1.5, P=0.4)

Case	$W/W_{Meer(P=0.4)}$	PM	J33	J10	W
LE	0.860	0.995	0.995	0.995	0.995
Meer	1.000	0.5	0.624	0.7465	0.8145
HE	1.230	0.058	0.135	0.282	0.431

The weight ratios versus exceedance probability for different spectral shapes were plotted in Fig. D.1. As it can be seen from the figure, possibility of need for heavier armour stone than the calculated weight from Meer's equation with P=0.4 increases as spectral shape becomes narrower. For example considering the most probable (average) case, $W/W_{Meer(P=0.4)}$ =1 for PM, 1.04 for J33, 1.08 for J10 and 1.13 for W spectrum. It means that for the condition of structure slope, cotα=1.5, necessary weight of armour stone calculated by Meer formula with P=0.4 will be enough if the spectrum is PM.

But if spectrum is narrower than PM, then up to 13% increase of weight may be needed.

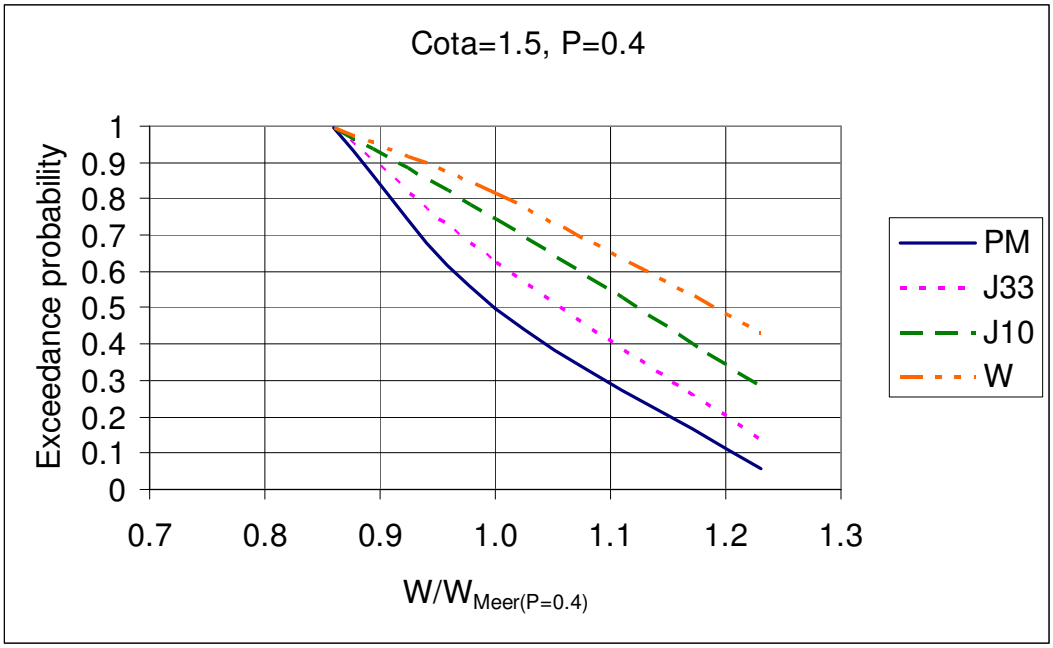

Fig.D.1 Weight ratio versus exceedance probability for different spectral shapes

Since PM and J33 are the widely used spectrums, it would be more practical to see occurrence probability of weight ratios for PM and J33 spectrums. Weight ratios versus exceedance probability plot of PM spectrum for all ζ_m in a range of 4.7-5.7and cotα=1.5 was given in Fig D.2. In the Fig. D.2, levels belongs to the most probable 20% (50%±10) and 60% (50%±30) of occurrence were drawn, also. From pdf of $\alpha_{extreme}$ for PM spectrum given in Fig 5.3, it was calculated that the most probable 60% of occurrence of $\alpha_{extreme}$ corresponds to $\mu_{\alpha extreme} \pm \sigma_{\alpha extreme}$ where $\mu_{\alpha extreme}$ =0.0089 and $\sigma_{\alpha extreme}$ =0.0007 as given in Table 5.1. The most probable 60% of occurrence of $\alpha_{extreme}$ corresponds to $\mu_{\alpha extreme} \pm 0.3\sigma_{\alpha extreme}$.

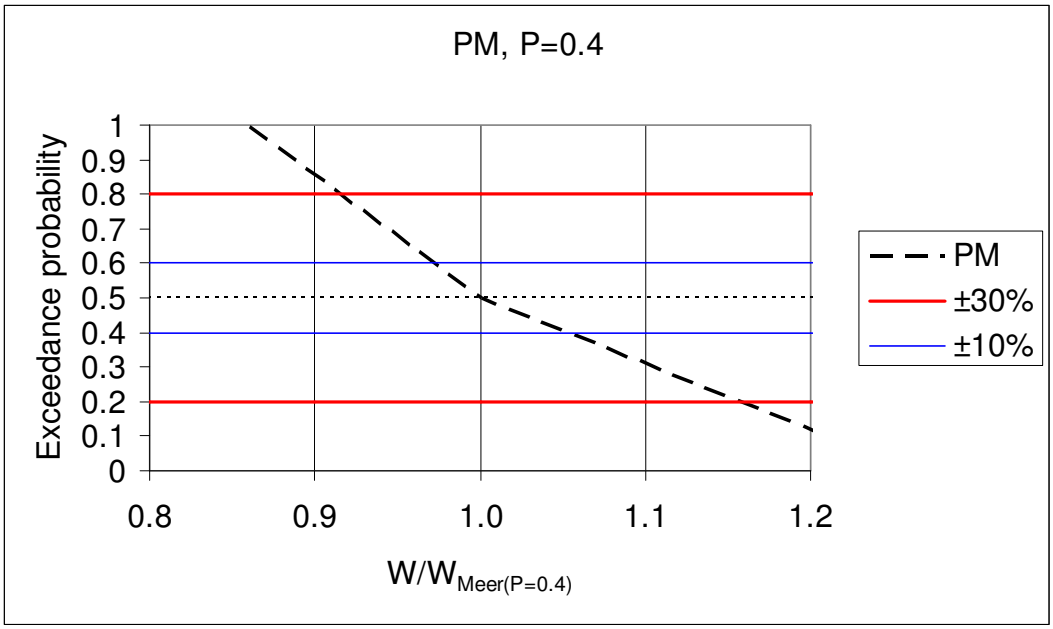

Fig.D.2 Exceedance probability of weight ratios for PM spectrum (cotα=1.5, P=0.4)

Repeating the procedure for the spectrum J33, weight ratios versus exceedance probability plot of J33 spectrum for all ζ_m in a range of 4.7-5.7 and cotα=1.5 was drawn in Fig D.3. In the Fig. D.3, levels belongs to the most probable 20% (50%±10) and 60% (50%±30) of occurrence were drawn, also. From pdf of $\alpha_{extreme}$ for J33 spectrum given in Fig 5.3, it was calculated that the most probable 60% of occurrence of $\alpha_{extreme}$ corresponds to $\mu_{\alpha extreme} \pm \sigma_{\alpha extreme}$ where $\mu_{\alpha extreme}$ =0.0093 and $\sigma_{\alpha extreme}$ =0.0008 as given in Table 5.1. The most probable 60% of occurrence of $\alpha_{extreme}$ corresponds to $\mu_{\alpha extreme} \pm 0.3\sigma_{\alpha extreme}$.

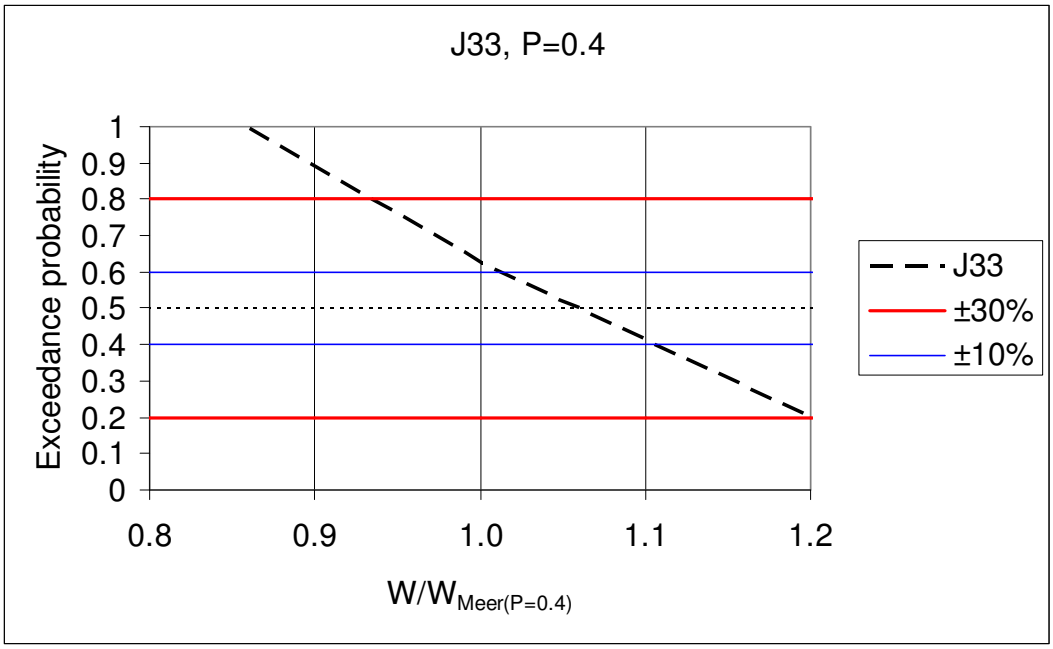

Fig.D.3 Exceedance probability of weight ratios for J33 spectrum (cotα=1.5, P=0.4)

D.2 Computation for cotα=1.5 and P=0.45

Then, exceedance probabilities of experiment cases LE and HE to Meer's equation with P=0.45 for all ζ_m in a range of 4.7-5.7, weight ratios for different spectral shapes were obtained and tabulated in Table D.2 for cotα=1.5.

Table D.2 Exceedance probabilities of weight ratios for different spectral shapes (cotα=1.5, P=0.45)

Case	$W/W_{Meer(P=0.45)}$	PM	J33	J10	W
LE	1.000	0.995	0.995	0.995	0.995
Meer	1.000	0.5	0.624	0.7465	0.8145
HE	1.500	0.058	0.135	0.282	0.431

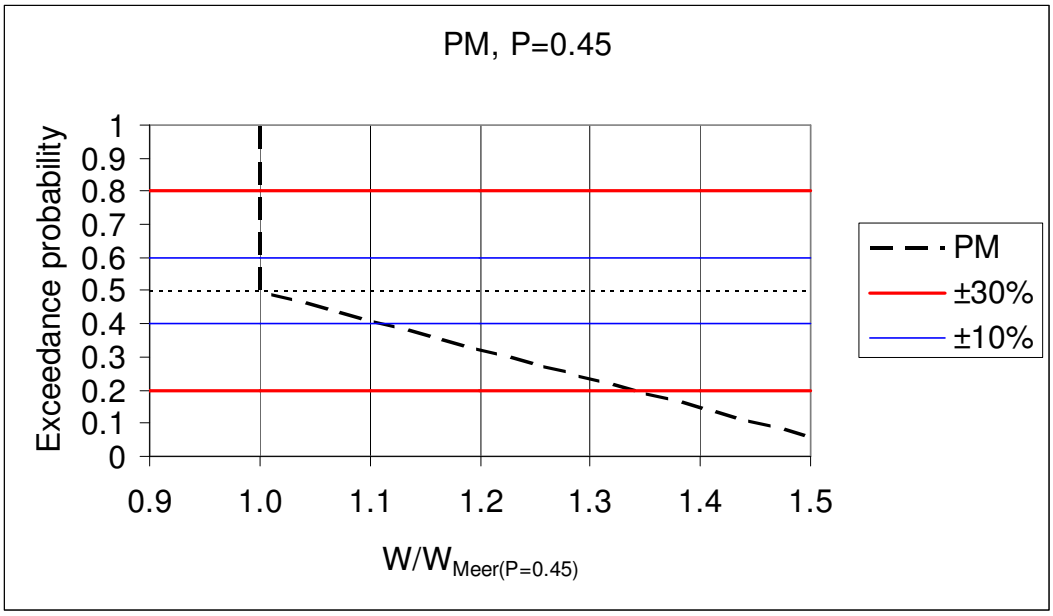

Fig.D.4 Exceedance probability of weight ratios for PM spectrum (cotα=1.5, P=0.45)

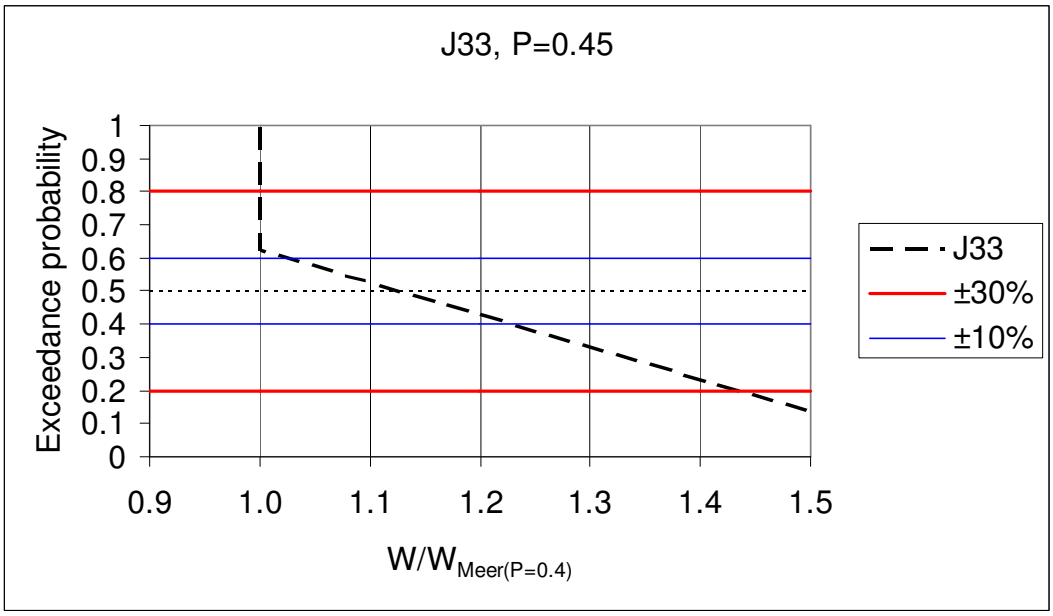

Fig.D.5 Exceedance probability of weight ratios for J33 spectrum (cotα=1.5, P=0.45)

Table D.3 Summary of the results on weight ratios of $W_{experiment}/W_{Meer}$ correspond to median (50%), ±10% and ±30% probabilities of $\alpha_{extreme}$ (cotα=1.5, ζ_m=4.7-5.9)

	30%	10%	median	-10%	-30%
PM, P=0.4	1.150	1.050	1.000	0.970	0.920
PM, P=0.45	1.330	1.120	1.000	1.000	1.000
J33, P=0.4	1.190	1.100	1.060	1.020	0.940
J33, P=0.45	1.430	1.230	1.130	1.030	1.000

D.3 Computation for cotα=3 and P=0.4

Table D.4 Exceedance probabilities of weight ratios for different spectral shapes (cotα=3, P=0.4)

Case	$W/W_{Meer(P=0.4)}$	PM	J33	J10	W
LE	0.940	0.995	0.995	0.995	0.995
Meer	1.000	0.5	0.624	0.7465	0.8145
HE	1.310	0.058	0.135	0.282	0.431

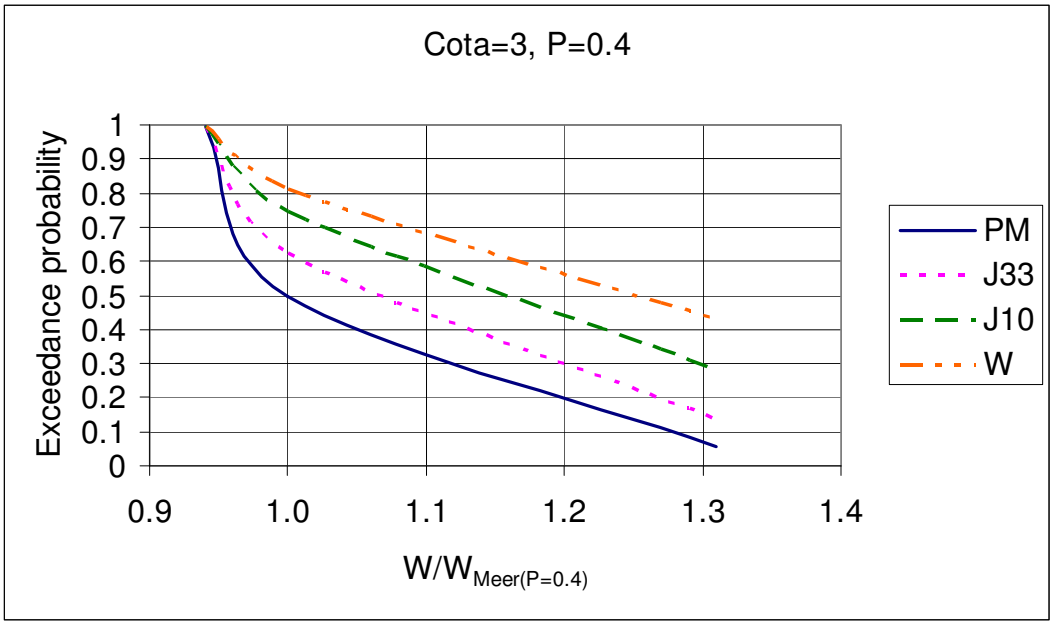

Fig.D.6 Weight ratio versus exceedance probability for different spectral shapes (cotα=3, P=0.4)

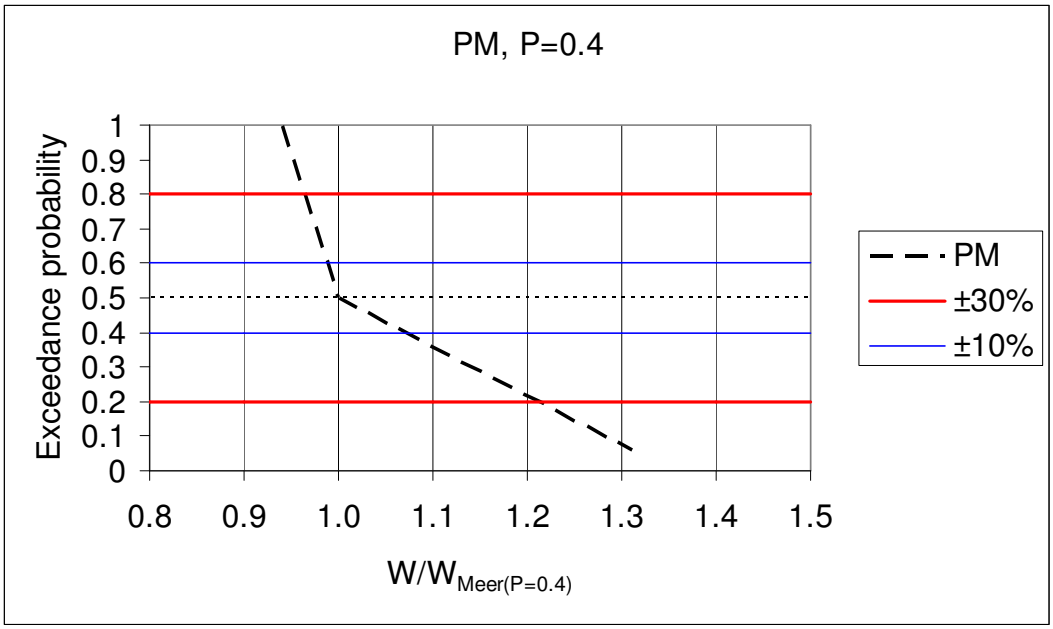

Fig.D.7 Exceedance probability of weight ratios for PM spectrum (cotα=3, P=0.4)

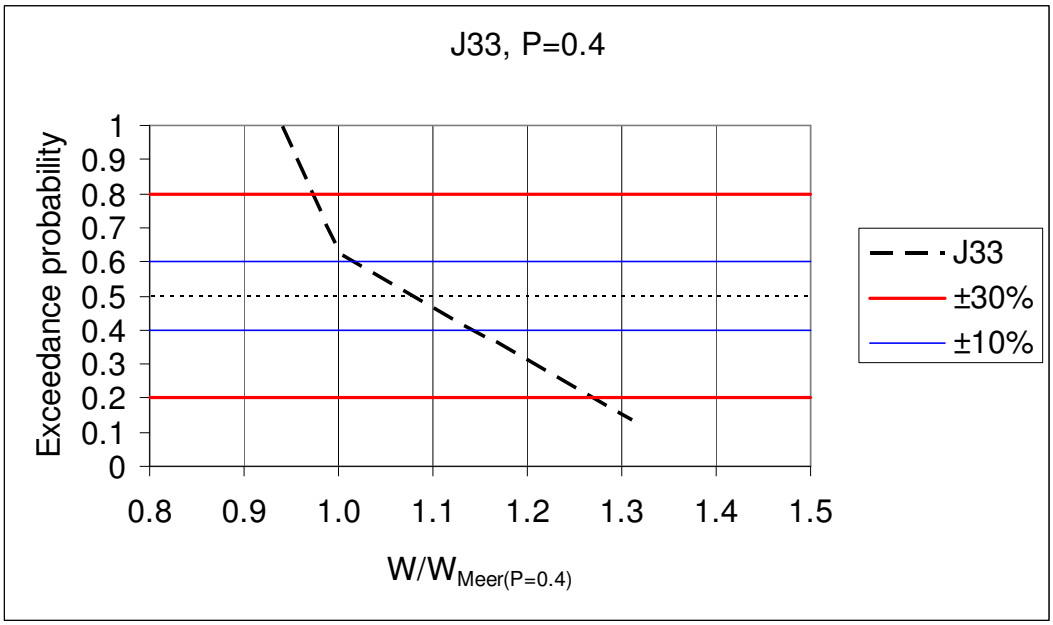

Fig.D.8 Exceedance probability of weight ratios for J33 spectrum (cotα=3, P=0.4)

D.4 Computation for cotα=3 and P=0.45

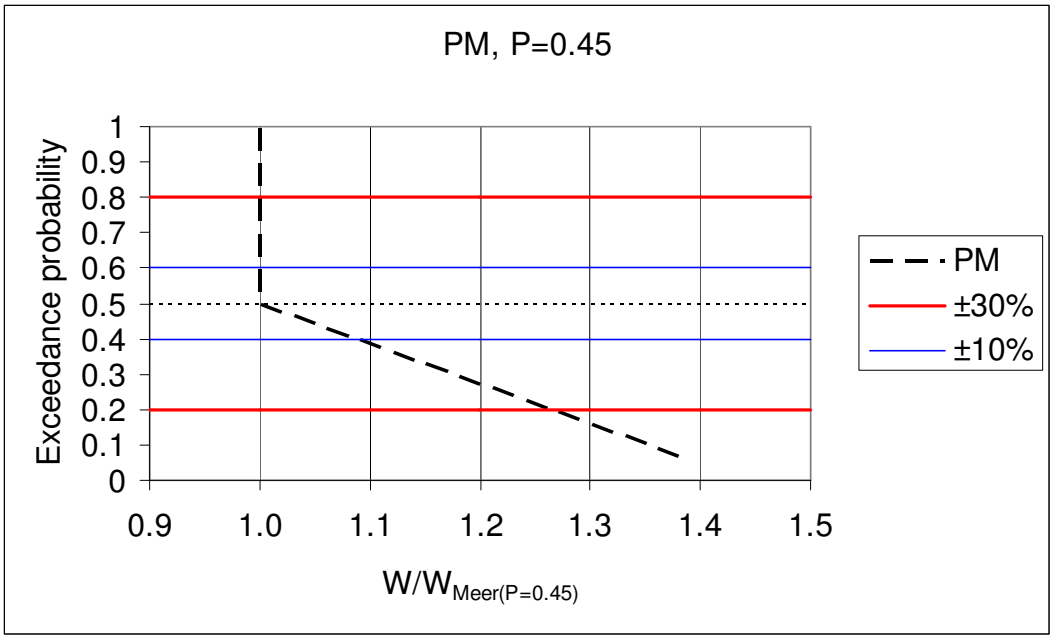

Fig.D.9 Exceedance probability of weight ratios for PM spectrum (cotα=3, P=0.45)

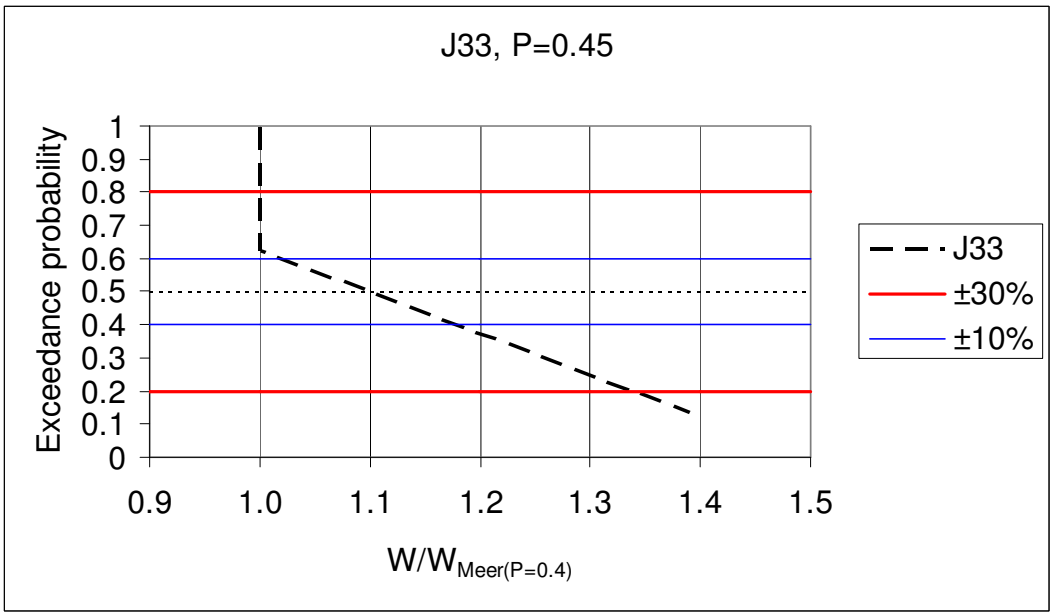

Fig.D.10 Exceedance probability of weight ratios for J33 spectrum (cotα=3, P=0.45)

Table D.5 Summary of the results on weight ratios of $W_{experiment}/W_{Meer}$ correspond to median (50%), ±10% and ±30% probabilities of $\alpha_{extreme}$ ($\cot\alpha$=3, ζ_m=1.9-2.7)

	30%	10%	median	-10%	-30%
PM, P=0.4	1.20	1.06	1.00	0.98	0.96
PM, P=0.45	1.25	1.09	1.00	1.00	1.00
J33, P=0.4	1.27	1.14	1.08	1.00	0.97
J33, P=0.45	1.34	1.17	1.10	1.00	1.00

VITA

Bergüzar Öztunalı Özbahçeci was born in Ankara on October 30, 1971. She graduated from the Civil Engineering Department of the Middle East Technical University in June 1993. She received her M.Sc. degree in Civil Engineering from the Middle East Technical University in September 1996. She was a research assistant in the Civil Engineering Department of Cumhuriyet University, Sivas, between 1994 and 1997. She studied as a research student in Disaster Prevention Research Institute of Kyoto University, Japan, between April 2001 and October 2002 as a Monbusho scholar of Japan Government. Since 1997, she has been working as a research engineer in Research Department of General Directorate of Construction of Railways, Ports and Airports which belongs to Ministry of Transport of Turkish Republic.